

STUDIES IN SOLID-GAS SYSTEMS:  
TITANIUM DIOXIDE AND UNSATURATED HYDROCARBONS

THESIS

presented for the degree of Doctor of Philosophy

by

IAIN SCOTT McLINTOCK, B.Sc.

University of Edinburgh.

1963.



# ABSTRACT OF THESIS

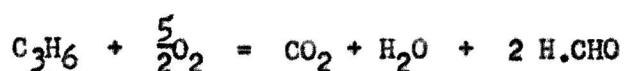
Name of Candidate IAIN SCOTT McLINTOCK  
Address \_\_\_\_\_  
Degree Ph.D. Date \_\_\_\_\_  
Title of Thesis STUDIES IN SOLID - GAS SYSTEMS: TITANIUM DIOXIDE AND  
UNSATURATED HYDROCARBONS.

Some properties of a laboratory prepared sample of  $\text{TiO}_2$  have been examined at  $25^\circ\text{C}$  under illumination by light of wavelength not less than  $3650\text{\AA}$ .

No dark adsorption of oxygen, ethylene or propylene was observed at  $25^\circ\text{C}$ , but photoadsorptions of each of these gases have been measured. Propylene was photoadsorbed only on  $\text{TiO}_2$  which had been pre-treated by a prior oxygen photoadsorption. The rate and extent of oxygen photoadsorption were increased by prior photoadsorption of either hydrocarbon and conversely. A series of alternate photoadsorptions could be carried out without apparent exhaustion of the solid.

The kinetics of photoadsorption followed a parabolic law in the initial stages of the uptake and the Elovich law in subsequent stages. The significance of the parabolic kinetics is obscure, but it is suggested that the Elovich kinetics result from an increasing energy of activation for photoadsorption with coverage. "Breaks" in the Elovich plots are taken to indicate the presence of at least two types of adsorption site. A new method of applying data to the Elovich law gives good agreement between the equation parameters and experimental rates.

The photo-oxidation of both hydrocarbons on illuminated  $\text{TiO}_2$  in the presence of oxygen at  $25^\circ\text{C}$  has been demonstrated. The overall oxidations fit the equations :



The adsorption and oxidation of formaldehyde, propylene oxide and ethylene oxide on  $\text{TiO}_2$  at  $25^\circ\text{C}$  have also been briefly studied.

The changes in the dark and photoconductance of  $\text{TiO}_2$  when oxygen, hydrocarbons and water vapour are brought in contact with it at  $20^\circ\text{C}$  have been measured.

The results of the conductivity measurements and the form of the kinetics of photoadsorption have been discussed generally. It is believed that some contribution has been made towards an understanding of the mechanisms of the surface processes involved.



To my Parents

## C O N T E N T S

	Page
INTRODUCTION	1
Properties of $\text{TiO}_2$	3
Photoreactions on $\text{TiO}_2$	10
Conductivity changes during adsorption on $\text{TiO}_2$	12
Photoadsorption and desorption on semiconductors	14
The kinetics of chemisorption	17
EXPERIMENTAL	20
EXPERIMENTAL RESULTS	
Photoadsorption on untreated $\text{TiO}_2$	30
Photoadsorption on "pre-treated" $\text{TiO}_2$	33
Reversibility of the photo-uptakes	35
Photoreaction of $\text{C}_2\text{H}_4\text{-O}_2$ mixtures	37
Photoreaction of $\text{C}_3\text{H}_6\text{-O}_2$ mixtures	43
Experiments with formaldehyde, ethylene and propylene oxide	51
Colour changes in $\text{TiO}_2$ during adsorption	55
Conductivity measurements	57
DISCUSSION	
Surface water and photoadsorption	65
Photoconductivity of $\text{TiO}_2$	67
Kinetics of photoadsorption	70

DISCUSSION (contd.)	Page
Mechanism of photoadsorption	76
Photo-oxidations on $\text{TiO}_2$	84
Adsorption of $\text{H}_2\text{O}$ vapour on $\text{TiO}_2$	89
Conclusion	92
TABIES	93
BIBLIOGRAPHY	113
ACKNOWLEDGMENTS	116

---

## INTRODUCTION

### INTRODUCTION

The high reflecting power of titanium dioxide has made it a valued component of many paints and a de-lustering agent for fabrics. But although in this respect it is more efficient than some other commercial additives such as white lead or barium sulphate, it has an additional and embarrassing property. In the presence of  $\text{TiO}_2$  and under the action of sunlight, slow fading of the paint and fabric dyes occurs, with the attendant phenomenon of "chalking", i.e. separation and flaking of the pigment from its vehicle. Widespread examples have now been reported of photochemical degradation of natural and synthetic fibres in the presence of  $\text{TiO}_2$ .

This ~~phenomenon~~ has been attributed over the past 30 years to many causes. These have ranged over such extremes as oxidation by perititanic acid or photosensitisation by the  $\text{TiO}_2$ . It is now established (1) (2) (3) that  $\text{TiO}_2$  absorbs in the ultra violet with a sharp absorption edge at c.  $4100\text{\AA}$ , and that it is this absorbed radiation which results in the troublesome photo-oxidations and photo-degradations (4) (5) (6). These systems are complex; a direct study of them, although useful, is not likely to result in a clear picture of the mechanisms involved in the photoreactions. Accordingly, the photoreactions of  $\text{TiO}_2$  with simpler organic systems have been investigated. Mandelic acid (7) in an aqueous suspension of  $\text{TiO}_2$ , for example, is photo-oxidised to benzaldehyde and carbon dioxide; the oxide itself is reduced to  $\alpha\text{-Ti}_2\text{O}_3$ . There is an undoubted correlation (7), among a range of  $\text{TiO}_2$  samples, between general photo-chemical reactivity and activity in the fading, chalking and degradation processes.

The idea (4) (6) that the active agent is atomic oxygen produced directly by photolysis of the lattice has now been abandoned. It is now believed that

that photoadsorbed oxygen is the oxidative species (8). This is, therefore, a surface reaction, and the electrical and optical properties of  $\text{TiO}_2$ , with their relations to surface phenomena and adsorption, are important in an approach to the problem.

FIG 1.

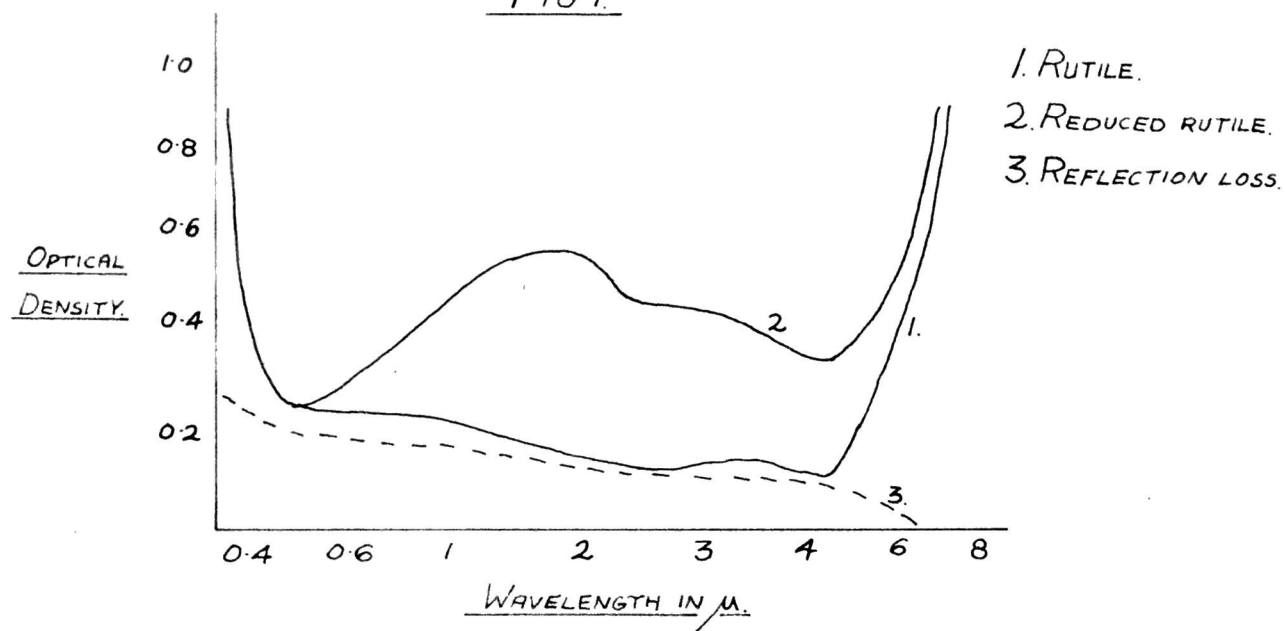


FIG. 2.

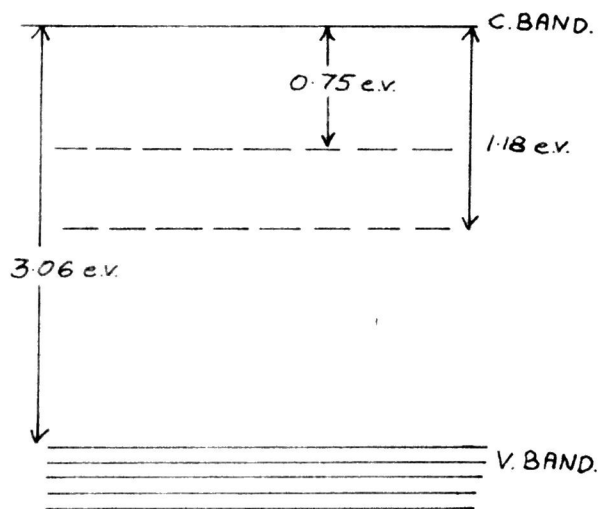
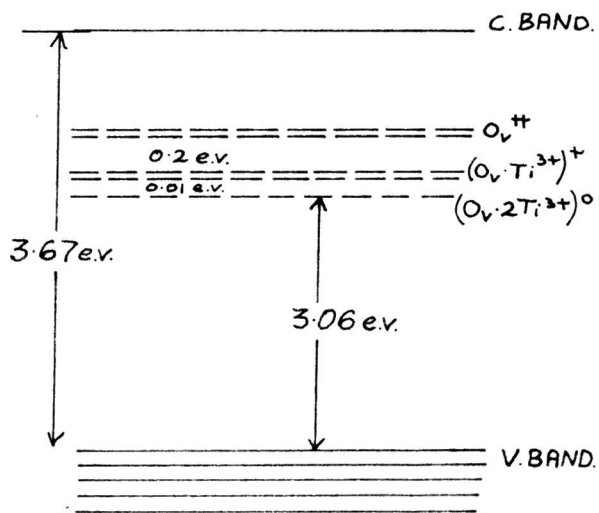


FIG. 3.



### Relevant properties of Titanium Dioxide

Titanium dioxide is a white solid existing in three crystal forms. Rutile and anatase are the two varieties present in pigments; the rare third variety, brookite, need not concern us here. In both rutile and anatase each Ti ion is surrounded by six oxygen ions, giving a slightly distorted octohedral structure. There is no definitive estimate of the extent of covalent bonding, but a number of independent observations (9) show a certain degree of covalent bonding to be present.

Curves of the variation of optical density of rutile with wavelength have been obtained from both diffuse reflection (3) and absorption measurements (1). The curve for "pure" rutile is shown in Fig. 1. The absorption edge at  $4100\text{\AA}$  is sharp at  $4^{\circ}\text{K}$  and reasonably sharp at room temperature; increasing temperatures, however, make it slightly less sharp and move it to higher wavelengths (2). Slight reduction of the dioxide ( $\text{H}_2$  for 2 minutes at  $600^{\circ}\text{C}$ ) alters the optical absorption considerably (Fig. 1) (1). The blue or black color of reduced rutile is consistent with Fig. 1. Bands have also been detected in the infra-red region (10) (11).

Band theory predicts that titanium dioxide should be an insulator. Most of the electrical data have been obtained (1) (12) (13) (14) from rutile and these show the oxide to be an oxygen-deficient n-type semiconductor. The current is, therefore, carried by quasi-free electrons produced from non-stoichiometric defect centres. This departure from stoichiometry is enhanced by reduction, in which case a rise in conductivity results.

The type of defect present in non-stoichiometric rutile has not yet been determined definitively. Previous to 1959 the defect centres were considered



(2) (4) (15) to be oxygen vacancies, associated with neighbouring polarised  $Ti^{3+}$  ions :



At low temperatures the electrons were mainly trapped on these  $Ti^{3+}$  sites, but thermal or optical energy could liberate them to produce conduction electrons and an ionised centre :



Singly and doubly-ionised centres.

More recent work by Cronmeyer (10) has sought to corroborate this picture. Work contemporary (14) (16) (17) with his, however, has presented strong evidence in favour of interstitial  $Ti^{3+}$  defects. Electron spin resonance spectra of reduced rutile in the liquid helium temperature range have been interpreted (17) as being due one or all of the three defects :

1. Interstitial  $Ti^{3+}$
2.  $Ti^{3+}$  on a site perturbed by an oxygen vacancy.
3. An unidentified centre whose presence is due to hydrogen incorporation in the lattice.

The semiconductivity of rutile can be varied also by the incorporation of altermvalent ions in the lattice (16) (17) (18). The results are interesting but as yet fairly inconclusive. Work by Ritchie et al (19) (20) in this Department has shown that conductivity changes occur in  $TiO_2$  during oxygen and ammonia adsorptions. Conductivity changes which occur during hydrogen adsorption (reduction) have been attributed (12) to an increased concentration of surface  $Ti^{3+}$  ions. Chemisorptions of these types can be regarded as giving rise to or destroying surface defect centres.

The white color of "pure" rutile darkens through yellow and blue to black under increasingly severe reducing conditions. These color changes have been attributed (21) to the formation of Paul-Schottky color centres, i.e. in this case oxygen vacancies associated with trapped electrons. (2) (4) (15). This would indicate the presence of oxygen-vacancy defects. It has been counter-proposed (14) that interstitial  $Ti^{3+}$  ions would also constitute a color centre. In any event, such color changes are imperfectly understood. Gebhart and Herrington (22) have carried out experiments which strengthen their view that discoloration is due to organic contamination from high vacuum grease. Rutile samples doped with altermvalent impurity ions also darken in color; photo-tropic effects in doped oxides, including  $TiO_2$ , have been discussed by McTaggart and Bear (8) (31) and Weyl and Forland (4).

Conductivity, (2) (15) (23) (24) Hall effect (15), thermopower (23) (25) and optical absorption (2) data have contributed to give some measure of

agreement on an energy-band structure for rutile. Conductivity measurements in the region 700-1100°C suggest an energy gap width ( $E_g$ ) of 3-4 e.v. between valence and conduction bands. Optical absorption and photoconductivity figures result in an  $E_g$  value of 2.8-3.1 e.v. Indecision as to the relation between optical and thermal activation energies has caused some ambiguity in the electronic energy level scheme for rutile. Some authors follow the treatment of Mott and Gurney (Electronic Processes in Ionic Crystals, Oxford Univ. Press 1940, p.160), which predicts an optical value always greater than the thermal value. In this event the relation between the two energies involves the values of optical and static dielectric constant. For rutile this leads to an optical value about five times greater than the thermal value (15). Other authors, meanwhile, appear to regard these two activation energies as identical.

Cronmeyer (1) (2), accordingly, has regarded the optical absorption edge and photo conductivity peak at  $0.4 \mu$  (3.06 e.v.) as due to the fundamental lattice absorption involving an electronic transition from valence band to conduction band. He thus arrives at a value 3.06 e.v. for  $E_g$ . His more recent work (10) has placed oxygen-vacancy levels 0.75 e.v. and 1.18 e.v. below the conduction band (Fig. 2).

Breckenridge and Hosler (15), however, have regarded the  $0.4 \mu$  edge as responsible for an electronic transition between oxygen-vacancy levels and conduction band, where these are 0.62 e.v. apart. They consider that on a thermal basis the optical activation energy (3.06 e.v.) should be scaled down to 0.62 e.v. by the appropriate factor  $1/5.1$ . Their proposed energy scheme is shown in Fig. 3. Thermodynamic considerations support their idea that the

impurity levels are produced by thermal decomposition at high temperatures (350-950°C) and with an appropriate activation energy. The density of impurity centres may be high enough to produce a narrow impurity conduction band. Paramagnetic data of Ehrlich (26) can be explained on the basis of a donor impurity band about 0.04 e.v. wide. The results of various workers give a range of values in the order of 0.1 e.v. for the depth of the donor band below the conduction band. In the case of non-interacting donor centres (no donor band formed) this value is generally slightly higher. These results are summarised in reference (9) page 671.

These energy schemes have been derived mainly from measurements carried out on single crystals of reduced rutile. The defects in these samples have been regarded as oxygen vacancies but, as mentioned previously, there is now some doubt as to the validity of this assumption. Frederikse and co-workers have proposed (16) a conductivity mechanism which involves defects of the interstitial cation type. At very low temperatures ( $\leq 4^\circ\text{K}$ ) the electrons are trapped on the interstitial titanium ions by self-polarisation of the surrounding lattice; as such they are termed "polarons". Conduction at these temperatures is in a narrow polaron band. At higher temperatures (say  $\sim 8^\circ\text{K}$ ) these electrons can be freed from their state of self-induced polarisation and become available for conduction in a narrow impurity band. This band is associated with the 3d levels of  $\text{Ti}^{4+}$  ions. The necessary activation energy rises from about 0.01 e.v. at temperatures less than  $50^\circ\text{K}$  to about 0.08 e.v. at room temperature.

The photoconductivity of  $\text{TiO}_2$  with respect to wavelength shows a maximum in the vicinity of the optical absorption edge (1) (2). There is a longer

wavelength effect extending into the near infra-red. Ritchie and co-workers in this Department have studied the effect of adsorbed oxygen and ammonia on the photo conductivity of  $\text{TiO}_2$  samples. These results will be discussed later. It is established that surface effects play an important part in the overall conductivity.

The preparation of  $\text{TiO}_2$  by hydrolysis of titanium salts produces an oxide in a high state of hydration. Latty has shown (27) that this water is lost in an exothermic reaction between room temperature and  $350^\circ\text{C}$ , with a maximum in the rate of dehydration at around  $170^\circ\text{C}$ . Gregg has shown (28) that most of the water is lost at temperatures less than  $500^\circ\text{C}$  but that a small portion is retained to be desorbed almost explosively at c.  $700^\circ\text{C}$ . This last temperature is in the region of the Tamman temperature. Gregg considers this to indicate circumstantially that the major portion of the water content is situated on the surface of the oxide rather than within the lattice. It is suggested (29) that water is bound to  $\text{TiO}_2$  by a wide range of energies. Three types of binding are proposed.

1. Removed below  $100^\circ\text{C}$ . Molecular water.
2. Removed in the range  $100-300^\circ\text{C}$ . Held by hydrogen bonds.
3. Removed only at  $>300^\circ\text{C}$ . Chemisorbed as OH groups.

A small but sharp infra-red absorption band at 0.4 e.v. is observed in all rutile crystals and has been attributed to OH groups. Yates has employed (30) infra-red methods in an investigation of surface water on  $\text{TiO}_2$ . His results show that some molecular water is present after evacuation at  $150^\circ\text{C}$  but that only OH groups remain after treatment at  $350^\circ\text{C}$ . There is an indication, also, that two types of surface OH occur on anatase but only one on rutile. The

character of surface water has here been shown to depend to a large extent on the method of sample preparation.

It is evident that the surface of a  $\text{TiO}_2$  sample will normally be partially covered with various forms of adsorbed water. This surface "impurity" may be expected to affect the electrical, adsorptive and catalytic properties of the solid. Its presence must be recognised in a consideration of such properties. Maclean has shown (20) that oxygen photo adsorption alters the binding between adsorbed water and surface; photo adsorbed oxygen displaces approximately equimolar amounts of surface water.

McTaggart and Bear (31) have reported that the phototropic properties of  $\text{TiO}_2$  depend on the presence of water on the surface.

Photo reactions on titanium dioxide

Ritchie et al (19) (20) (32) have studied the photo adsorption of  $O_2$  and of NO on  $TiO_2$  at  $25^\circ C$  and c. 50 mm. pressure. After addition of  $O_2$  or NO to previously evacuated  $TiO_2$  a slow, small uptake of NO was observed in the dark, but no corresponding change in pressure occurred in the case of  $O_2$ . On illumination with light absorbed by the  $TiO_2$  a relatively rapid pressure decrease occurred with both NO and  $O_2$ . The photo uptakes of each gas were of the same order of magnitude. The rate and amount of photo uptake depended on such variables as light intensity and wavelength, ambient pressure, temperature and stage of uptake, as well as on sample structure and pretreatment. At low initial pressures (c 1 m.m.) the oxygen photo adsorption was complete to within 0.01 m.m. but the pressure decrease in the nitric oxide photo reaction amounted to only 75% of the initial pressure. The remaining gas phase here was nitrous oxide. Maclean (20) later showed that some nitrous oxide was retained by the surface until the sample was evacuated. The surface photo reaction



has now been proposed. The absence of a detectable dark or photo uptake of hydrogen, carbon monoxide or nitrous oxide has been reported by Kennedy (32). But Russian workers have recently reported (33) a photo adsorption of hydrogen in the range  $0-200^\circ C$ . The influence of sample preparation on surface properties is again indicated.

It was found (32) that the kinetics of the oxygen uptake depended on sample structure and preparation. In some samples the entire photo adsorption followed a parabolic expression of the form,

$$(\Delta p + p_0)^2 = k t + p_0^2$$

where  $\Delta p$  is the pressure decrease at time  $t$  and  $k$  and  $p_0$  are constants. In

other samples such an expression described the initial stages only, and an exponential expression was followed in the later stages. This expression was of the form

$$(P-\Delta p) = p e^{-kt} \qquad k = \text{constant}$$

where  $\Delta p$  is the pressure decrease after time  $t$  and  $P$  is a constant considered to correspond to the total possible photo uptake. Maclean (20) reports different kinetics for this photo adsorption. In the initial stages his oxygen photo uptakes adhered to the Elovich rate equation (see page 17); the later stages followed exponential kinetics similar to those mentioned above. Maclean has reported (20) identical kinetics for the nitric oxide photo uptake.

These kinetics have been interpreted (32) on the basis of a two-site mechanism. Reversible adsorption on a limited number of sites of type A leads to a surface species  $A^+O^-$ . The trapping of photoelectrons gives an  $AO^-$  centre from which the  $O^-$  is free to migrate to sites of type B. The kinetics are here parabolic, controlled by the migration process. The eventual trapping of a positive hole gives the final irreversibly adsorbed species  $B^+O^-$ . It is assumed that the exponential kinetics take over when the number of B sites available becomes the controlling factor.



Conductivity of  $\text{TiO}_2$  - variation on adsorption of gases

Ritchie et al (19) (20) have studied the conductivity changes associated with oxygen uptake on  $\text{TiO}_2$  pellets at room temperature. In the dark oxygen at 50 mm. pressure produced a small decrease in resistance. This effect was reversed on evacuation. Illumination of an evacuated sample caused a large decrease in resistance. This effect was slowly reversed on discontinuation of the illumination. Oxygen produced a large decrease in this photo conductance; here the effect was not reversed by evacuation in the dark. Maclean has measured the effect of ammonia at room temperature on the dark and photoconductivities of  $\text{TiO}_2$ . Ammonia produced an almost instantaneous decrease in the dark resistance, followed by a small and slow increase to a constant value. (The final resistance value was always less than the original value before admission of ammonia.) Illumination of the sample at this stage produced a further resistance decrease which was smaller than that experienced in the absence of ammonia; the final resistance value, however, corresponded to that of the photo conductance which would have been observed in vacuo. The resistance changes here were also reversed on evacuation or discontinuation of illumination.

Kennedy (34) has since then studied the conductivity of  $\text{TiO}_2$  films in the range 20-140°C, using a variety of pre-treatments. The dark conductivity depended on pre-treatment and on temperature. Activation energies of the order 0.7 e.v. were quoted for the dark conductance. In two respects his results disagreed with those obtained previously for the  $\text{TiO}_2$  pellets. In the first place, oxygen (5.0 mm) increased the value of dark resistance. Secondly, at 26°C the decay in the photo conductance was incomplete even after long periods in the dark. At 120°C, however, the decay was rapid and complete for short

periods of pre-illumination. It was confirmed that the increase in resistance brought about by oxygen photo adsorption was not reversed by evacuation in the dark; treatment at 120°C in vacuo caused a small decrease in the 20°C dark resistance after such oxygen treatment. These photoeffects have been tentatively explained on the basis of a slightly modified scheme of oxygen photo adsorption.

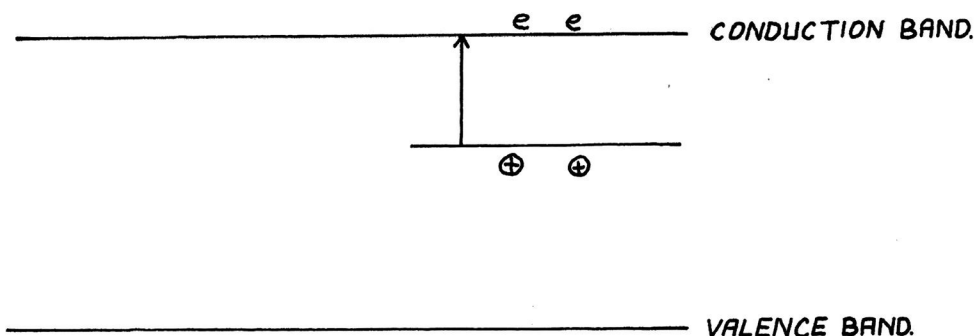
Photoadsorption and desorption on semiconductors

It has been well established experimentally that the rate and extent of gas adsorption processes at semiconductor surfaces can be altered by illuminating the system with radiation of suitable wavelength. In general, the gaseous component of the system does not absorb the radiation, and the observed effects are the result of the solid having absorbed incident radiation. An adsorption which is promoted in this way is termed a "photo adsorption". The term "photo desorption" is given to an analogous desorption. The effect of the absorbed radiation is to excite electrons into conducting levels; this results in the observed photo conductance. It is apparent that illumination has altered the electronic equilibrium of the semiconductor. The electronic factor has frequently been emphasised in adsorption and catalytic studies, and electron transfer between gas and solid is involved in many chemisorptions. It is, therefore, to be expected that illumination of a semiconductor will be capable of altering its properties in relation to gas adsorption. Photo adsorption and photo desorption have been reported (19) (20) (32) (67) (35-43) for a number of systems. The experimental methods have involved both direct measurements of gas pressure and indirect measurements involving properties of the semiconductor such as photo conductance.

In the  $ZnO-O_2$  system low oxygen pressures have been used and both photo adsorption and photo desorption have been observed. In previous studies on  $TiO_2$  the use of higher gas pressures (10-50 m.m.) has placed the emphasis on photo adsorption. It has been mentioned earlier (p. 10) that photo adsorptions of oxygen and of nitric oxide have been observed on  $TiO_2$  at  $25^\circ C$ . Ritchie et al (19) have reported that illumination does not promote adsorption of carbon

monoxide, water vapour or hydrogen. Russian workers have recently reported a photo adsorption of hydrogen on  $\text{TiO}_2$  (cf. p. 10). On the other hand, illumination has been reported (44) to inhibit hydrogen adsorption on  $\text{ZnO}$ .

There are at least two sets of conflicting ideas which attempt to predict whether photo adsorption will occur in a particular system. These can be illustrated by reference to an n-type semiconductor, where the effect of the illumination is to excite electrons from donor impurity levels to the conduction band,



Schwab (45) considers that electron transfer between gas and solid involves energy levels in the conduction band. The increased number of electrons in the conduction band during illumination will promote the adsorption of oxygen as  $\text{O}^-$ , but will not promote the adsorption of electron donors such as hydrogen.

On the other hand Gray (46) considers that the electron transfer process occurs at the impurity levels. Illumination decreases the number of electrons at these levels but produces positive holes there. The adsorption of electron donors such as hydrogen will be enhanced by illumination but the adsorption of electron acceptors, e.g. oxygen, will not be promoted.

The experimental results outlined above indicate that neither of these points of view describe the situation adequately. Illumination appears to promote adsorption of both electron acceptors and electron donors. It is of interest, therefore, to extend the experimental studies to other gases and to see whether photo adsorption can be qualitatively explained in terms of their electronic structures and probable direction of electron transfer.

Photo adsorption is undoubtedly an electronic phenomenon, involving the electronic structures of both gas and solid. A shared characteristic of oxygen and nitric oxide is their possession of an unpaired electron; the photo adsorption of each of these gases could be related to this common electronic property. The double-bonded system of unsaturated hydrocarbons suggests itself as an electronic system which could profitably be investigated in relation to photo adsorption in  $\text{TiO}_2$ . Adsorption of these hydrocarbons has been considered (47) (48) to involve formation of a positively-charged species and it is possible that this will be reflected in photo adsorption effects.

The possibility that photo-oxidation of the hydrocarbon will occur on illuminated  $\text{TiO}_2$  provides a potential extension of these investigations to the field of photocatalysis. In turn, this could be linked with the photo-oxidising action of  $\text{TiO}_2$  on paints and fabrics.

### The Kinetics of chemisorption

A general comprehensive treatment of the kinetics of chemisorption is still very much in the future. But one rate law which has been extensively explored in an attempt to systematise the large body of chemisorption data is the Elovich rate law. This is an empirical expression introduced by Elovich in 1939. Later work, notably in the first instance by Taylor and Thon (49) (50), has shown the applicability of the Elovich equation to a variety of chemisorption reactions. The Elovich equation and its significance in the field of chemisorption has recently been reviewed by Low (51).

In its differentiated form the Elovich equation is :

$$\frac{dq}{dt} = a e^{-\alpha q}$$

where  $q$  is the amount of gas chemisorbed at time  $t$  and  $\alpha$  and  $a$  are constants.  $a$  should equal the initial rate ( $\frac{dq}{dt}$ ) when  $q$  is zero. For a chemisorption which follows the Elovich equation a plot of  $\log$  (rate) against  $q$  will be linear.

The equation is not generally applied in this form but instead in one of its integrated forms.

Typical of these is the expression :

$$q = \frac{2.3}{\alpha} \log (t + t_0) - \frac{2.3}{\alpha} \log t_0$$

where  $t_0 = \frac{1}{\alpha a}$  is a parameter whose value is chosen to give a straight-line plot of  $q$  against  $\log (t + t_0)$ .  $\alpha$  is then obtained from the gradient of this line, and subsequently  $a$  from the relation  $t_0 = \frac{1}{\alpha a}$ . Numerical methods of determining  $\alpha$  and  $a$  have also been employed in contrast to the graphical

methods outlined above. These methods are cited in reference (51) page 269. Elovich plots sometimes consist (49) of more than one linear portion, each of which has its own value of  $\alpha$  and of  $\underline{a}$ . The possible significance of such breaks has been discussed by Low (51) along with the related variation of  $\alpha$  and  $\underline{a}$  with temperature and pressure. One outstanding result is that the  $\underline{a}$  values calculated from the Elovich plots are generally very much less than the experimental rates at  $q = 0$ . On the basis of the differential Elovich equation they should be equal.

A number of proposed mechanisms of chemisorption lead to the Elovich rate law. The sole fact of the adherence of a particular set of data to this law is, therefore, no sign of a unique mechanism. The use of the equation has been criticised (52) - (54) on these grounds. In its defence it is claimed that the equation provides some basis of comparison for the proliferate data of chemisorption kinetics. The fact, too, that many mechanistic approaches to chemisorption have resulted in the Elovich equation has divested it of its purely empirical nature.

Most of the proposed chemisorption mechanisms which lead to the Elovich rate law fall into one of two categories.

- (i) Models involving the generation of adsorption sites by the presence of the adsorbate gas itself. The process described by the Elovich equation is then the slow destruction of the sites by adsorption of the gas. Discrepancies arise between  $\underline{a}$  values and experimental rates because this slow process is preceded by a fast adsorptive process concerned with site-generation. So far, no workers have fitted a kinetic equation to this initial process. Cimino and others (55)

consider that in most cases  $\underline{a}$  loses all physical meaning, although a physical significance can be given to  $\alpha$ . It is believed that  $\alpha$  measures the rate of deceleration of the slow process.

- (11) Models which picture the adsorbate as having to surmount a potential barrier whose height increases with coverage. Important among these are those models which involve electron transfer between gas and surface (42) (56) (57). The model proposed by Gundry and Tompkins involves the transition of an adsorbed atom from an initial to a different chemisorbed state. The tendency among models of this type is to regard the Elovich law as an approximation which is valid only at certain stages in the chemisorption. The physical meaning of  $\alpha$  and  $\underline{a}$  becomes even less tangible.

A full account of the numerous suggested models of chemisorption is given in reference (51) p.p. 362-307.

The photoadsorption of oxygen, ethylene and propylene on  $\text{TiO}_2$  will later be examined kinetically in the framework of the Elovich rate law. The character of the initial fast process, and the relation between  $\underline{a}$  values and experimental rates, will receive particular attention.



EXPERIMENTAL

Fig. 4

Reaction vessel, actual size.

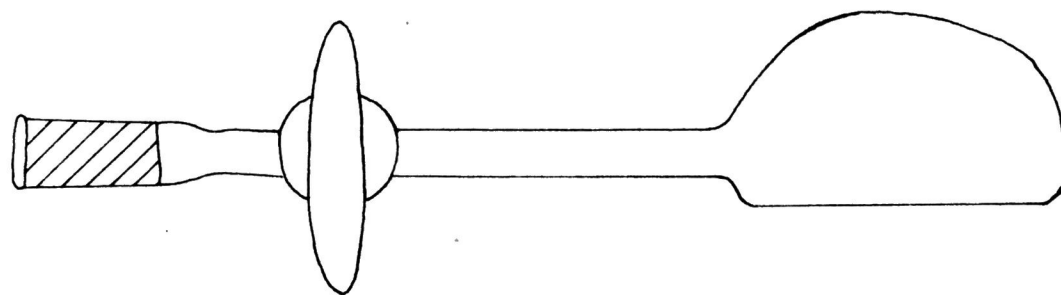
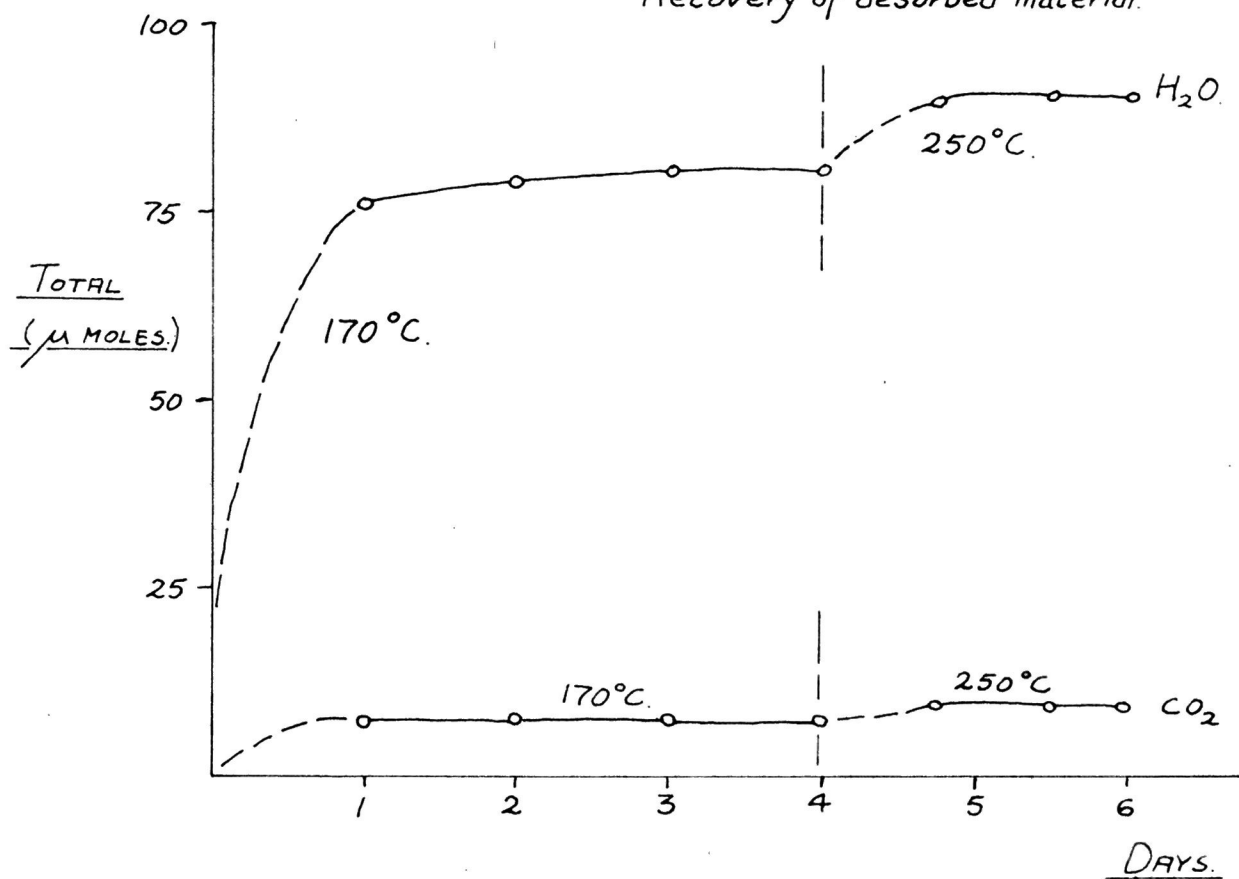


Fig. 5.

Evacuation of a  $\text{TiO}_2$  film.  
Recovery of desorbed material.



## EXPERIMENTAL

The experimental results fall into two categories. The first involves measurements of gas uptake and photoreaction on films of  $\text{TiO}_2$ . The second is concerned with conductivity changes of  $\text{TiO}_2$  pellets in contact with gases and vapours.

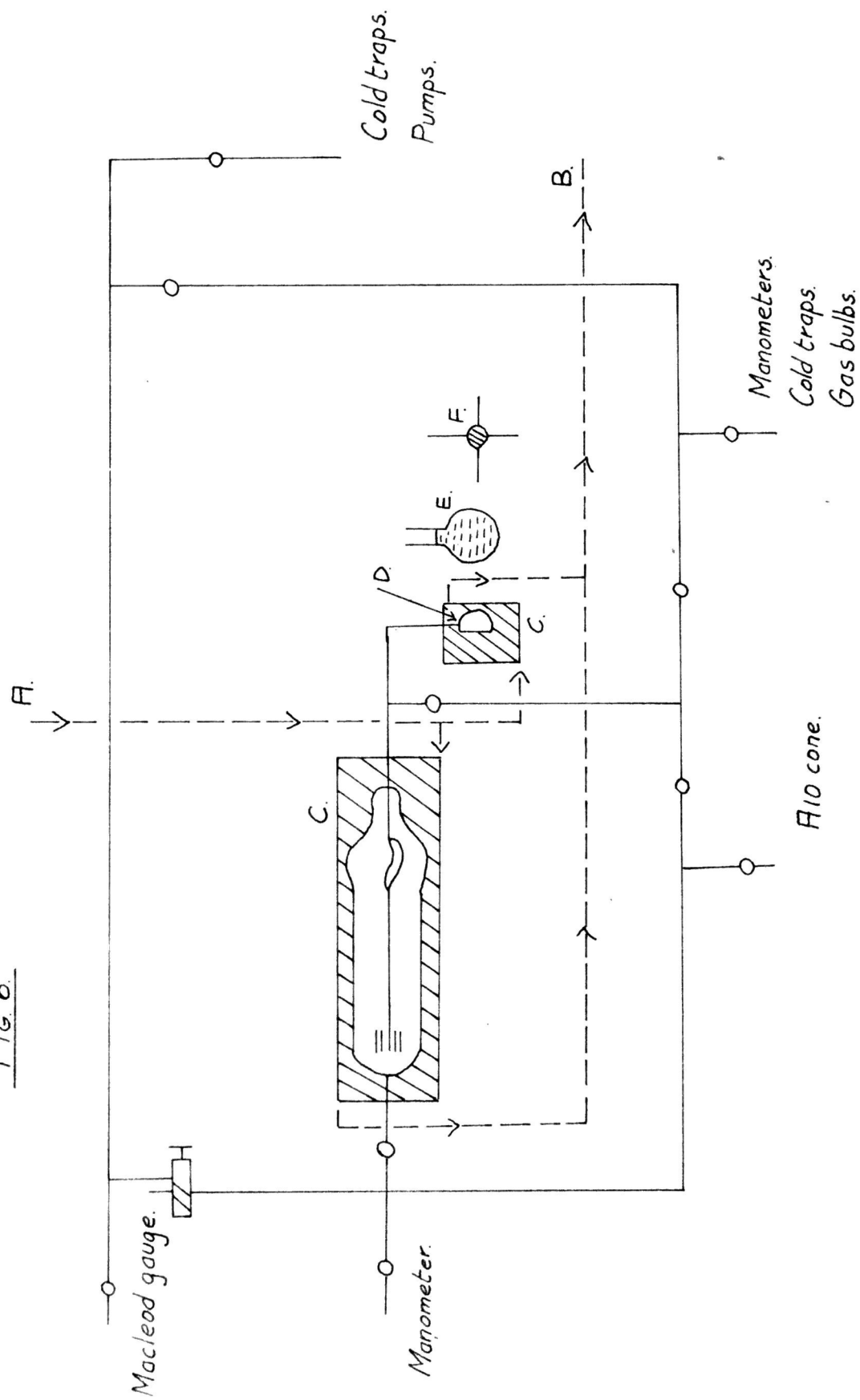
### Photoadsorption measurements

#### (1) Preparation of films.

Films for adsorption experiments were prepared by introducing a weighed quantity (c. 0.1 g) of ground  $\text{TiO}_2$  into reaction vessels of the type shown in Fig. 4. The solid was made into a slurry on the flat side of the vessel with 0.2 ml. distilled water. Evaporation of the water resulted in a thin and reasonably uniform layer of the dioxide on the flat side of the vessel.

Evacuation ( $10^{-5}$  mm.) of such films at room temperature produced measurable quantities of desorbed water vapour even after several weeks. It is difficult under certain conditions to differentiate between water from this source and water produced from a surface reaction between adsorbed gases. Maclean (20) has pointed this out in his report on the photoadsorption of oxygen and other gases on  $\text{TiO}_2$ . In the present experiments this problem was obviated by evacuating the films at a higher temperature ( $170^\circ\text{C}$ ) in a small furnace. Negligible ( $0.2 \mu$  moles per day) amounts of water vapour were desorbed after 4-5 days of this treatment. In agreement with the results of Iatty (27) and of Gregg (29) the surface was not completely dehydrated at this temperature; an increase in the temperature of evacuation after the completion

Fig. 6.



A. CONSTANT HEAD. C. CONSTANT TEMPERATURE JACKET. E.  $\text{CuSO}_4$  SOLUTION.  
 B. RETURN FLOW TO THERMOSTAT. D. REACTION VESSEL. F. LIGHT SOURCE.

of the usual pre-treatment at  $170^{\circ}\text{C}$  resulted in the desorption of further appreciable quantities of water vapour. Small quantities of carbon dioxide were also desorbed at  $170^{\circ}\text{C}$ . Typical data obtained for the dehydration of a film are given in Fig. 5. This film was evacuated at  $20^{\circ}\text{C}$  for 2 hours before raising the temperature gradually to  $170^{\circ}\text{C}$ . The products were condensed out in a trap at liquid nitrogen temperatures and analysed by the vapour pressure technique described later. A blank run, in which an evacuated reaction vessel with no  $\text{TiO}_2$  film was heated to  $170^{\circ}\text{C}$ , demonstrated that no desorption from the glass surfaces occurred under these conditions.

When exposed to the atmosphere, films dehydrated at  $170^{\circ}\text{C}$  readsorbed water vapour extremely rapidly. Reaction vessels were accordingly fitted with a high vacuum tap and kept under high vacuum during transfer to the photoadsorption-measurement apparatus.

It is believed that such pretreatment ( $170^{\circ}\text{C}$  for 4-5 days) gave a satisfactory production of reproducibly hydrated  $\text{TiO}_2$  surfaces. Water recovered under the same conditions and following a photoreaction was, therefore, assumed to have originated from the photoreaction.

#### (11) Apparatus

The apparatus used in the measurement of photoadsorption reactions is illustrated in Fig. 6. Basically it consisted of a Bourdon gauge system capable of measuring small pressure changes in a thermostatted reaction space of constant volume. The movement of the Bourdon gauge pointer was followed visually through a telescope fitted with a graduated scale. The apparatus was built from soda-glass tubing. Apiezon L grease was used on all taps and joints. Gases were stored in bulbs attached to the apparatus. The total

pressure of gas in the reaction system was measured by either mercury monometers or the Bourdon gauge itself (for smaller pressures). A standing vacuum of  $10^{-5}$  mm. was attained by the use of a mercury diffusion pump, backed by a rotary oil pump. Traps at liquid nitrogen temperatures protected these pumps from the effects of condensable vapours.

The film in the reaction vessel D. was illuminated from the light source F, which was a voltage-stabilised 125 watt Osira mercury vapour lamp. The copper sulphate solution (100 g.  $\text{CuSO}_4 \cdot 5\text{H}_2\text{O}$  per litre) acted as an infra-red filter and as a focusing lens.

The reaction space and the jacket of the Bourdon gauge were maintained at a constant temperature by water circulated from a tank thermostatted to  $25^\circ\text{C} \pm 0.01^\circ\text{C}$ . by a Sunvic control and a chloroform-mercury switch. The water was pumped from this tank to a constant-head device and thereafter flowed in a divided stream round the gauge jacket and round the reaction vessel, before its return to the tank. Any small change in the temperature of the pumped water affected both sides of the gauge system and did not cause any appreciable movement of the pointer.

### (iii) Experimental procedures

The methods of calibration of the Bourdon gauge and the volume of the reaction space are fully described in reference (32). Reaction-space volumes were of the order 30 ml. and gauge sensitivities of the order 0.07 mm. per division.

The study of an adsorption process involved first of all introducing a known pressure of gas (or gases) into the reaction space and gauge jacket. This was then allowed to reach the temperature of the thermostatted system.

Pressure decreases due to any dark reaction were noted from the time of admittance of the gas. When the system had become stabilised, the time was noted and the film was illuminated by removing a shutter from the light source. Pressure decreases were taken at suitable time intervals and the results were tabulated as pressure decreases (scale divisions) with respect to time of illumination.

Normally gas pressures of about 30 mm. were employed for simple adsorption measurements. The total pressure decrease never exceeded 2 mm. The adsorptions were, therefore, studied under virtually constant pressure conditions; the rate of adsorption was shown to be insensitive to gas pressure alterations in this range.

Pressure decreases resulting from illumination of mixtures of gases were obtained in the same manner. In these instances the mixture was held in the dark at thermostat temperature for a period long enough to ensure adequate mixing of the gases.

(iv) Analysis of photo adsorption data

A plot of pressure decrease against time was obtained for each photo adsorption. Rates corresponding to various stages of uptake were obtained from such curves by graphical differentiation. Pressure decreases are quoted in scale divisions, time in minutes and rates in divs/minute. Appropriate plots of pressure decreases, time and derived rate values were used to evaluate the kinetics of the photo adsorptions.

(v) Recovery of products

The products of the surface reaction were sited on the solid, but in some cases also in the gas phase. The gas phase was removed for analysis by

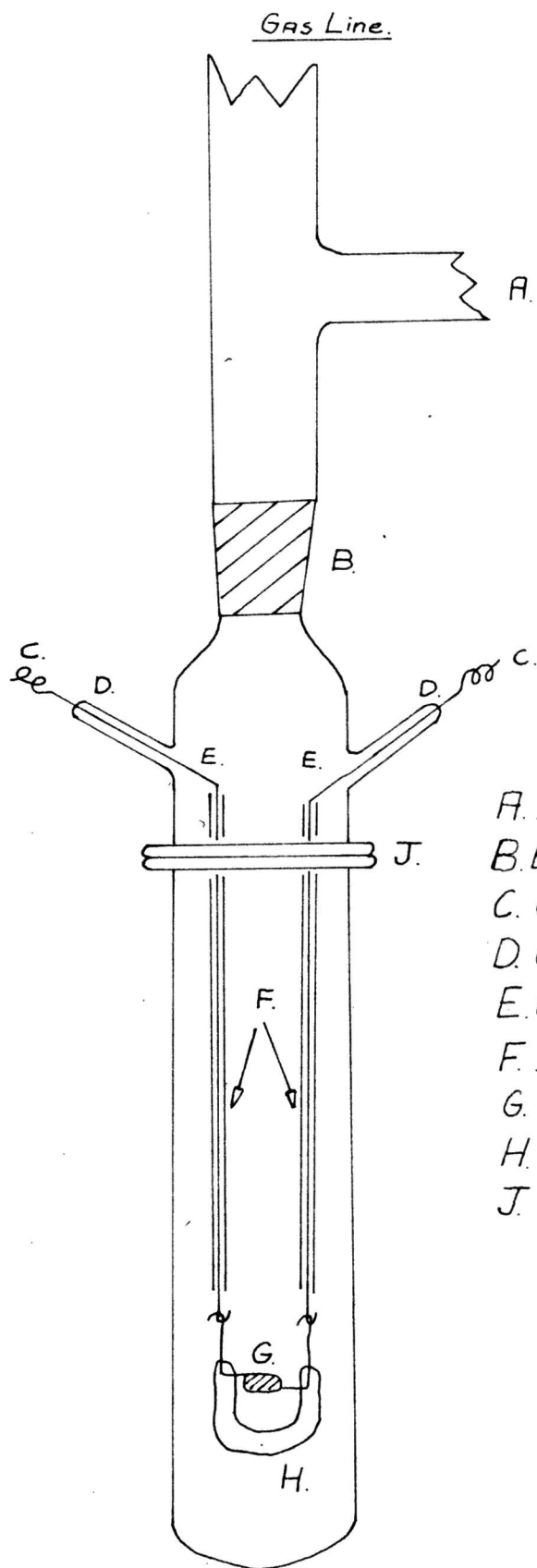


FIG 7.

CONDUCTIVITY CELL.

ACTUAL SIZE.

- A. IONISATION AND PIRANI GAUGES.
- B. B19 JOINT.
- C. COAXIAL CABLE.
- D. GLASS-METAL SEALS.
- E. PLATINUM LEADS.
- F. INSULATING SHEATHS.
- G.  $TiO_2$  BRIDGE.
- H. SILICA HORSESHOE.
- J. GROUND-GLASS FLANGE JOINT.



freezing out a known proportion of it. Other products were desorbed from the solid by evacuation in a small furnace at  $170^{\circ}\text{C}$  for periods ranging from one to twenty-four hours. The desorbed material was condensed out in a trap at liquid nitrogen temperatures; provision was made for its analysis at any stage of the evacuation. At no stage of this procedure was the film exposed to the atmosphere.

#### Conductivity measurements

These were carried out in the cell illustrated in Fig. 7. This cell was attached to a high vacuum apparatus built of pyrex and with Apiezon L grease on all taps and joints. Pressure down to  $10^{-5}$  mm. mercury were attained with an oil-diffusion pump, backed by a rotary oil pump. The hardness of the vacuum was measured by an ionisation or a Macleod gauge. Gas pressures were measured by either mercury manometers or a Pirani gauge. Bulbs for the storage of gases, and appropriate cold traps were attached to the apparatus.

The  $\text{TiO}_2$  sample was prepared in the form of a pellet which bridged the 1 mm. gap between two platinum contacts attached to the silica horse-shoe H (Fig. 7). The pellet was prepared from a suspension of finely ground  $\text{TiO}_2$  and distilled water. A drop of the suspension was placed between the contacts and evacuation removed the water to give a stable bridge of the dioxide. Evacuation ( $10^{-5}$  mm.) at  $20^{\circ}\text{C}$  for several hours gave a steady pellet resistance value of between  $10^{+10}$  and  $10^{+13}$  ohms. The pellet system was adopted after various trials involving deposition of thin films of  $\text{TiO}_2$  from a cloud of hydrolysed  $\text{TiCl}_4$ . The pellet system had the advantages of ease of preparation,

reproducibility of results and permanence of specimen. Added to this, the  $\text{TiO}_2$  sample used in preparation of the pellets was that used in the photo adsorption measurements. There were not likely to be any differences in the physical or chemical state of the dioxide used in the preparation, except for a higher water content of the pellets.

The resistance of the dioxide bridge was measured by an E.I.L. Vibron Electrometer and Resistance-measuring unit. Platinum-soda glass seals carried the electric circuit from the coaxial leads of the Electrometer to the platinum contacts of the cell (Fig. 7). The cell was screened by a copper sheath to which was attached the high potential lead of the Electrometer.

A voltage-stabilised 125 watt Osira mercury vapour lamp was used as a light source to produce a photoconductance in the pellet. Removal of infra-red radiation and some focusing of the illumination were provided for by a flask of copper sulphate solution (100 g.  $\text{CuSO}_4 \cdot 5\text{H}_2\text{O}$  per litre). No provision was made to thermostat the system; adequately steady resistance values were achieved without this. The Electrometer was attached to a recording galvanometer which could produce a direct plot of the current flowing through the film.

It was ascertained that the currents flowing through the film were directly proportional to the applied voltage in the range 0-480 volts. All measurements were made with an applied voltage of 120 volts, supplied from a dry battery.

The resistance changes resulting from illumination of the pellet or from admission of gas to the system were noted against time. The large resistance changes which occurred were conveniently plotted as the log of the resistance (ohms) against time (minutes).

### Analytical procedures

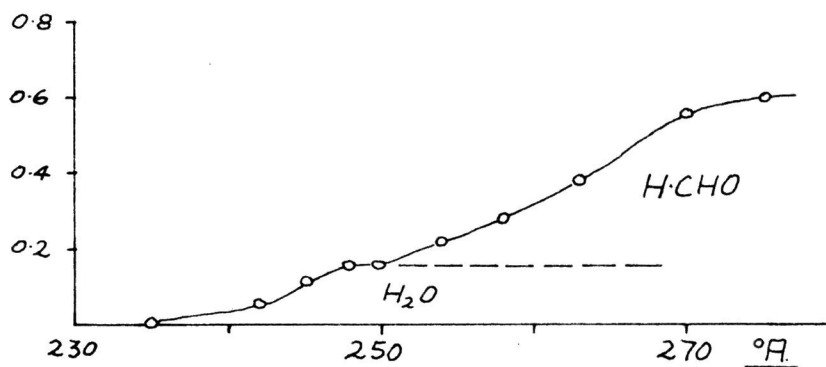
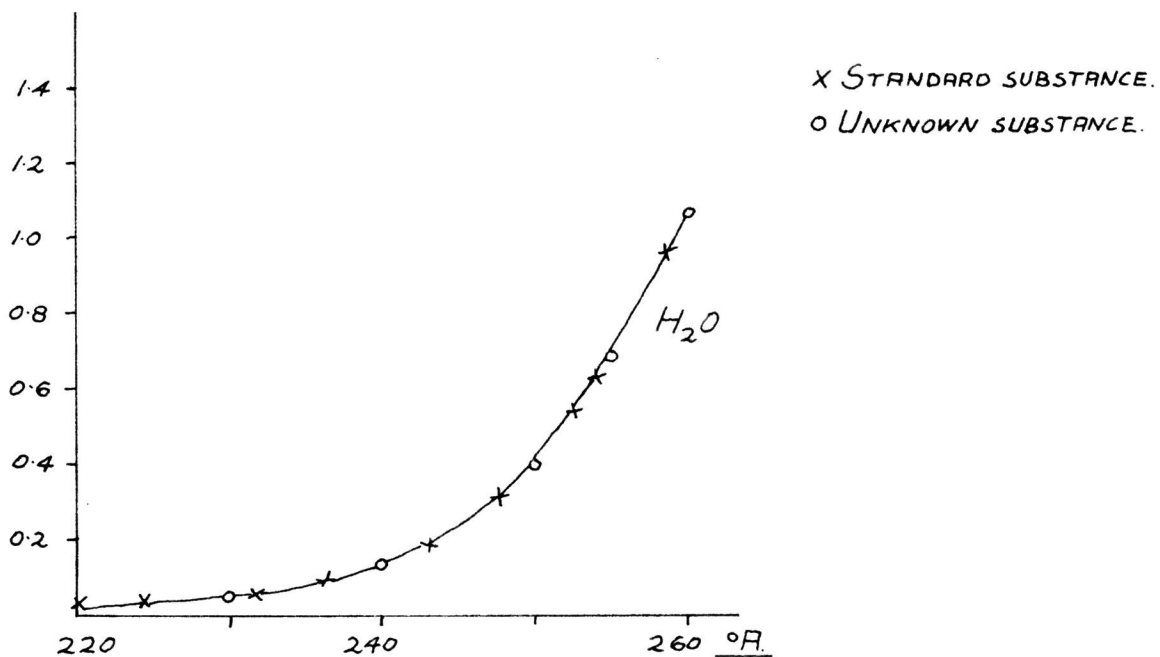
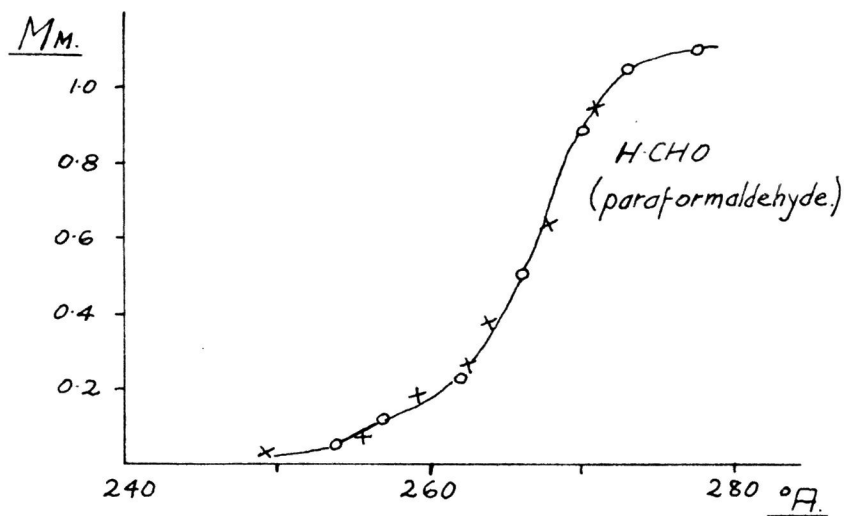
On the completion of a photoadsorption experiment the reaction vessel was transferred to a subsidiary soda glass vacuum system, fitted with a non-thermostatted Bourdon gauge. Any remaining gas phase was condensed into one of several cold traps and kept for analysis. The reaction vessel could then be evacuated through a cold trap (liquid  $N_2$ ) and its temperature gradually raised to  $1700^\circ C$  in an electric furnace. The film was then isolated under  $10^{-5}$  mm. pressure and in contact with the cold trap until no further material was desorbed. This normally took several hours.

The material obtained in this way consisted of oxygen, hydrocarbons, carbon dioxide, water vapour and paraformaldehyde. These, in general, were easily separable into two fractions by distillation; each fraction was then analysed independently by taking measurements of vapour pressure against temperature.

The Bourdon gauge was calibrated to give pressures in m.m. of mercury. At temperatures below  $-120^\circ C$  the temperature of the sample was obtained from a calibrated thermocouple taped to the cold trap. The cooled trap was enclosed by a Dewar flask which had been flushed out with liquid nitrogen. Simultaneous measurements of pressure and temperature were taken while the temperature rose slowly and spontaneously from  $-190^\circ C$ . Above  $-120^\circ C$  the temperature of the sample was controlled by a Dewar flask full of low boiling petroleum ether, cooled with liquid air. The temperature was raised in a controlled fashion by passing dry air through a copper coil immersed in the ether; the coil also acted as a stirrer. The temperature and vapour pressure were allowed to equilibrate for 10 minutes after each increase in temperature.

FIG 8.

TYPICAL VAPOR PRESSURE AGAINST TEMPERATURE CURVES.



Temperatures were measured by pentane thermometer.

The results were plotted to give curves of the types shown in figs. 8 and 8a. Each step in the curves was compared with literature vapour pressure data; this tentatively identified the species responsible. Experimental curves with standard substances confirmed the identification. The volumes of appropriate sections of the apparatus were known to the nearest 0.1 ml. and the number of moles of each constituent could therefore be obtained from the ideal gas equation. The method was sensitive enough to detect  $0.1 \mu$  moles of any constituent.

The qualitative presence of each constituent was confirmed finally by both infra red and gas chromatographic methods. Any species which did not condense at liquid  $N_2$  temperatures was assumed to be oxygen.

The presence of formaldehyde on the dioxide following illumination was confirmed in all instances by spot-testing a sample of the solid with carbazole in concentrated sulphuric acid (Feigl, Spot Tests: Organic applications, page 241). Appropriate blank tests demonstrated that formaldehyde had resulted from a photoreaction on the solid.

### Chemicals

#### Oxygen

B.O.C. cylinder oxygen was passed over  $P_2O_5$  into the vacuum system and distilled at liquid  $N_2$  temperatures.

#### Ethylene

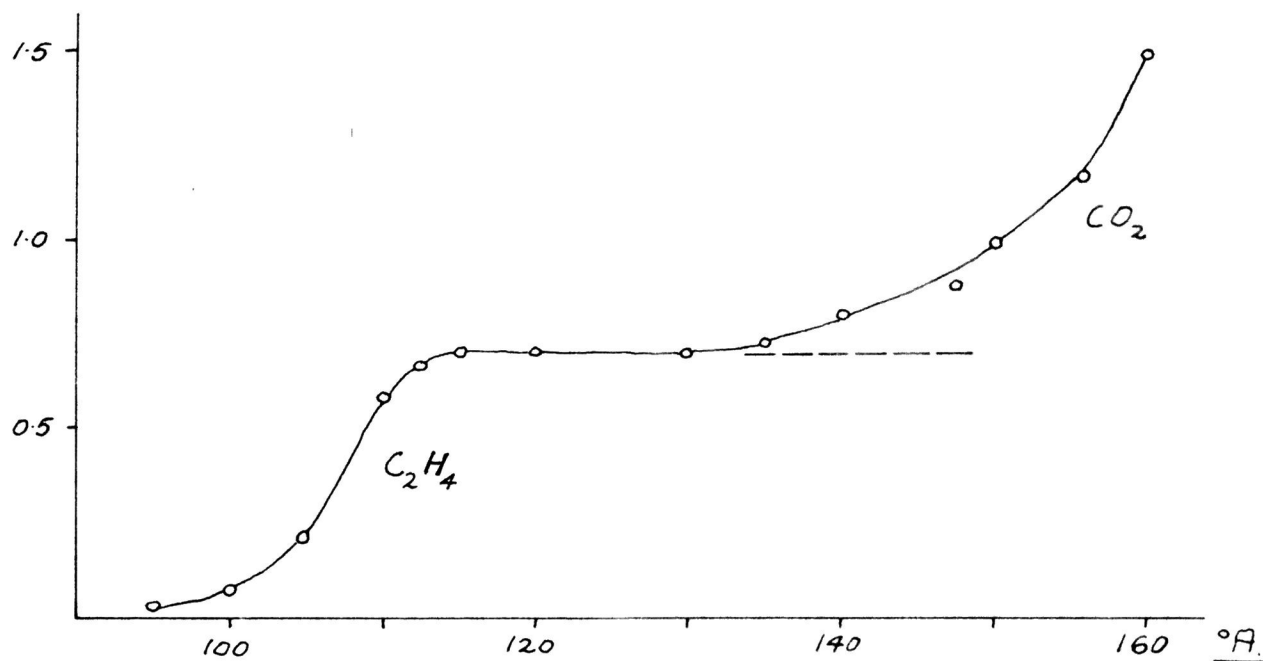
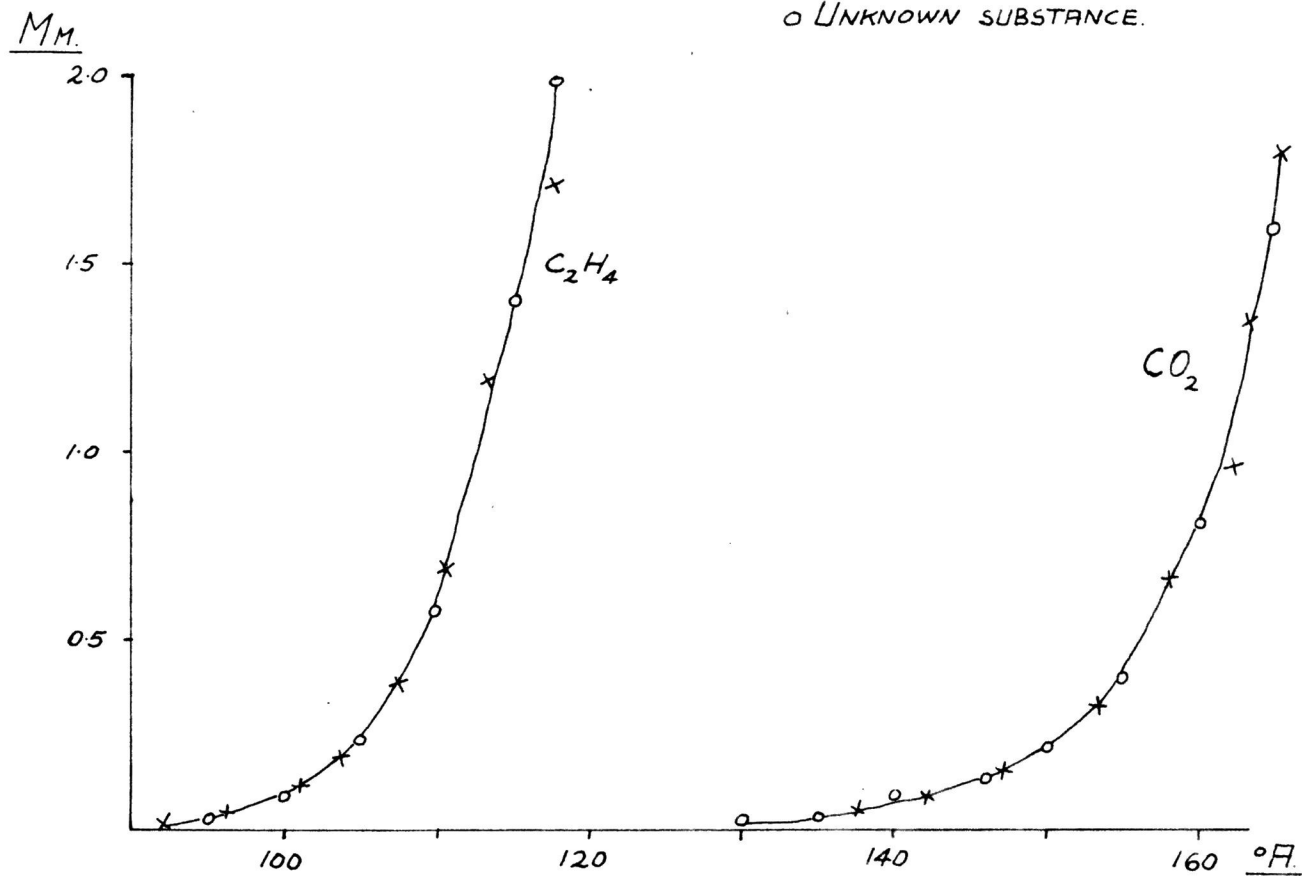
Cylinder ethylene was passed over  $P_2O_5$  and fractionally distilled at liquid  $N_2$  temperatures.

FIG. 8A.

TYPICAL VAPOR PRESSURE AGAINST TEMPERATURE CURVES.

x STANDARD SUBSTANCE.

o UNKNOWN SUBSTANCE.



Propylene

Prepared by dehydration of ~~sec-butyl~~<sup>propyl</sup> alcohol using  $P_2O_5$  as dehydrating agent. It was purified by repeated distillation at  $-160^\circ C$  and then at  $-80^\circ C$ .

Water was thoroughly degassed in the vacuum system by repeated freezing at  $-80^\circ C$  and distillation.

B.D.H. ethylene oxide, propylene oxide and benzene were dehydrated over  $P_2O_5$  in the vacuum line. Dissolved gases were removed by suitable distillations.

Paraformaldehyde was prepared by evaporation of 10% formalin.

Pure formaldehyde was prepared from the polymer by heat treatment in vacuo.

Where appropriate, gas chromatographic methods were used to establish the purity of reagents.

Titanium dioxide The single sample of  $TiO_2$  used in the investigations was prepared from  $TiCl_4$  by the method of Weiser and Mulligan (58). 30 g. of  $TiCl_4$  were added slowly to a 2.7 molar NaCl solution (500 ml.) and the mixture was refluxed for 2 hours. The liberated HCl was neutralised with solid NaOH. The supernatant liquid was decanted off. The titania gel was washed repeatedly with distilled water and centrifuged down (but with difficulty). The oxide so obtained was dried in an oven at  $170^\circ C$  for 12 hours and then at  $100^\circ C$  over  $P_2O_5$  for 30 hours. The final product was a white powder which was stored in the dark.

A B.E.T. surface area determination, using argon as adsorbate, gave a value of  $100\text{ m}^2$  per g. for a sample prepared in this way and then evacuated for 5 days at  $170^\circ C$ . Using a different method of surface area determination

(adsorption of dyes from solution) (59) (60), Gregory (61) has confirmed that  $\text{TiO}_2$  samples prepared in the manner described above had surface areas of the order  $100 \text{ m}^2$  per g.



EXPERIMENTAL.

RESULTS

$\Delta b(\text{divs})$

Fig. 9

$O_2$  PHOTOGRAPH ON UNTREATED  $TiO_2$

x DATA OF TABLE 1.

o DATA OF TABLE 2.

23.7 at 7220 mins.

27.7 at 7540 mins.

t (mins.)

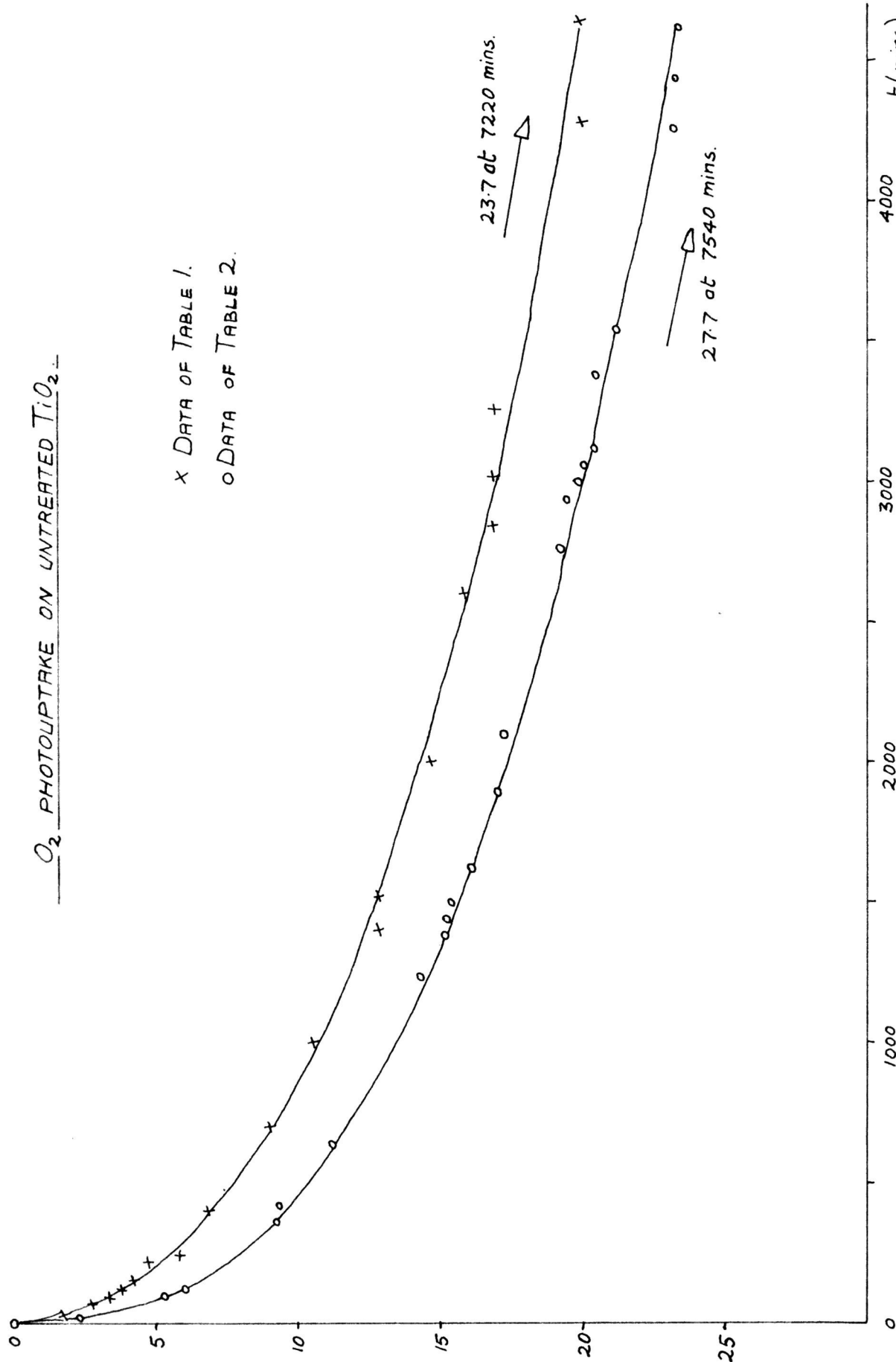
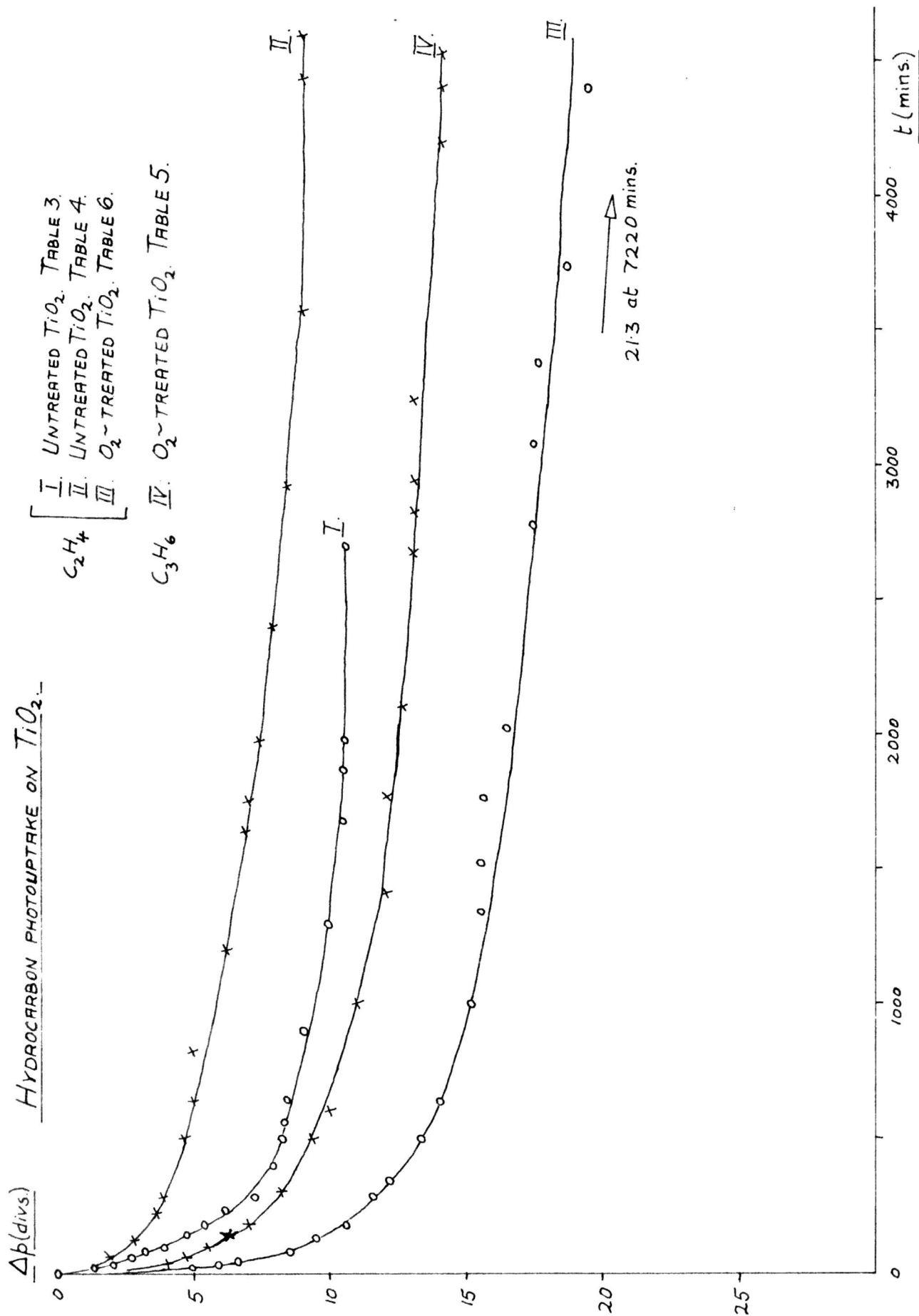


FIG. 10.

HYDROCARBON PHOTOUP TAKE ON  $TiO_2$ .



## EXPERIMENTAL RESULTS

### The photoadsorptions of oxygen, ethylene and propylene on untreated TiO<sub>2</sub>.

The term "untreated" signifies that the photoadsorption was not preceded by a photoadsorption of another gas.

Photoadsorption data for oxygen and for ethylene on untreated TiO<sub>2</sub> films at 25°C are presented in Tables 1-4 and Figs. 9 and 10. These illustrate the degree of reproducibility which was encountered. Gas pressures of 30-40 mm. were employed. There was no measurable adsorption of either gas in the dark after admission to the reaction system, although the possibility of a very rapid small dark adsorption during admission of the gas cannot be discounted. No dark or photoadsorption of propylene was observed under these conditions.

Rate data derived from the photoadsorption measurements were used to evaluate the kinetics of the process. The ethylene photoadsorption data of Table 3 are used to illustrate the adopted procedure. In the initial stages a plot of  $\frac{1}{R}$  (where R = rate in divs/minute) against q was linear. (q =  $\Delta p$  in divisions); this is illustrated in Fig. 11. This means that:

$$\frac{1}{R} = Kq + C$$

$$\therefore \frac{dt}{dq} = Kq + C$$

$$\therefore t = \frac{K}{2} q^2 + Cq + L$$

and if q = 0 when t = 0, then L = 0

$$\therefore t = \frac{K}{2} q^2 + Cq$$

FIG. 11.

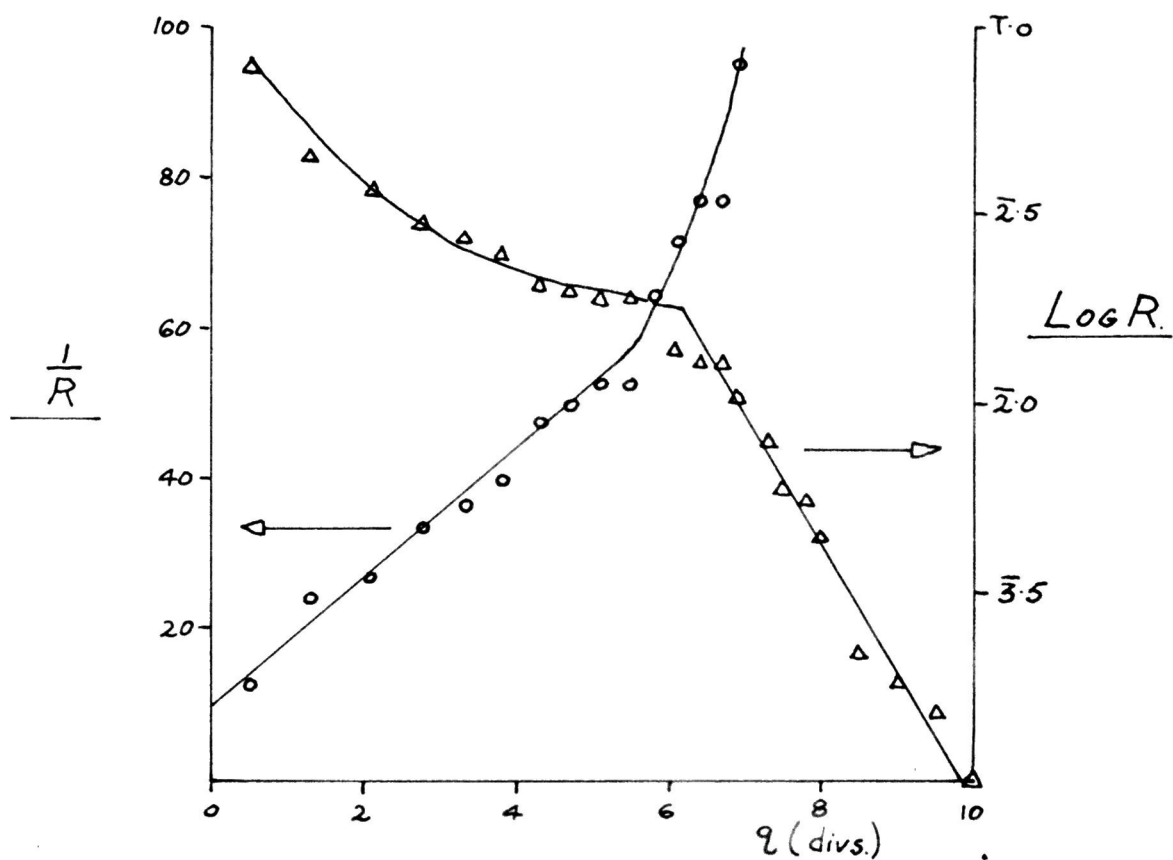
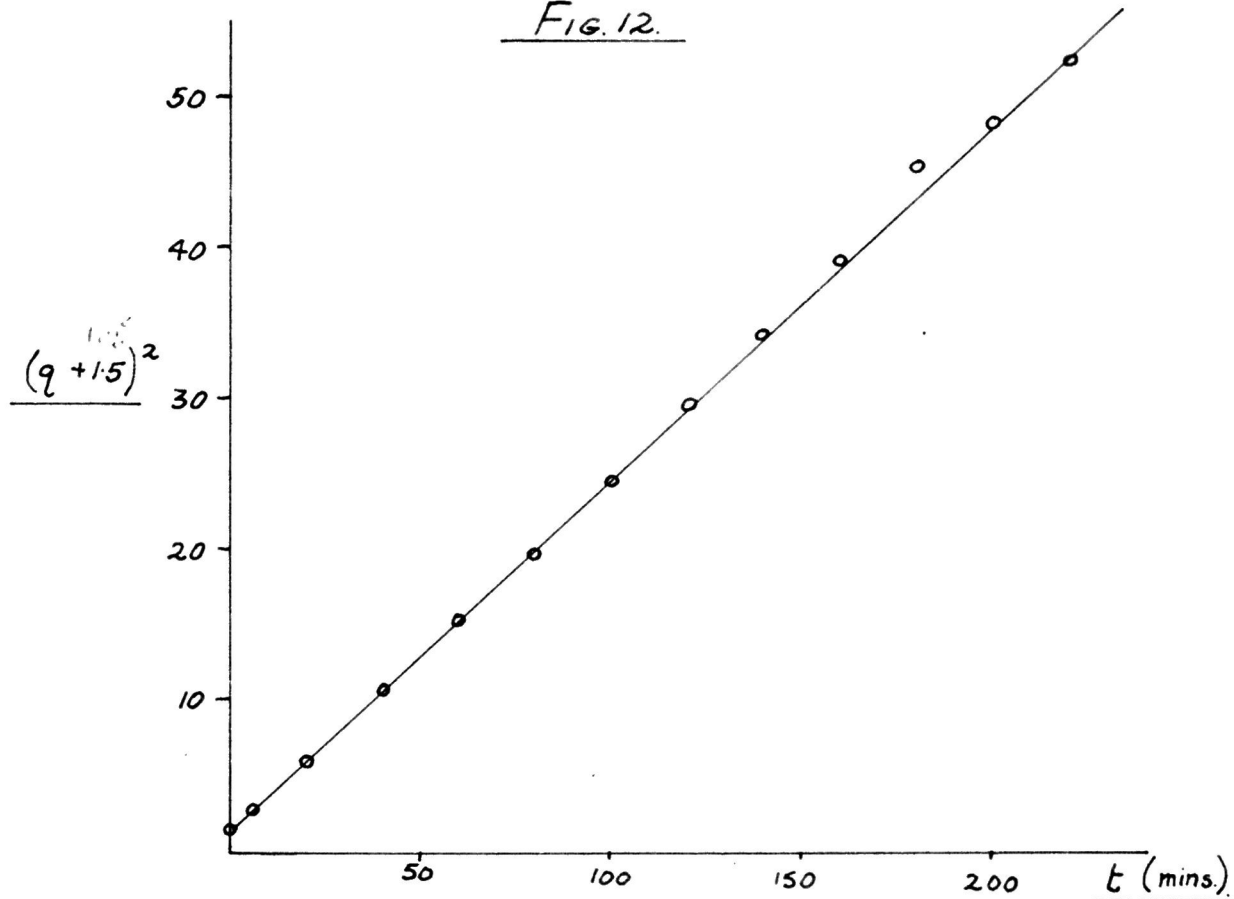


FIG. 12.



$$\begin{aligned} \text{Now } \frac{K}{2} (q + q_0)^2 &= \frac{K}{2} q^2 + K q q_0 + \frac{K}{2} q_0^2 & q_0 &= \text{constant} \\ &= \frac{K}{2} q^2 + K q q_0^2 + \text{constant} \end{aligned}$$

$$\therefore t = \frac{K}{2} (q + q_0)^2 - \text{constant} \quad \text{where } q_0 = \frac{C}{K}$$

$$\therefore t = \frac{K}{2} (q + q_0)^2 - \frac{K}{2} q_0^2$$

$$\therefore (q + q_0)^2 = \frac{2}{K} t + q_0^2$$

The values of  $k$  and  $c$  (and hence of  $q_0$ ) are given by the gradient and intercept of the  $\frac{1}{R}$  against  $q$  plot. The  $q_0$  value in this case is 1.15 and the initial stages of the photoadsorption can be represented by the expression:

$$(q + 1.15)^2 = 0.23 t + 1.3$$

A plot of  $(q + 1.15)^2$  against  $t$  is linear and is illustrated in Fig.12.

In the later stages of the photoadsorption a plot of  $\log (R)$  against  $q$  was linear (Fig.11) showing that the process was then described by the Elovich equation,

$$\frac{dq}{dt} = ae^{-\alpha q} \quad (\text{see page 17})$$

All the oxygen and ethylene photoadsorptions could be described by a similar type of initially parabolic and finally Elovich kinetics (cf. page 11). The integrated form of the Elovich equation was used to obtain a more precise formulation of the later stages of the uptake. A discussion of this

procedure is reserved for a later stage (page 70 et seq.)

The total pressure decrease recorded in the oxygen photoadsorption experiments will vary with time but the rate of photo-uptake after several thousand minutes of illumination was effectively zero. At this stage the oxygen photo-uptake corresponded to 40-50  $\mu$  moles  $O_2$  per g. of  $TiO_2$ . This was taken as a rough estimate of the photoadsorptive capacity of the dioxide for oxygen. The corresponding figure in the ethylene case was about 20  $\mu$  moles per g.  $TiO_2$ .

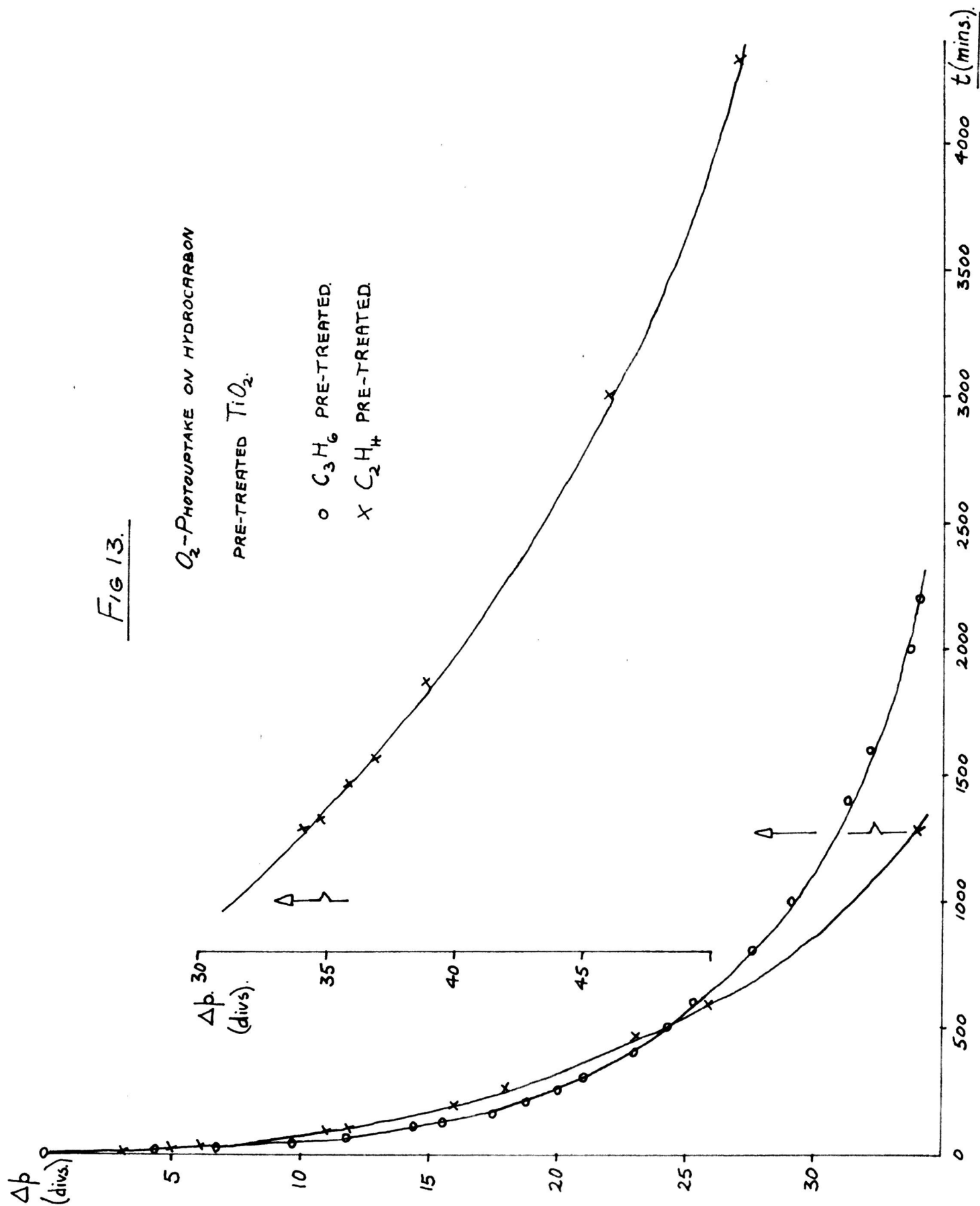
Fig 13.

O<sub>2</sub>-PHOTOGRAPH ON HYDROCARBON

PRE-TREATED TiO<sub>2</sub>.

○ C<sub>3</sub>H<sub>6</sub> PRE-TREATED.

× C<sub>2</sub>H<sub>4</sub> PRE-TREATED.





Photoadsorption on pre-treated  $\text{TiO}_2$

The term "pre-treated" signifies that the film had been pre-treated by a prior photoadsorption of either oxygen or hydrocarbon. It was found that the rate and extent of a photoadsorption were altered if it was preceded by a photoadsorption of another gas. Again gas pressures of 30-40 mm. were employed.

Whereas no photo-uptake of propylene was observed on a fresh film, the hydrocarbon was photoadsorbed on a film pre-treated with oxygen. Oxygen pre-treatment increased the rate and extent of ethylene photoadsorption. The corresponding rates of uptake were generally greater for ethylene than for propylene. Experimentally, the procedure involved photoadsorption of a known amount of oxygen followed by removal of the oxygen gas phase before the hydrocarbon photoadsorption. It was established, however, that an increased hydrocarbon photoadsorption occurred if the oxygen pre-treated film was illuminated in vacuo or heated to  $170^\circ\text{C}$  in vacuo for 24 hours prior to the hydrocarbon photoadsorption. Tables 5 and 6 present typical data obtained for photoadsorptions on oxygen pre-treated  $\text{TiO}_2$ ; pressure decrease against time curves for these data are given in Fig.10.

Conversely, pre-photoadsorption of either hydrocarbon increased both the rate and extent of oxygen photoadsorption. The results quoted were again selected as being typical of a reproducible set of experiments. These results are presented in Tables 7 and 8 and Fig. 13.

A full analysis of the kinetics of these photoadsorptions will again be postponed until the discussion. But it can be stated here that the kinetics were similar to those on films which had not been pre-treated. Parabolic

FIG 14.

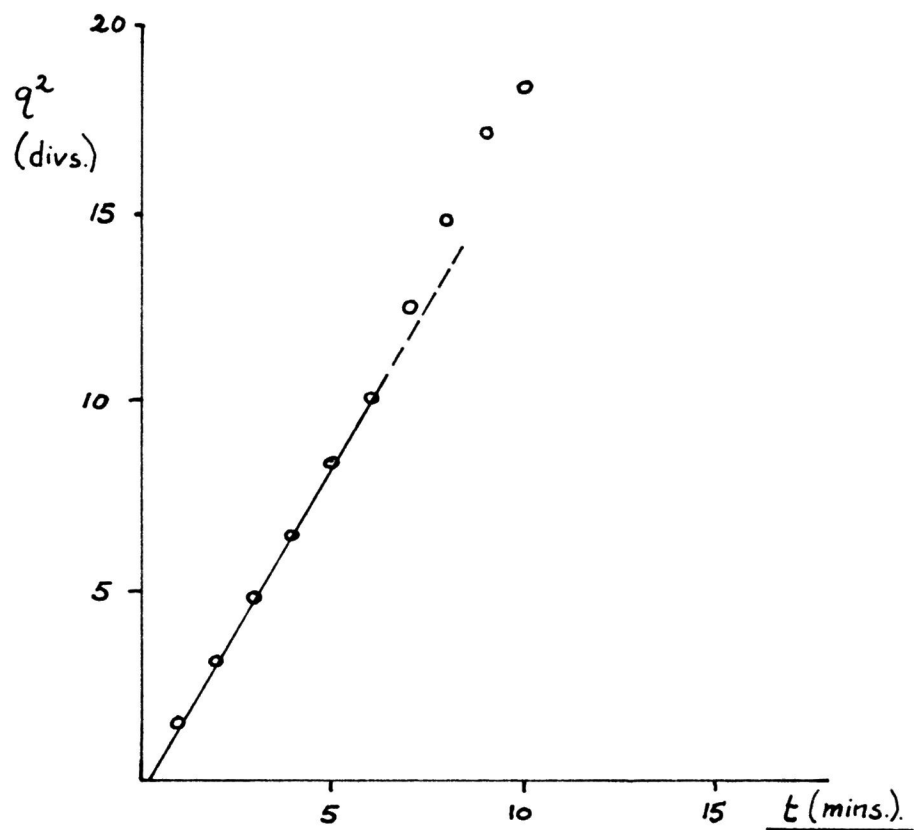
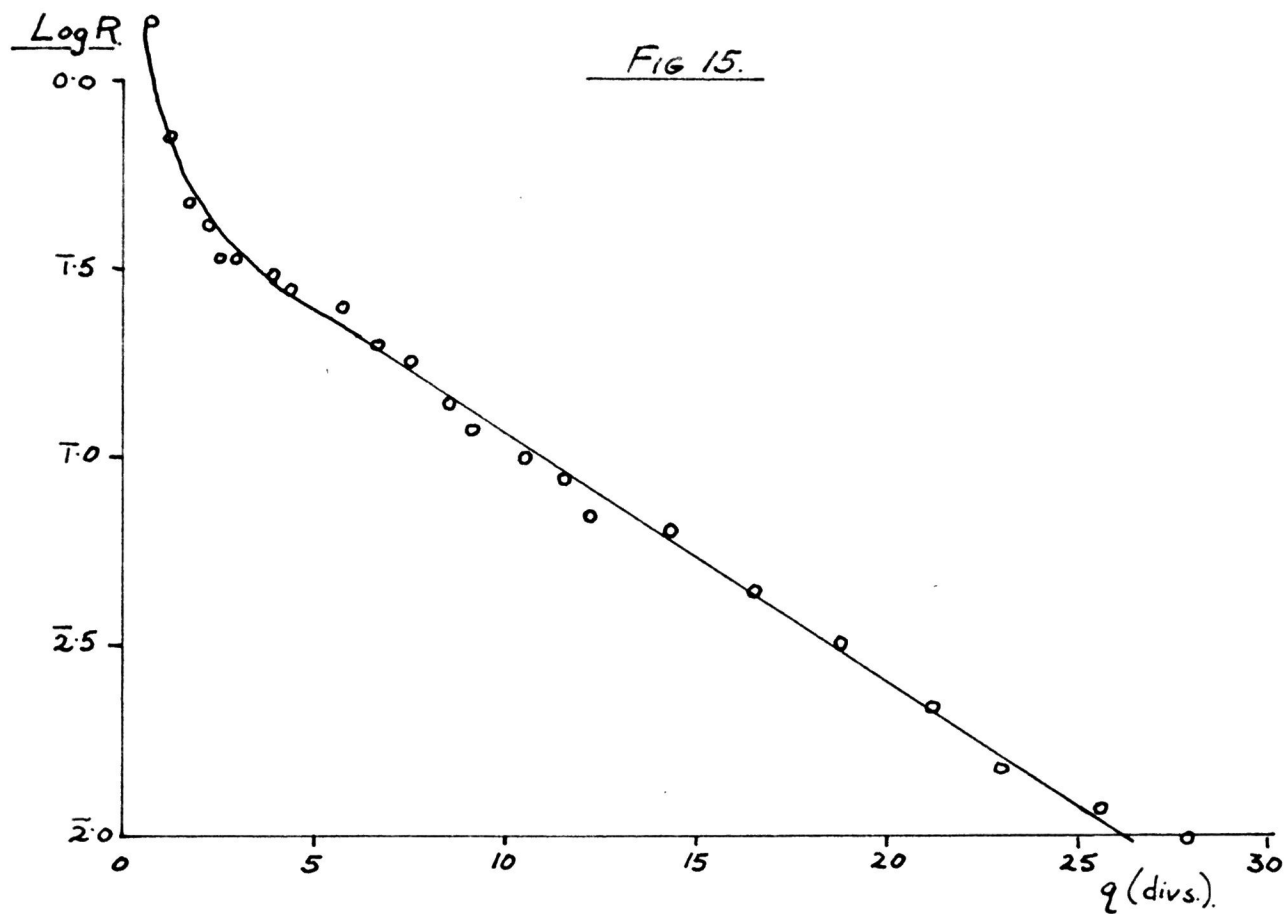


FIG 15.



kinetics were again followed in the initial stages and the later stages were again described by the Elovich rate law. The oxygen photoadsorption of Table 7 is taken as an example. This process was first described by the parabolic expression :

$$q^2 = 1.75 t - 0.4$$

and a plot of  $q^2$  against  $t$  is presented in Fig.14. A  $q_0$  value was normally involved in the parabolic stages of the hydrocarbon photoadsorptions (cf. pages 31 and 72 ). The eventual linearity of a  $\log R$  against  $q$  plot shows that the oxygen photoadsorption of Table 7 eventually obeyed the Elovich rate law (Fig.15). Derived rate values are tabulated in Table 7a.

Alternate photoadsorption of oxygen and hydrocarbon could be carried out without any apparent exhaustion of the  $TiO_2$ , when the film was briefly evacuated at room temperature between each photoadsorption. It is to be noted that a saturation effect was encountered later when  $170^\circ C$  evacuation was carried out between oxygen and propylene photoadsorptions (page 44 ).

### Reversibility of the photo-uptakes

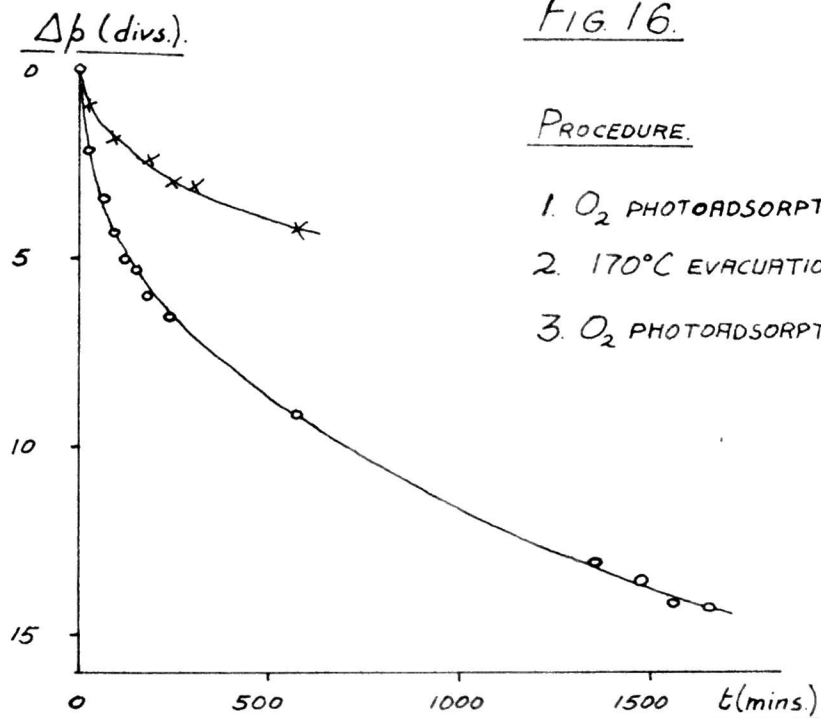
The reversibility of the photo-uptakes was studied by the evacuation procedure outlined on page 23. The evacuated ( $10^{-5}$  m.m.) film, with its photoadsorbed species, was isolated over a cold trap (liquid  $N_2$ ) for periods up to 24 hours. The reaction vessel was placed in a furnace and its temperature could be varied between  $20^\circ\text{C}$  and  $c.300^\circ\text{C}$ .

#### (1) Photo-uptake of oxygen.

Photoadsorbed  $O_2$  was not recovered as such by evacuation at temperatures up to  $170^\circ\text{C}$ . In this sense the photoadsorption of oxygen was regarded as irreversible. In addition, no pressure ~~d~~ecrease was observed in the in/ Bourdon system when films which had photoadsorbed  $O_2$  were illuminated in an initial vacuum of  $10^{-5}$  mm. at  $25^\circ\text{C}$ . If photo~~a~~dsorption was occurring it must, de/ therefore, have corresponded to a pressure increase of less than  $10^{-2}$  mm.

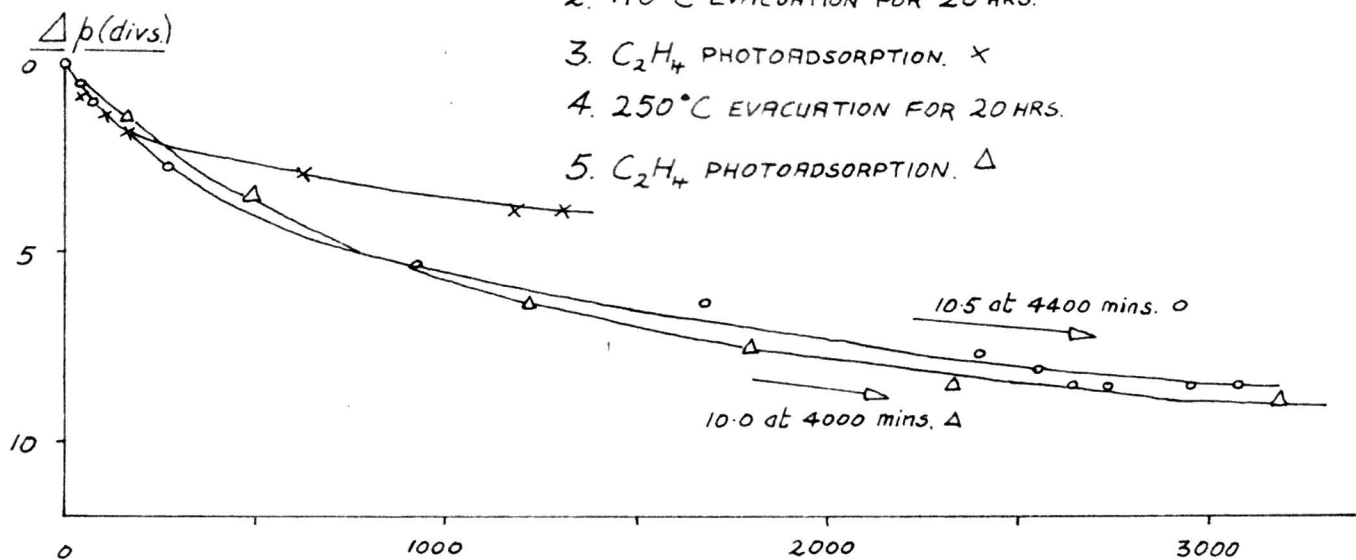
Pre-treatment of the sample with ethylene or propylene did not affect the above results, but it did affect the nature of the desorbed products. Evacuation ( $170^\circ\text{C}$ ) of a non-pretreated film after photoadsorption of  $O_2$  resulted in the recovery of small amounts of  $CO_2$  and water vapour. The relation between amount of  $O_2$  photoadsorbed and the amount of  $CO_2$  and water recovered was not established. But evacuation ( $170^\circ\text{C}$ ) of a film on which  $O_2$  had been photoadsorbed after pretreatment with either of the hydrocarbons produced  $CO_2$ , water vapour and formaldehyde. The latter was obtained as paraformaldehyde, with a characteristic vapour pressure against temperature curve (Fig.8). The absolute amounts of each product were small ( $2-3 \mu$  moles). No attempt was made at this juncture to determine the reactions quantitatively.

FIG 16.



PROCEDURE.

1.  $C_2H_4$  PHOTOADSORPTION.  $\circ$
2.  $170^\circ C$  EVACUATION FOR 20 HRS.
3.  $C_2H_4$  PHOTOADSORPTION.  $\times$
4.  $250^\circ C$  EVACUATION FOR 20 HRS.
5.  $C_2H_4$  PHOTOADSORPTION.  $\Delta$



(ii) Photo-uptake of ethylene.

No ethylene or other product was recovered by evacuation ( $10^{-5}$  mm) at temperatures up to  $250^{\circ}\text{C}$  after a photoadsorption of ethylene at  $25^{\circ}\text{C}$ . Pre-treatment of the film with oxygen did not affect this result. Ethylene photoadsorption was thus assumed to be irreversible under these conditions. Again, no photoadsorption was detectable on illuminating the film in vacuo in the Bourdon gauge system. de/

(iii) Photo-uptake of propylene.

As reported on page 33, photoadsorption of propylene occurred only on films which had been pre-treated with oxygen. Evacuation ( $170^{\circ}\text{C}$ ) resulted in the recovery of a small amount of propylene,  $\text{CO}_2$ , water vapour and formaldehyde. The photoadsorption of propylene thus appeared to be partly reversed by evacuation at  $170^{\circ}\text{C}$ . It was evident that large variations occurred in the small amounts of the other three desorbed products.

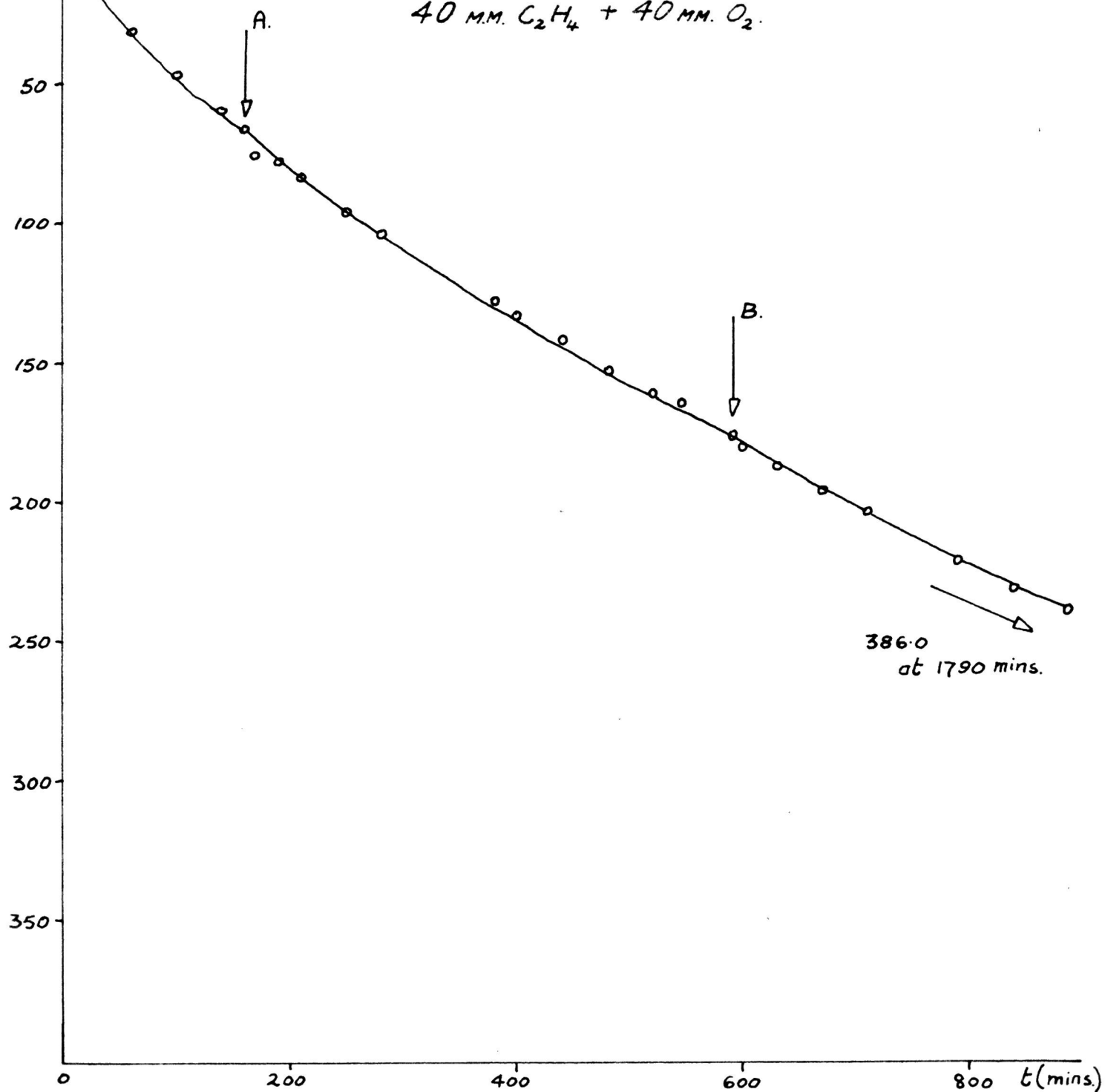
It was stated above that  $\text{O}_2$  and ethylene photoadsorption on non-pretreated films appeared to be irreversible in that photoadsorbed gas could not be recovered on evacuation at  $170^{\circ}\text{C}$ . Nevertheless, this thermal evacuation did renew the capacity of the film for further photoadsorption of the same gas. The second photo-uptake was always less than the photo-uptake which preceded the evacuation. No correlation was found between extent of thermal evacuation and increased capacity for photoadsorption, but the effect is illustrated by Fig.16.

Pre-treatment of a fresh film at  $250^{\circ}\text{C}$  instead of  $170^{\circ}\text{C}$  did not result in an increased capacity for ethylene photoadsorption.

$\Delta p$  (divs.)

FIG 17.

40 mm.  $C_2H_4$  + 40 mm.  $O_2$ .



Photoreaction of ethylene-oxygen mixtures

No pressure changes were observed in an ethylene-oxygen mixture over  $\text{TiO}_2$  films at  $25^\circ\text{C}$  in the absence of illumination. Large pressure decreases were observed when the system was illuminated. The rate of the pressure change decreased with time during the illumination of any one mixture. Nevertheless, very large pressure decreases (100 mm or more) could be followed without any apparent saturation of the oxide. After prolonged illumination of a mixture, carbon dioxide was detectable in the gas phase.

No pressure decreases were observed in the absence of  $\text{TiO}_2$ . In one experiment a mixture of 36 mm. ethylene and 8 mm.  $\text{O}_2$  was illuminated at  $25^\circ\text{C}$  in a reaction vessel which contained no  $\text{TiO}_2$  film. No pressure change was observed during 300 mins. of illumination. Analysis of the gas phase (vapor pressure and infra red) showed that its initial composition was unchanged. The pressure decreases can, therefore, be attributed to a photoreaction involving  $\text{TiO}_2$ .

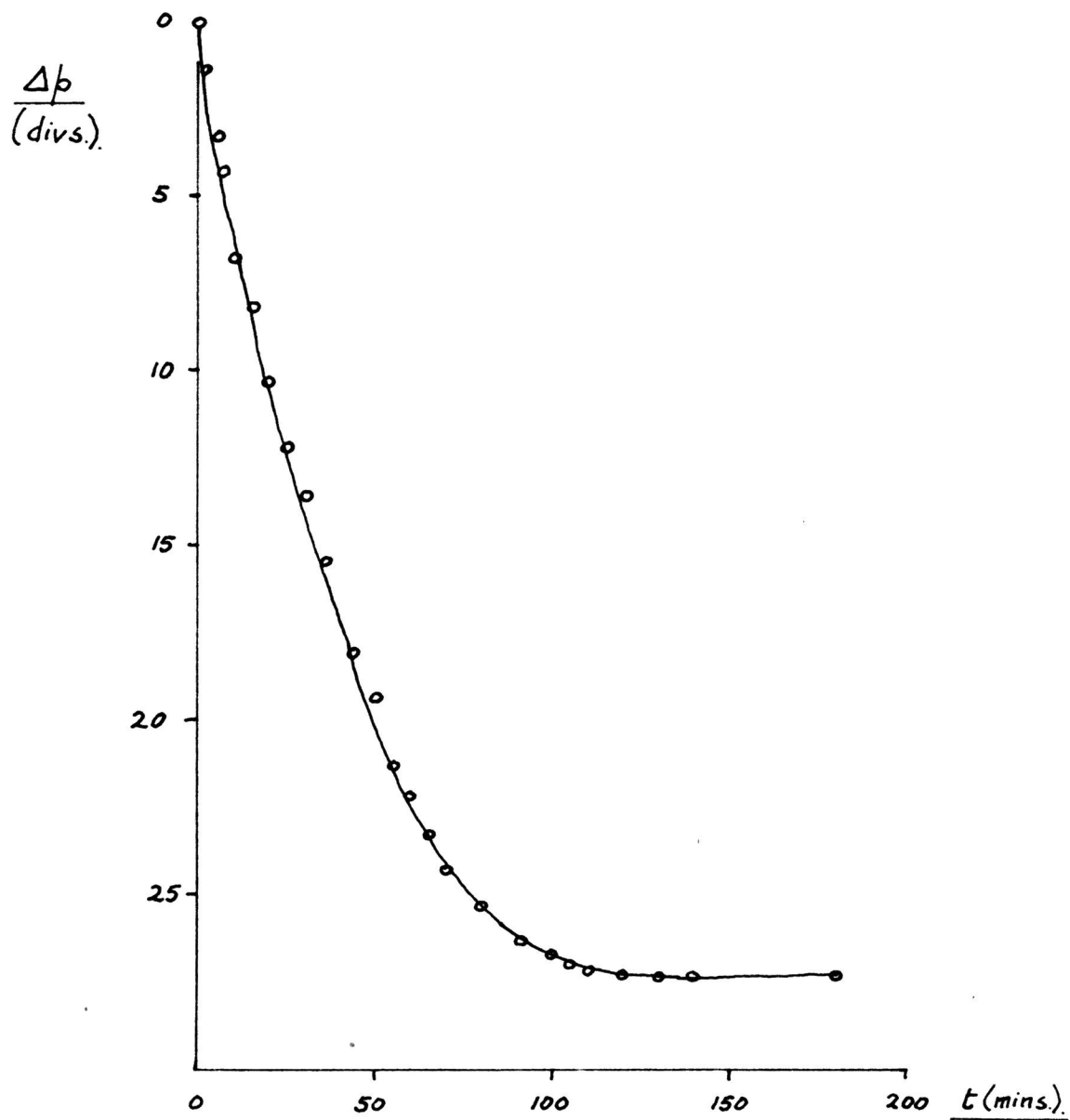
The experimental procedure adopted initially in the study of the ethylene-oxygen- $\text{TiO}_2$  system was as follows. A known pressure of one gaseous constituent was brought in contact with a  $\text{TiO}_2$  film in the reaction system. The second gaseous constituent was added to give a known total pressure. Any dark reaction was noted. After standing in the dark for periods up to 2 hours, the system was illuminated. Values of pressure decrease (divs) were taken against time. A sample of the gas phase present after illumination was analysed qualitatively by vapour pressure and infra red methods.

Data obtained from a mixture of 40 mm. ethylene and 40 m.m. oxygen are presented in Table 9 and Fig.17. A total pressure decrease of <sup>386</sup>~~193~~ divs (<sup>30</sup>~~15~~ mm.)



FIG. 18.

8.6 mm.  $C_2H_4$  + 1.65 mm. (21.3 divs.)  $O_2$ .



occurred over 1790 mins. of illumination. The rate of the pressure decrease fell from  $\overset{0.96}{0.48}$  divs/min. at  $t = 1$  min. to  $\overset{0.14}{0.07}$  divs/min. at  $t = 1790$  mins. Points A, B, C, D and E represent overnight interruptions in illumination without removal of the gas phase. It is evident that a slight increase in rate occurred on re-illumination, after these periods in the dark. Small pressure decreases (2 divs) occurred during these dark periods; these are not included in the pressure decreases of Table 9 and Fig.17. A qualitative analysis of the gas phase showed the presence of ethylene, carbon dioxide and a gas (presumed  $O_2$ ) which did not condense at liquid  $N_2$  temperatures.

It seemed probable from these results that  $TiO_2$  acted as a catalyst in a photo-oxidation of ethylene. Experiments were, therefore, conducted to ascertain whether the amounts of ethylene and oxygen involved in the pressure decreases bore a simple relation to each other.

#### Ratio of ethylene-oxygen in the photoreaction.

A photoadsorption of ethylene at 39 mm. pressure was carried out for 4300 mins. The rate of photoadsorption was then virtually zero and 1.4  $\mu$  moles of ethylene had been adsorbed. Illumination was discontinued. No further photoadsorption was observed when the ethylene pressure was increased to 80 mm. and then decreased to 8.6 mm. A small "injection" of 21.3 divs (1.73 mm.) oxygen was then added in the dark to 8.6 mm. ethylene. No reaction was observed in the dark, but a rapid pressure decrease occurred on illumination; this pressure change was complete after 180 minutes, when the pressure had fallen by 27.3 divs. The ethylene was treated in a similar manner with six further "injections" of oxygen. Pressure decreases against time for the first injection are plotted in Fig.18. The amount of oxygen and the total

pressure decrease for each addition are summarised in Table 10.

Table 10

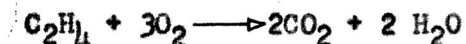
Gauge sensitivity 0.0776 mm./div.

Volume of reaction system = 27.5 ml.

<u>Amount of O<sub>2</sub> added. (divs.)</u>	<u>Total pressure decrease. (divs.)</u>
21.3	27.3
24.6	33.7
10.7	13.7
4.5	6.9
20.3	28.4
28.0	38.0
<u>27.1</u>	<u>31.9</u>
136.5 divs. = 15.7 $\mu$ moles.	179.9 divs. = 20.6 $\mu$ moles.

The gas phase which remained was analysed in the subsidiary Bourdon system. It consisted of 7.2  $\mu$  moles ethylene and 0.8  $\mu$  moles CO<sub>2</sub>.

Thus at the start of the experiment the surface was saturated with respect to ethylene and the reactants were present in the gas phase as 12.7  $\mu$  moles ethylene and 15.7  $\mu$  moles O<sub>2</sub>. At the completion of the experiment the gas phase consisted of 7.2  $\mu$  moles ethylene and 0.8  $\mu$  moles CO<sub>2</sub> with no residual oxygen; the surface was again presumably saturated with respect to ethylene. On this basis, 1 mole ethylene reacts with  $\frac{15.7}{12.7-7.2} = 2.9$  mole O<sub>2</sub>. This result is in approximate agreement with the oxidation equation :



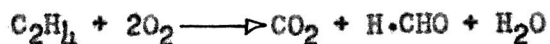
if it is assumed that CO<sub>2</sub> and H<sub>2</sub>O were largely retained by the surface. This

TABLE II

Reaction between  $O_2$  and  $C_2H_4$  over illuminated  $TiO_2$ 

Film	Initial pressures (m.m)		Reactants used up ( $\mu$ moles)		Products ( $\mu$ moles)			
	$O_2$	$C_2H_4$	$O_2$	$C_2H_4$	$CO_2$	H. CHO	$H_2O$	$CO_2/C_2H_4$
1	20	3.5	8.3	1.7	3.3	1.4	1.1	1.95
2	20	4.0	9.4	2.2	4.5	1.5	1.4	2.05
3	20	3.5	5.3	1.4	2.9	1.0	1.0	2.10
4	20	3.0	10.7	2.5	4.8	1.6	1.2	1.90
Average = 4.3					Average = 2.0			

would imply that no  $O_2$  was additionally photoadsorbed as such on the  $TiO_2$  surface. If  $O_2$  is photoadsorbed in this way, then incomplete oxidation is a possibility. The recovery of formaldehyde in previous experiments (page 35) suggests that such an incomplete oxidation might involve :



Having established that a definite photoreaction appeared to be occurring on the surface of the solid, an attempt was made to investigate the total products of the reaction.

#### Products of the photoreaction.

A mixture of ethylene and oxygen at known partial pressures was illuminated over a  $TiO_2$  film until a reasonably large pressure decrease (5-6 mm.) had occurred. The photoreaction was discontinued and the resultant gas phase was analysed quantitatively (vapor pressure measurements). After a pressure decrease of 5-6 mm. only trace amounts of  $CO_2$  were detected in the gas phase. The film was then held under vacuum at  $170^\circ C$  for up to 70 hours. Carbon dioxide, water and formaldehyde were recovered and analysed quantitatively (vapor measurements, cf. Fig. 8 and 8a.). Carbon dioxide desorption did not occur after 24 hours at  $170^\circ C$ ; no further water or formaldehyde were recovered after 30 hours. Formaldehyde was determined on the assumption that the vapour pressure of the paraformaldehyde which formed on condensation of the products was due to monomeric formaldehyde. The experiment was repeated on different films of  $TiO_2$ . The results are summarised in Table 11 in terms of  $\mu$  moles of reactants used up and products recovered.

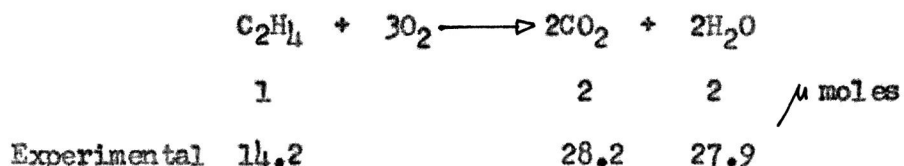
The following facts are apparent from Table 11 :-

- (a) Oxygen disappeared from the gas phase in amounts greater than those required for complete oxidation of the ethylene to carbon dioxide and water.
- (b) Although the average  $\text{CO}_2/\text{C}_2\text{H}_4$  ratio is exactly 2.0, formaldehyde in appreciable amounts was recovered as a partial oxidation product.
- (c) The total carbon content of the products invariably exceeded that of the reacted ethylene.
- (d) On evacuating the films at  $170^\circ\text{C}$ , water was not recovered in amounts which corresponded to a complete photo-oxidation of ethylene.

One explanation of the majority of these facts rests on the assumption that oxygen is photoadsorbed on free  $\text{TiO}_2$  surface as well as entering into a photo-oxidation of ethylene. The relatively large amounts of oxygen involved in the photoreaction are explicable in this event. The most likely source of excess carbon in the products is carbon dioxide adsorbed on the dioxide during its preparation; photoadsorption of  $\text{O}_2$  on fresh  $\text{TiO}_2$  surfaces has been shown (20) (cf. page 35) to result in subsequent desorption of  $\text{CO}_2$  on evacuation. It thus seems that the integral value of 2.0 for the  $\text{CO}_2/\text{C}_2\text{H}_4$  ratio must be regarded as fortuitous.

It is obvious that the complications of adsorption on sites which do not participate in the photo-oxidation and the errors arising from the presence of previously adsorbed  $\text{CO}_2$  will be minimised by a long and extensive oxidation in which large amounts of reactants are used up. An experiment of this type has been carried out by Macfarlane (62) in this Department. He used a  $\text{TiO}_2$

film which had been evacuated ( $10^{-3}$  mm. only) at room temperature prior to the experiment. An oxygen photoadsorption was then carried out until the reaction had practically ceased. A gas phase of 14.22 mm. ethylene and 70.9 mm. oxygen were illuminated over the film for 155 hours, after which time no further pressure decreases were observed. A vapour pressure analysis of the gas phase showed that it consisted of  $\text{CO}_2$  and oxygen only, with negligible amounts of residual ethylene. The film was then evacuated ( $10^{-3}$  mm.) for 20 hours at room temperature;  $\text{CO}_2$  and water were recovered and analysed in the Bourdon system. There was no evidence for the recovery of formaldehyde. The total  $\text{CO}_2$  recovered, inclusive of that released from the film during the photoreaction, corresponded to a pressure of 28.2 mm. in the reaction system and the desorbed water to a pressure of 27.9 mm. This analysis agrees well with the stoichiometric equation:



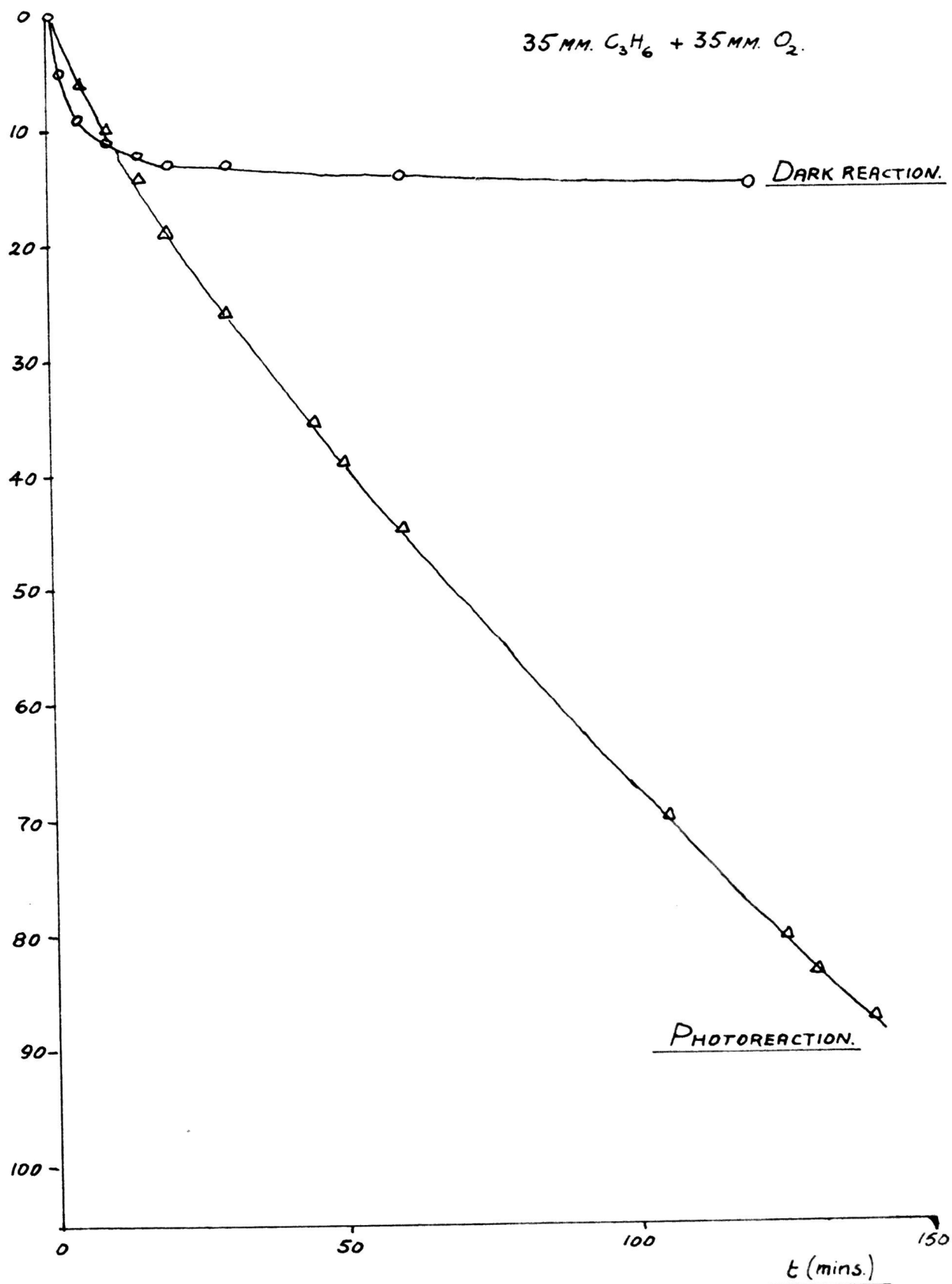
for the overall photoreaction

Carbon dioxide is not generally recovered in such amounts from  $\text{TiO}_2$  on evacuation at room temperature. It is reasonable to assume that the 28.2 mm. of  $\text{CO}_2$  were a product of the photoreaction. The situation as regards the water is less clear, since room temperature evacuation of the film prior to the experiment will leave a high content of surface water. The room temperature evacuation procedure has the advantage, however, of dispelling any doubts as to the source of recovered  $\text{CO}_2$ . A complete photo-oxidation of ethylene to  $\text{CO}_2$  and water is indicated under these conditions.

$\Delta p(\text{divs.})$

FIG. 19.

35 mm.  $\text{C}_3\text{H}_6$  + 35 mm.  $\text{O}_2$ .





Photoreaction of propylene - oxygen mixtures

Small pressure changes occurred in the dark in a propylene-oxygen mixture in contact with  $\text{TiO}_2$  at  $25^\circ\text{C}$ . In addition, large pressure decreases were observed when the system was illuminated. The general pattern of behaviour on illumination paralleled that observed in the ethylene-oxygen system. Again the rate of pressure decrease fell with time during illumination of any one mixture, and large pressure decreases of 100 mm. or more could be followed without any apparent saturation of the solid, provided that both propylene and  $\text{O}_2$  were present in the gas phase. After prolonged illumination  $\text{CO}_2$  was released into the gas phase. Once again a blank experiment ( $\text{TiO}_2$  absent) showed that the pressure decreases did not occur in the absence of  $\text{TiO}_2$ . The propylene-oxygen system differed from its ethylene analogue in that pressure decreases occurred in the dark.

The experimental procedure involved here was that outlined on page 37 for the investigation of the ethylene-oxygen counterpart. Dark reactions could be measured only after addition of the second gaseous constituent had been completed. These additions required some 30 secs. to effect. The pressure changes observed in the dark are therefore expected to be smaller than the actual values of dark uptake.

Table 12 and Fig.19 present data obtained from a mixture of 35 mm. propylene and 35 mm.  $\text{O}_2$  in contact with a  $\text{TiO}_2$  film at  $25^\circ\text{C}$ . Propylene was added to 35 mm.  $\text{O}_2$  until the total pressure became 70 mm. Pressure measurements were taken as soon as the addition of propylene was complete. A dark reaction of at least 15 divs. (0.12 mm) occurred in 120 minutes, after which its rate became effectively zero. When the system was illuminated, a further pressure

decrease of 87.5 divs. occurred over 140 minutes. The rate of the photo-reaction fell from approx. 1.0 divs/min. at  $t = 1$  min to approx 0.5 divs/min. at  $t = 140$  mins.

The size of the dark pressure decrease varied from film to film. Its amount varied between 10 divs and 100 divs (0.8-8.0 mm.). In fact, an increase in pressure rather than a decrease was observed on occasions. The value of a pressure increase never exceeded 10 divs.

In a second type of experiment a film was prepared whose capacity for photo-uptake from a purely propylene gas phase or from a purely oxygen gas phase was virtually zero. A film of such characteristics was prepared by a series of oxygen photoadsorption, in vacuo treatment at  $170^{\circ}\text{C}$  and propylene photoadsorptions. The sequence and results of this procedure is now outlined. Gas pressures of 35 m.m. were used in the photoadsorptions.

1. Normal 5 days evacuation at  $170^{\circ}\text{C}$ .
2. Oxygen photoadsorption ( $2.8/\mu$  moles in 2800 mins.).
3. 22 hours in vacuo at  $170^{\circ}\text{C}$ .  $\text{CO}_2$  ( $0.8/\mu$  moles) and  $\text{H}_2\text{O}$  ( $0.6/\mu$  moles) were desorbed.
4. Oxygen photoadsorption ( $0.8/\mu$  moles in 1200 mins.).
5. 20 hours in vacuo at  $170^{\circ}\text{C}$ .  $\text{CO}_2$  ( $0.4/\mu$  moles) and  $\text{H}_2\text{O}$  ( $0.4/\mu$  moles) were desorbed.
6. Propylene photoadsorption ( $1.3/\mu$  moles in 1860 mins.)
7. 10 hours in vacuo at  $170^{\circ}\text{C}$ .  $\text{CO}_2$  and  $\text{C}_3\text{H}_6$  (total of  $0.3/\mu$  moles) were desorbed.
8. Oxygen photoadsorption ( $3.9/\mu$  moles in 1700 mins.)
9. 12 hours in vacuo at  $170^{\circ}\text{C}$ .  $\text{CO}_2$  ( $1.8/\mu$  moles,  $\text{H}_2\text{O}$  ( $0.2/\mu$  moles) and  $\text{CH}_2\text{O}$  ( $0.2/\mu$  moles) were desorbed.

10. Propylene photoadsorption ( $0.2\mu$  moles in 1450 mins.)
11. When the propylene gas phase was replaced by oxygen no photoadsorption was observed over 600 mins. of illumination.

It is evident that at this stage virtually no pressure decreases occurred when the film was illuminated in contact with propylene or with oxygen. In addition, vacuum treatment of the film for 12 hours at  $170^{\circ}\text{C}$  did not result in the desorption of large amounts of material.

90 mm.  $\text{O}_2$  were now introduced to the reaction system in the dark. Propylene was added as quickly as possible to give a total pressure of 110 m.m. A dark reaction (pressure decrease) of 109d(8.5 mm.) occurred in the first 1100 mins. after the complete addition of propylene. On illumination the pressure decreased by 660 divs (51 mm.) over 3260 mins. Illumination was then discontinued. The final gas pressure was 50 mm.

The volume of the reaction system was 31.4 ml. That portion of it enclosed by the Bourdon gauge and the reaction vessel top was 16.4 ml. The reaction vessel tap was closed and the 16.4 ml. sample was held in contact with liquid  $\text{N}_2$  temperatures for 1 hour. After this time a portion of it ( $37\mu$  moles) had not condensed; this  $37\mu$  moles was assumed to be oxygen. The  $7\mu$  moles which had condensed were shown (vapor pressure and gas chromatography) to consist of  $\text{CO}_2$  only. The remainder of the gas phase (volume 15.0 ml) was transferred to the subsidiary system in the reaction vessel. The gas phase was pumped off for  $\frac{1}{2}$  hour through a trap cooled in liquid  $\text{N}_2$  and the system was then isolated for 20 hours at  $20^{\circ}\text{C}$  in vacuo and in contact with the cold trap.  $10.0\mu$  moles of  $\text{CO}_2$  were obtained and identified as before; no other substance was detected in the desorbed material. On the basis of the gas-phase

analysis reported above, this second sample of the gas phase would contain  $6.5\mu$  moles of  $\text{CO}_2$ . It appears that  $3.5\mu$  moles of  $\text{CO}_2$  were desorbed from the film at  $20^\circ\text{C}$ .

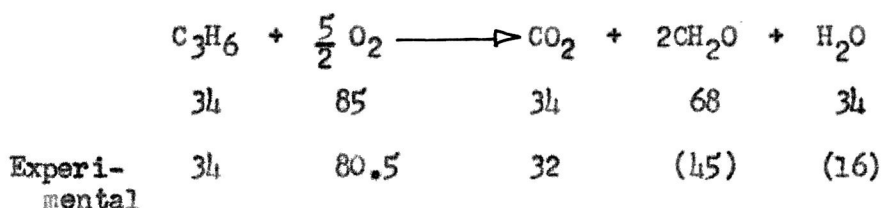
The film was then heated in vacuo for 22 hours and desorbed material was condensed in a cold trap (liquid  $\text{N}_2$ ). Only trace amounts of non-condensable material were obtained. After 2 hours in the furnace the film had reached a temperature of  $140^\circ\text{C}$  and  $42\mu$  moles of material had been desorbed. After another  $1\frac{1}{2}$  hours no further material had been desorbed but the temperature had risen to  $155^\circ\text{C}$ . The temperature of the film was gradually raised to  $170^\circ\text{C}$ . After a further 18 hours a further  $34\mu$  moles of material were recovered. In 22 hours, therefore, at temperatures up to  $170^\circ\text{C}$  a total of  $76\mu$  moles of condensable products were desorbed from the film.

Of these  $76\mu$  moles a portion ( $15\mu$  moles) did not condense at  $-70^\circ\text{C}$ . This portion consisted of  $\text{CO}_2$  only. The remainder consisted of water and formaldehyde. The ratio of the amounts present was difficult to determine directly since the vapor pressures of the ice and paraformaldehyde produced by condensing the mixture are similar. An estimate of this ratio was obtained by expanding the entire  $61\mu$  moles into a volume large enough to ensure that the saturation vapor pressure of each constituent was not exceeded. A representative sample of the mixture could then be analysed by taking vapor pressure measurements (cf. Fig.8). The estimated ratio of formaldehyde to water vapor was 2.8 to 1, on the assumption that the vapor pressure of the paraformaldehyde was due to monomeric formaldehyde. Of the  $61\mu$  moles, therefore, an estimated  $45\mu$  moles were formaldehyde and  $16\mu$  moles were water.

The above analyses can be summarised by saying that  $\text{CO}_2$ , water and

formaldehyde were obtained as products of a photoreaction between propylene and  $O_2$  in the presence of  $TiO_2$  at  $25^\circ C$ . 90 mm  $O_2$  ( $152 \mu$  moles) and 20 mm propylene ( $34 \mu$  moles) were illuminated over  $TiO_2$  after a pressure decrease of at least 8.5 mm. in the dark. Although the  $TiO_2$  showed no separate photoadsorption of propylene or of  $O_2$ , a pressure decrease of 51 mm was observed during 3260 minutes of illumination. The final gas phase consisted of  $71.5 \mu$  moles  $O_2$  and  $13.5 \mu$  moles  $CO_2$ , with no detectable propylene. On evacuation of temperatures up to  $170^\circ C$  a further  $18.5 \mu$  moles of  $CO_2$  were obtained, along with  $45 \mu$  moles formaldehyde and  $16 \mu$  moles water.

It appears, then, that  $34 \mu$  moles propylene reacted with  $80.5 \mu$  moles  $O_2$ . The recovered products consisted of  $32 \mu$  moles  $CO_2$ ,  $45 \mu$  moles formaldehyde and  $16 \mu$  moles water. The carbon content of the reactants is  $102 \mu$  moles and of the recovered products  $79 \mu$  moles. It is obvious that  $23 \mu$  moles of carbon had been "lost" on the  $TiO_2$ . If both formaldehyde and water were retained by the surface of the dioxide the gas phase analytical figures agree fairly well with the reaction :



The figures refer to the quantities ( $\mu$  moles) corresponding to the oxidation of  $34 \mu$  moles propylene.

It may be noted that evacuation at  $170^\circ C$  for 22 hours did not result in the quantitative recovery of water produced by the photoreaction. A similar retention of water by the surface has been mentioned previously (page 41) in the case of the ethylene-oxygen photoreaction.

### Comparison of rates of photo-uptake

A striking result of the above experiment is the fact that large pressure decreases (dark and photo) were observed in a propylene oxygen gas phase in contact with a  $\text{TiO}_2$  film which showed no appreciable uptake of each gas individually. An experiment was next carried out on another film with the intention of comparing the separate rates of propylene and oxygen photo-uptake with the rate of pressure decrease in an illuminated propylene-oxygen gas phase.

The film was one which had been treated with various amounts of propylene and oxygen, and immediately prior to the experiment a photo-uptake of 140 divs ( $18.3 \mu$  moles) of oxygen had been adsorbed in a photo-uptake. 35 mm. propylene were then added in the dark to the evacuated film; no pressure changes were observed in the dark. On illumination for 60 minutes, a photoadsorption of propylene occurred, with an initial rate of 0.27 divs/min and a final rate of 0.07 divs/min. The propylene was then replaced by 35 mm. oxygen and this system was illuminated (no dark reaction) for 150 minutes, during which time the rate of oxygen photo-uptake fell from 0.74 divs/min. to 0.07 divs/min. The oxygen photoadsorbed over these 150 minutes was 33 divs ( $43.5 \mu$  moles). Propylene was then added in the dark to give a total pressure of 70 mm. A small (15 divs) pressure decrease occurred in the dark and was complete within a few minutes. On illumination, a pressure decrease was observed, with an initial rate of 0.64 divs/min., falling to 0.49 divs/min. after 35 minutes of illumination. The amount (140 divs) of oxygen photoadsorbed during the initial illumination in oxygen was some four times greater than that photo-adsorbed (33 divs) during the second illumination; it therefore seems reasonable to take the figure 0.27 divs/min. as the maximum rate of photo-uptake of propylene on the film at the stage prior to treatment with the gas mixture.

The rate of oxygen photo-uptake at this same stage was observed, as above, to be 0.07 divs/min.

On the basis of the figures given above it can be assumed that the maximum rate of combined propylene and oxygen photo-uptakes would be  $(0.27 + 0.07) = 0.34$  divs/min. This figure is nearly half that of the rate of pressure decrease (0.64 divs/min.) in an illuminated mixture of propylene and oxygen under the same conditions and at the same stage in the history of the film. This result may be taken to indicate that the pressure decreases observed in propylene-oxygen mixtures are not merely the sum of two photo-uptakes, i.e. of propylene and of oxygen, and that a more direct photo-oxidation occurs when both are present in the gas phase. The existence of a more reactive photo-adsorbed species when both gases are present now appears to be a possibility. The pressure decreases observed in the dark when propylene-oxygen mixtures are in contact with  $\text{TiO}_2$  suggest that such a reactive surface species may be formed to some extent in the absence of illumination. It is not known to what extent changes in the surface during this dark reaction may alter the rate of a subsequent photo-reaction; the results of this experiment must therefore be regarded as inconclusive. It can be noted here, however, that the existence of an initially photoadsorbed and reactive form of surface oxygen is discussed later under the heading of the mechanism of oxygen photoadsorption.

#### Qualitative detection of formaldehyde after photoreaction

It was evident that  $\text{CO}_2$  was a product of a surface photoreaction between adsorbed propylene and oxygen, since it was released into the gas phase after prolonged illumination. It seemed possible that the formaldehyde was a

product of the 170°C evacuation and not a direct product of the photoreaction. Therefore a sample of a  $\text{TiO}_2$  film was spot-tested with carbazole reagent (page 27) immediately after photoreaction in a propylene-oxygen mixture over the film. A positive result here showed that formaldehyde was indeed produced on the  $\text{TiO}_2$  during the course of the illumination. The sensitivity of the spot test was such that 5 % of formaldehyde could be detected.



Experiments with formaldehyde, ethylene oxide and propylene oxide

Formaldehyde appeared as a photo-oxidation product of both ethylene and propylene on  $\text{TiO}_2$  surfaces at  $25^\circ\text{C}$ . A brief investigation was therefore undertaken to ascertain whether formaldehyde was itself oxidised under the same conditions. It also seemed possible that ethylene and propylene oxides might be intermediates in the photo-oxidation of their respective hydrocarbons. The capacity of the  $\text{TiO}_2$  sample for both ethylene and propylene oxides at  $25^\circ\text{C}$  was also briefly investigated.

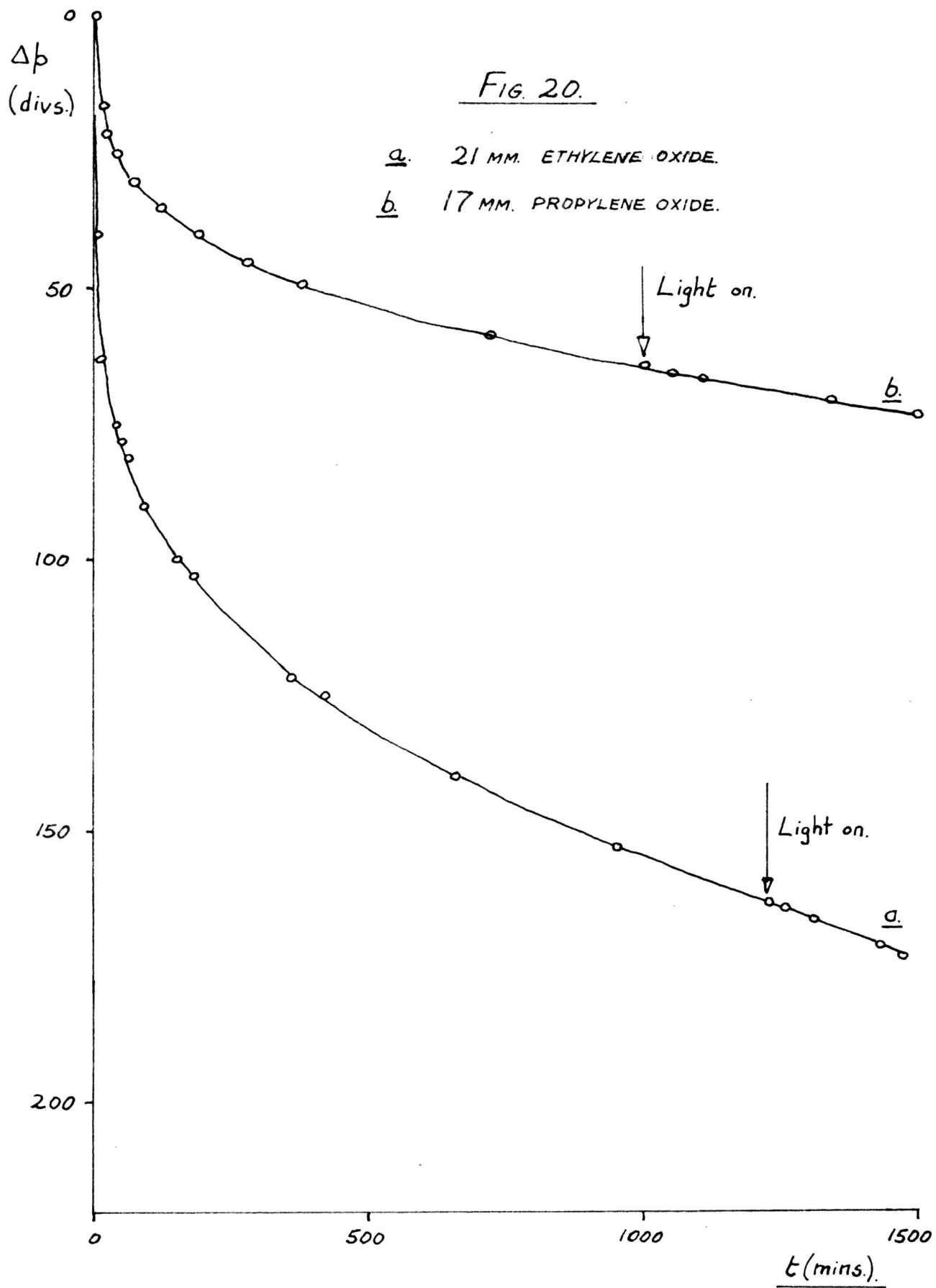
1. Formaldehyde

Formaldehyde was prepared by gentle heating of paraformaldehyde in a side-tube of the vacuum apparatus. The aldehyde obtained in this way in situ was brought in contact with a  $\text{TiO}_2$  film prepared in the normal way. The gaseous formaldehyde re-polymerised readily to give a white deposit of para-formaldehyde on the walls of the apparatus. For this reason no pressure measurements were taken.

No changes were observed in a  $\text{TiO}_2$  film in contact with formaldehyde gas in the absence of illumination, even after periods of up to 24 hours. On illumination a blue-grey color was detectable on the oxide within 5 mins.; after several hours of illumination the colour had darkened to steel-blue. Evacuation of the film at  $20^\circ\text{C}$  resulted in the recovery of some formaldehyde. Evacuation at  $170^\circ\text{C}$  for about 20 hours reversed the colour change almost completely and resulted in the recovery of larger quantities of formaldehyde but no other detectable substance.

When  $\text{O}_2$  (10 m.m.) was added to the above system before illumination





the same results were recorded. If anything, the colour change was less pronounced. On evacuation for 20 hours at 170°C (after two days of illumination) no more than  $4 \mu$  moles of CO<sub>2</sub> were detected.

These results indicate that extensive photo-oxidation of formaldehyde to CO<sub>2</sub> did not occur on TiO<sub>2</sub> at 25°C even in the presence of oxygen. A weak photoadsorption of formaldehyde is indicated.

## 2. Ethylene oxide

When ethylene oxide (21 mm.) was admitted to a TiO<sub>2</sub> film at 25°C in the Bourdon reaction system, large pressure decreases were observed in the dark (Fig.20). A blank experiment showed that no detectable adsorption occurred on the glass surface. Illumination had no effect (Fig.20) on the rate of the pressure decrease. The colour of the dioxide changed from white to light cream during the dark adsorption.

The ethylene oxide was replaced by 20 mm. of O<sub>2</sub>. No appreciable pressure decrease was observed in the dark but on illumination the pressure decreased by 97 divs (7.5 mm.) in 390 mins. The photoreaction was interrupted at this point and the O<sub>2</sub> was replaced by ethylene oxide. Large amounts of ethylene oxide (>40 mm.) were taken up rapidly within 5 mins. Subsequent to this no further pressure decreases were observed in the dark or on illumination. The film changed in colour from white to cream.

The gas phase was then removed and the film was heated for 20 hours in vacuo at 170°C. The colour of the film darkened from cream to light brown.

The evacuated film was transferred again to the pressure-measurement system. 22 mm. of O<sub>2</sub> were added in the dark at 25°C. No pressure

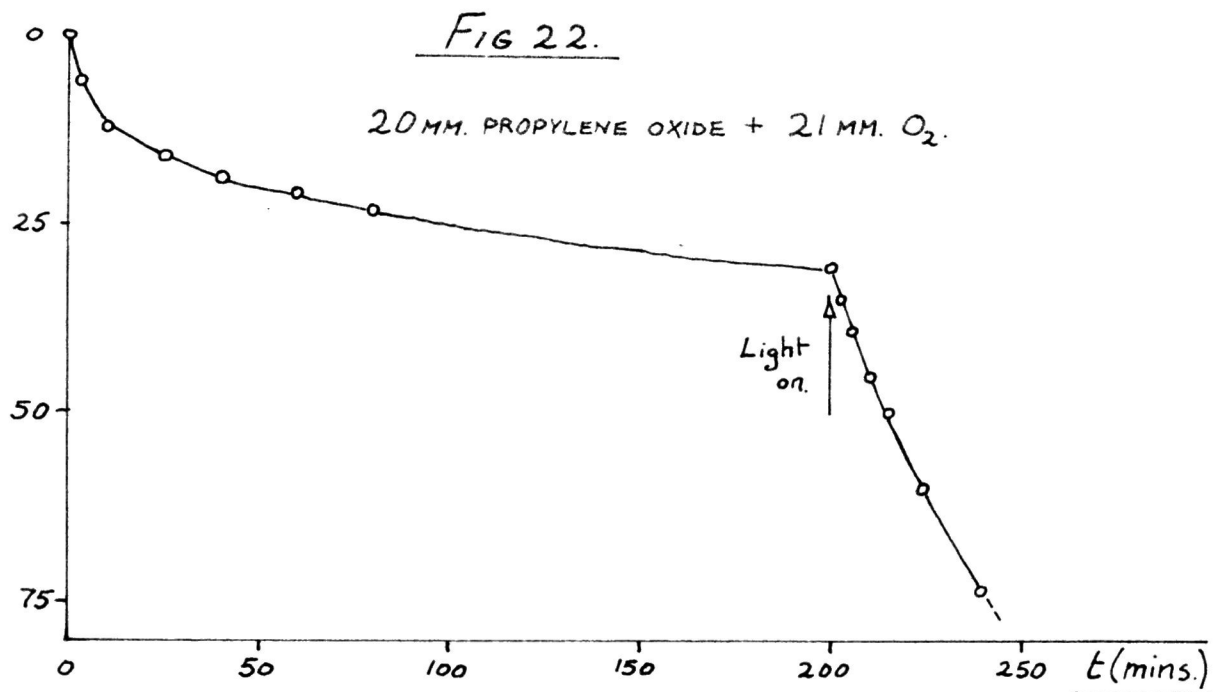
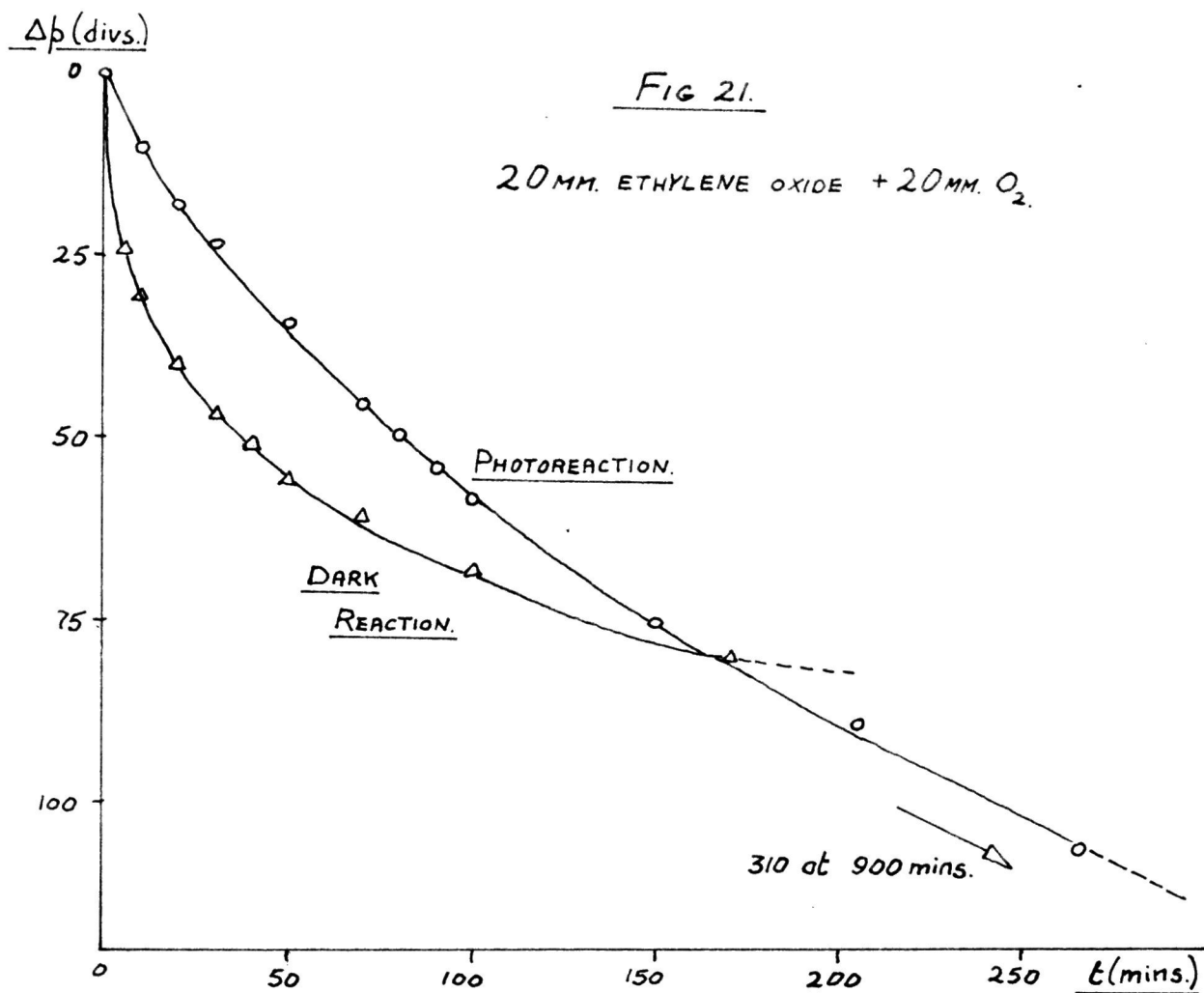
decrease was observed. Ethylene oxide was added to give a total pressure of 42 mm. A measured pressure decrease (dark) of 80 divs (6.2 mm.) occurred in the 170 mins. which followed the completion of the addition (Fig.21). On subsequent illumination a photo-uptake of 24 mm. occurred in 900 mins; the pressure decrease (divs) over the first 265 mins. is illustrated in Fig.22. The film was finally a light cream colour, which darkened to light brown on evacuation at 170°C.

Further experiments showed that the uptake of ethylene oxide in the dark was reversed (at least partly) on evacuation at 20°C. Oxidation products included CO<sub>2</sub>, water and formaldehyde, all of which were desorbed from the TiO<sub>2</sub> on evacuation at 170°C. Spot-testing showed that formaldehyde was present on the film following adsorption but prior to thermal evacuation.

### 3. Propylene oxide

Pressure decreases were observed when propylene oxide was admitted to TiO<sub>2</sub> films at 25°C. Illumination caused no appreciable increase in the rate of the pressure decrease. Fig.20 illustrates the uptake which occurred in 1500 mins. from 17 mm. of propylene oxide, the reaction being discontinued at this stage. During this uptake the colour of the solid darkened from white to cream; this change became more pronounced on heating in vacuo.

The propylene oxide was replaced by 21 mm. O<sub>2</sub>. No pressure decrease was observed in the dark, but on illumination a pressure decrease of 32.2 divs (2.5 mm.) was observed over 20 mins. Illumination was discontinued at this stage and propylene oxide was added to give a total pressure of



40 mm. The pressure decreases in the dark over the 200 mins. which followed the completion of the addition are shown in Fig.22, along with the pressure decreases which occurred during a subsequent short period of illumination. The experiment was terminated at this point and the film was finally cream coloured.

Further experiments showed that the dark uptake of propylene oxide was largely reversible at 20°C. CO<sub>2</sub>, water and formaldehyde were recovered (170°C evacuation) as oxidation products. Some oxidation appeared to occur even in the absence of oxygen. The presence of formaldehyde on the film, following treatment with propylene oxide but prior to thermal evacuation, was established by the carbazole spot-test.

### Color Changes in $\text{TiO}_2$ during photoadsorption

No colour changes were observed when  $\text{O}_2$  was photoadsorbed on  $\text{TiO}_2$  which had not been pre-treated.

A white to light-grey colour change occurred when ethylene was photoadsorbed on  $\text{TiO}_2$ . This colour change was partially reversed by several hours evacuation at  $170^\circ\text{C}$ . Colour changes occurred on both untreated and oxygen pre-treated samples.

A more pronounced colour change (white to blue grey) was observed during propylene photoadsorptions. Evacuation at  $170^\circ\text{C}$  reversed the change; the reversal was observed before extensive desorption of products had taken place. Photoadsorption of  $\text{O}_2$  was also effective in partly reversing the change.

No observable change in the colour of the oxide took place during photo-reaction where both  $\text{O}_2$  and ethylene were present in the gas phase. A similar negative effect was noted for the propylene-oxygen system. These two systems differed, however, in their behaviour during a subsequent evacuation at  $170^\circ\text{C}$ . The ethylene-oxygen system again produced no observable colour change in the oxide. But the film darkened to brown on  $170^\circ\text{C}$  evacuation after photoreaction in a propylene-oxygen gas phase. The brown colour lightened to cream when  $\text{O}_2$  was photoadsorbed on the sample at  $25^\circ\text{C}$ , and also during a second propylene-oxygen photoreaction at  $25^\circ\text{C}$ .

The colour changes associated with formaldehyde, ethylene oxide and propylene oxide have been noted in the previous section but are included here for the sake of completeness. No colour change was observed when formaldehyde was admitted to  $\text{TiO}_2$  in the dark. But the solid darkened to a pronounced blue-grey colour within 5 mins. of commencing illumination. The blue-grey colour was

removed completely by evacuation at 170°C.

Colour changes occurred during the dark adsorption of ethylene oxide and propylene oxide on  $\text{TiO}_2$ . In both cases the dioxide darkened from white to cream in colour. A subsequent 170°C evacuation darkened the sample even more (light brown). This colour change was completely reversed by a photoadsorption of  $\text{O}_2$ .

In the illuminated systems mentioned above colour changes were not normally observed on sections of the film which were not exposed to the illumination.



### Conductivity measurements

These measurements were carried out at 20°C on pellets of  $\text{TiO}_2$  powder, as described on page 24. The experiments studied the effect of the following on the resistance of the  $\text{TiO}_2$  pellets.

1. Illumination
2. Oxygen
3. Water vapour
4. Unsaturated hydrocarbons

1. and 2. were studied previously by Maclean (20) and by Kennedy (34). Kennedy used thin transparent films of  $\text{TiO}_2$  deposited on silica plates by hydrolysis of  $\text{TiCl}_4$ , while Maclean used pelleted preparations similar to those used in the present investigations.

In the present work it was first established that the presence of mercury vapour (from manometers, etc.) had no measurable effect on the dark or photo-resistances of the pellets at 20°C. This was ascertained by opening the evacuated pellets to that part of the vacuum line which contained the mercury manometers; no resistance changes were observed over several hours, in either the dark or illuminated pellets.

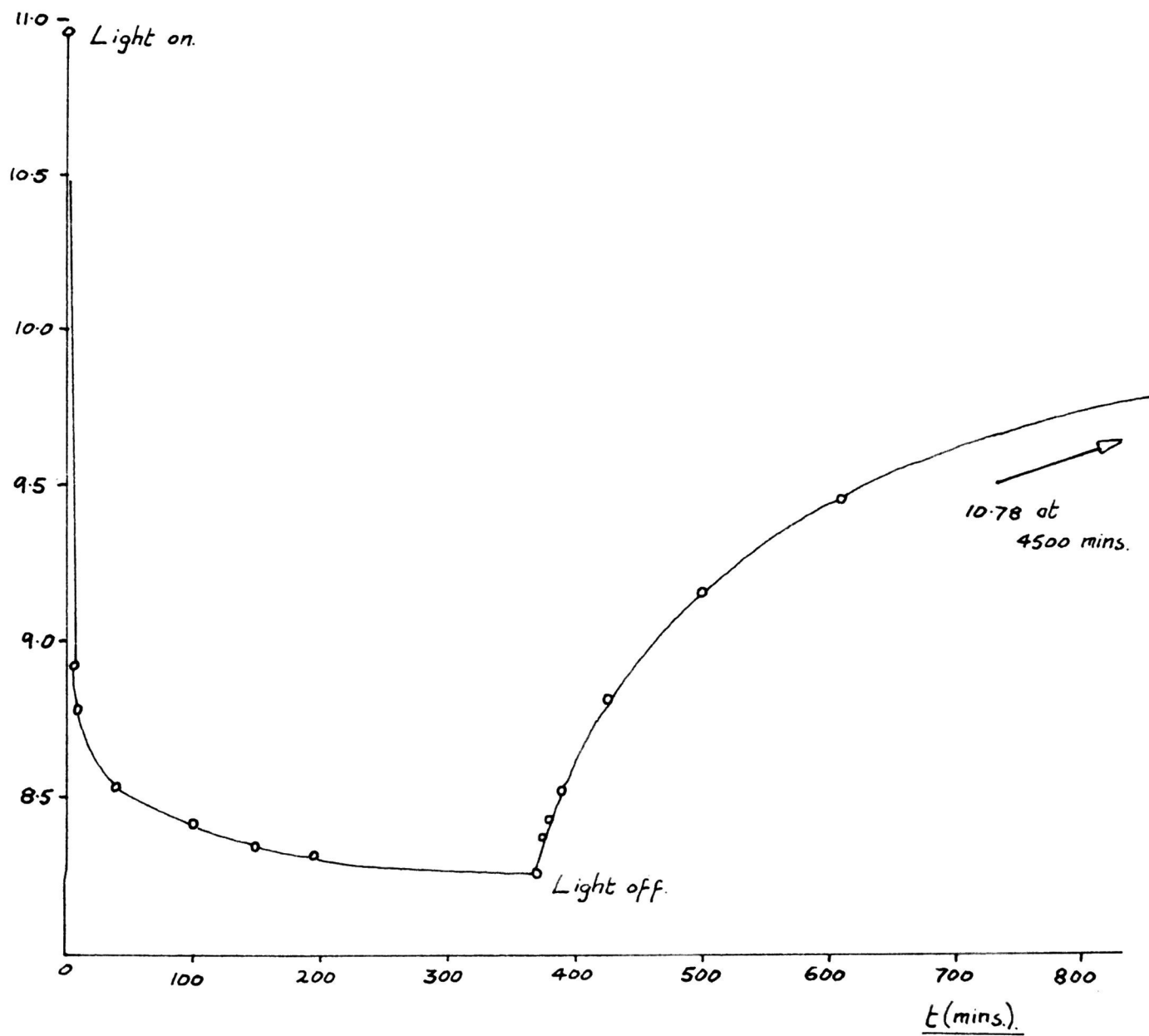
#### 1. Effect of illumination

Illumination of a  $\text{TiO}_2$  sample in vacuo ( $10^{-5}$  mm.) resulted in a rapid decrease in its resistance. The rate of decrease in resistance fell with time until a reasonably steady value of the photoconductive<sup>ity</sup> was established after c. 200 mins. When illumination was discontinued the resistance increased again, at first rapidly and then more slowly. A steady dark resistance

Fig. 23.

PHOTOCONDUCTANCE RISE AND DECAY.

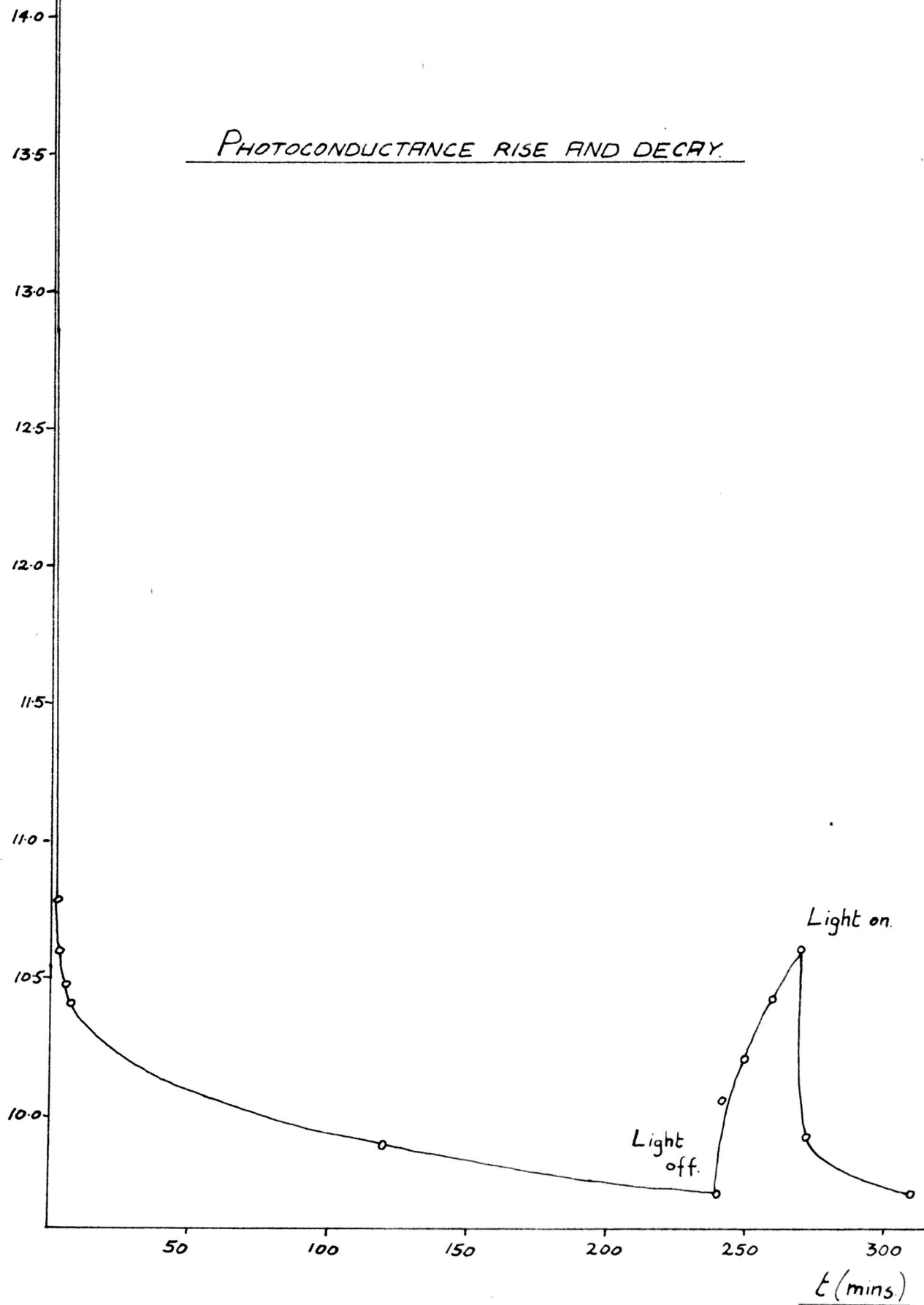
log r.



logr. Light on.

FIG. 24.

PHOTOCONDUCTANCE RISE AND DECAY.



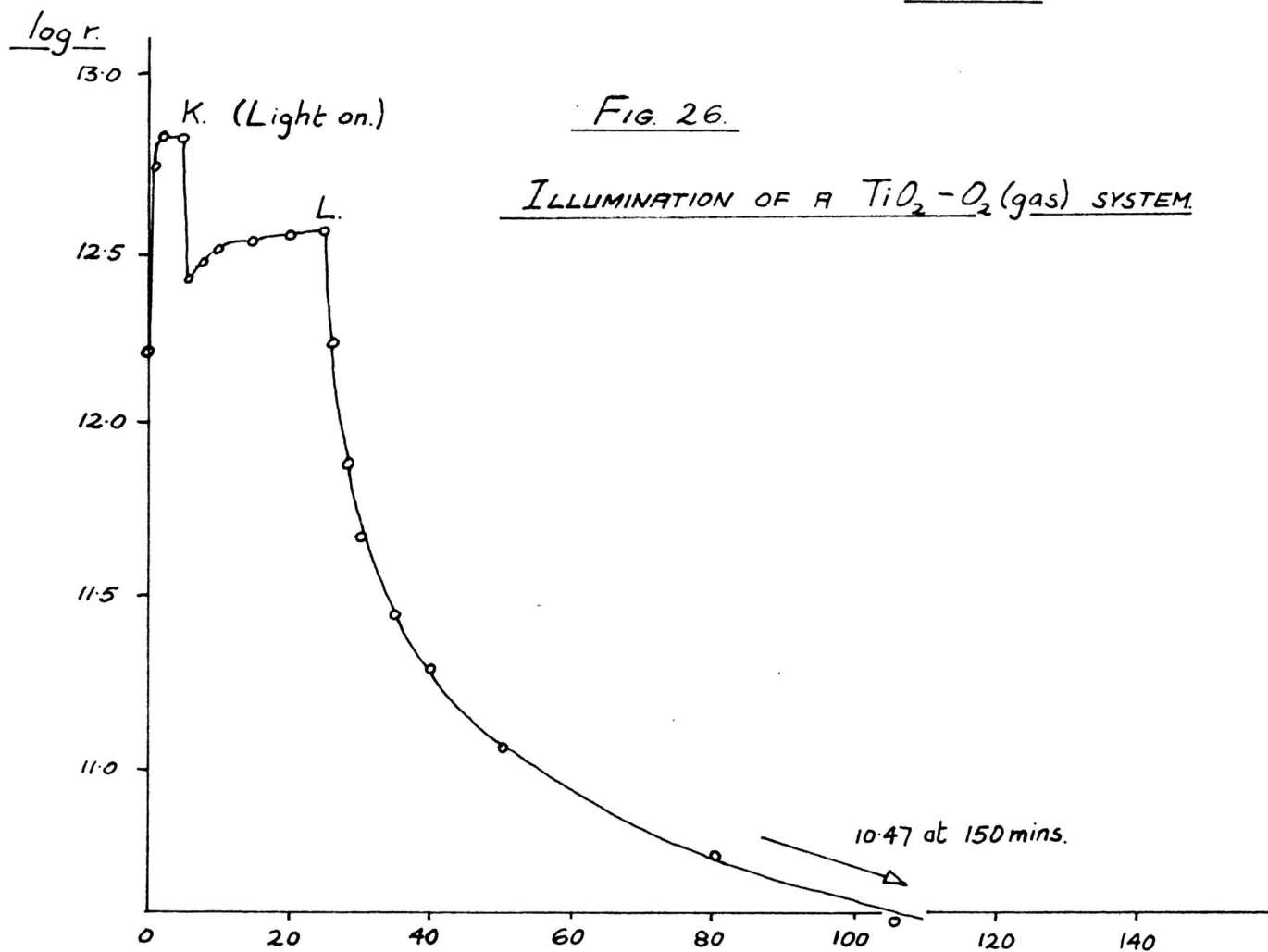
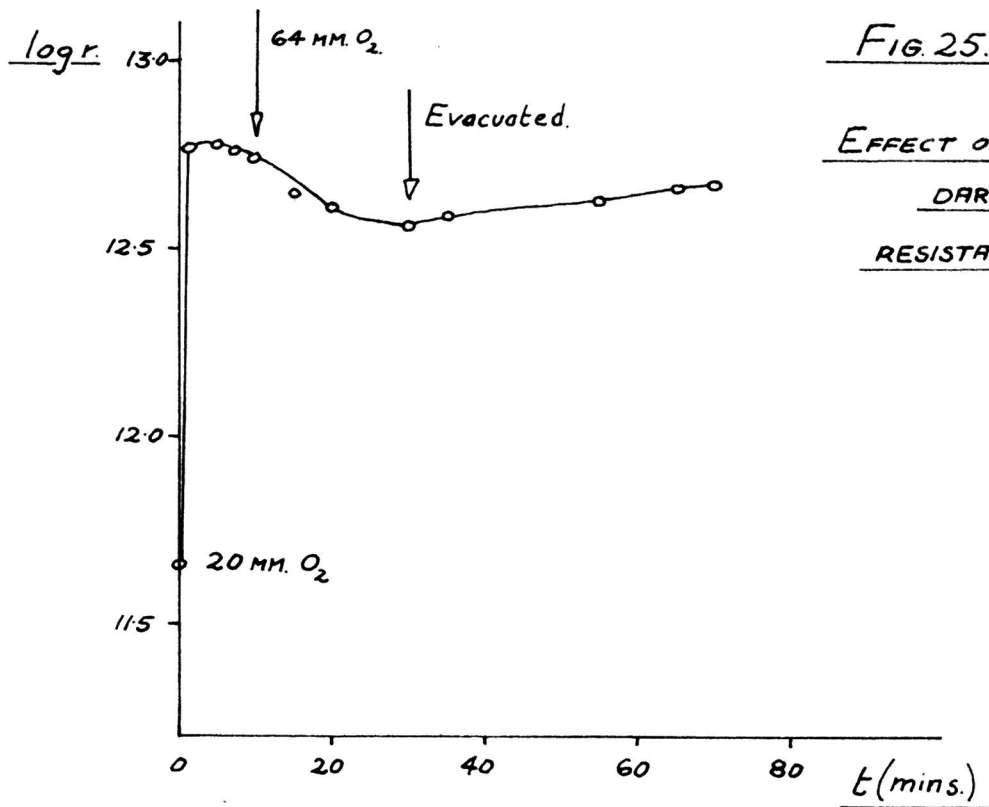
was established again 2-3 days after ceasing illumination. This new value of dark resistance was always less than the original dark resistance of the pellet. A typical illustration of the resistance changes occurring during and after illumination of a  $\text{TiO}_2$  pellet is given in Table 13 and Fig.23.

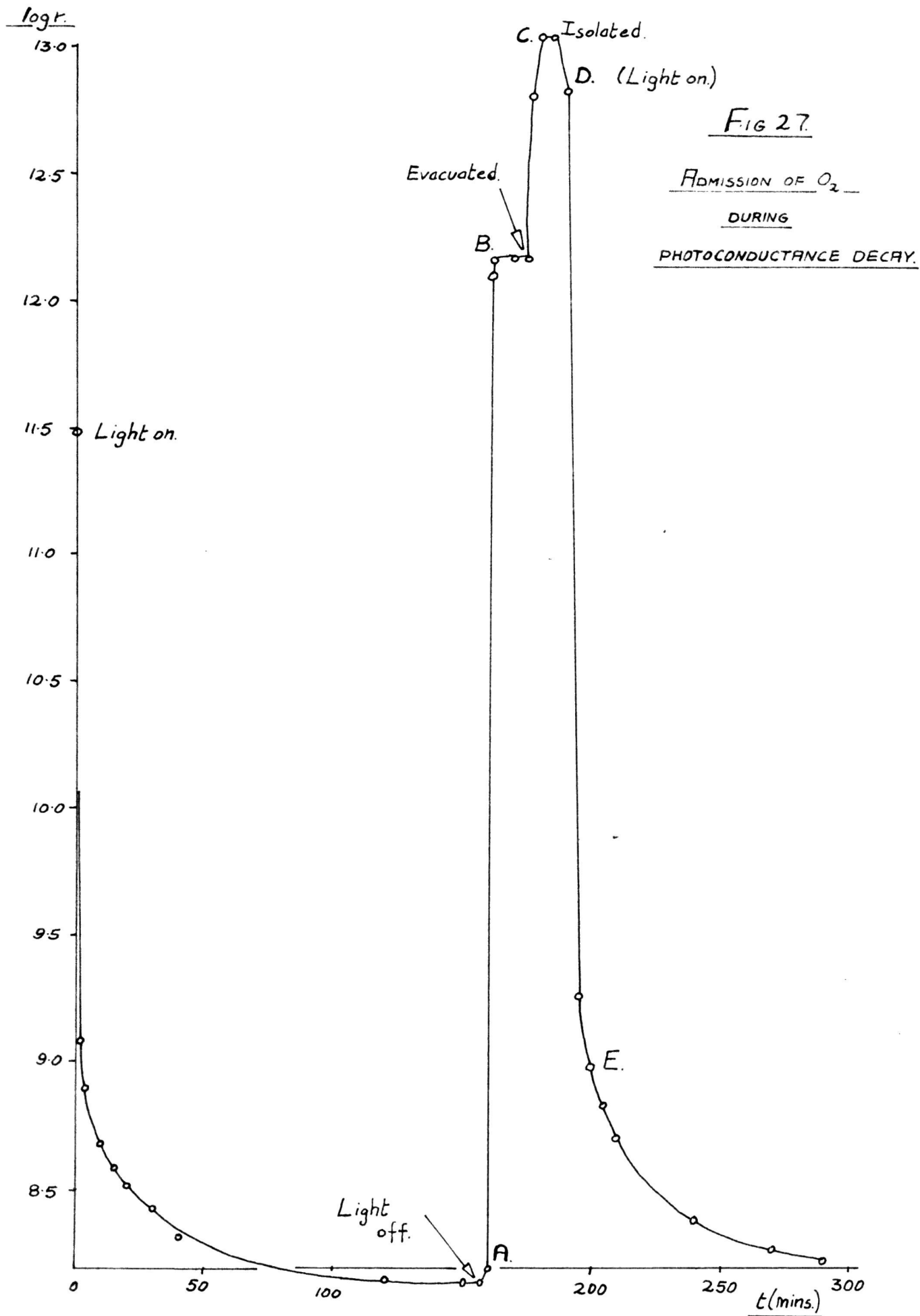
If illumination was re-commenced during the decay in the photoconductance the resistance of the sample again decreased. The rate of decrease in resistance during this second illumination was always greater than that over the same range of resistance values in the first illumination. Table 14 and Fig.24 present typical measurements. Here the resistance of the freshly illuminated sample fell from  $\log r = 10.60$  to  $\log r = 9.73$  in 230 mins; during the second illumination the resistance decreased between the same values in only 40 mins. Removal of the illumination after these 40 mins. produced an increase in resistance similar to that in Fig.23.

## 2. Effect of oxygen

The effect of  $\text{O}_2$  on both the dark and photoresistances was studied. Changes in resistance with time were measured for  $\text{TiO}_2$  pellets in contact with oxygen at pressures in the range 1-60 mm.

The dark resistance of a  $\text{TiO}_2$  pellet increased from  $4.62 \times 10^{11}$  ohms to  $5.97 \times 10^{12}$  ohms when 20 mm. dry  $\text{O}_2$  were introduced to the system (Table 15 and Fig.25). The resistance change was complete within 0.5 minute. Successive increases of  $\text{O}_2$  pressure to a maximum of 64 m.m. and over a period of 30 mins. produced no further increase in resistance; instead, the resistance fell slowly by a fraction of the original increase. The large initial increase in resistance was not removed by pumping at  $20^\circ\text{C}$ . In fact, the resistance increased again slightly during this evacuation (Fig.25). The



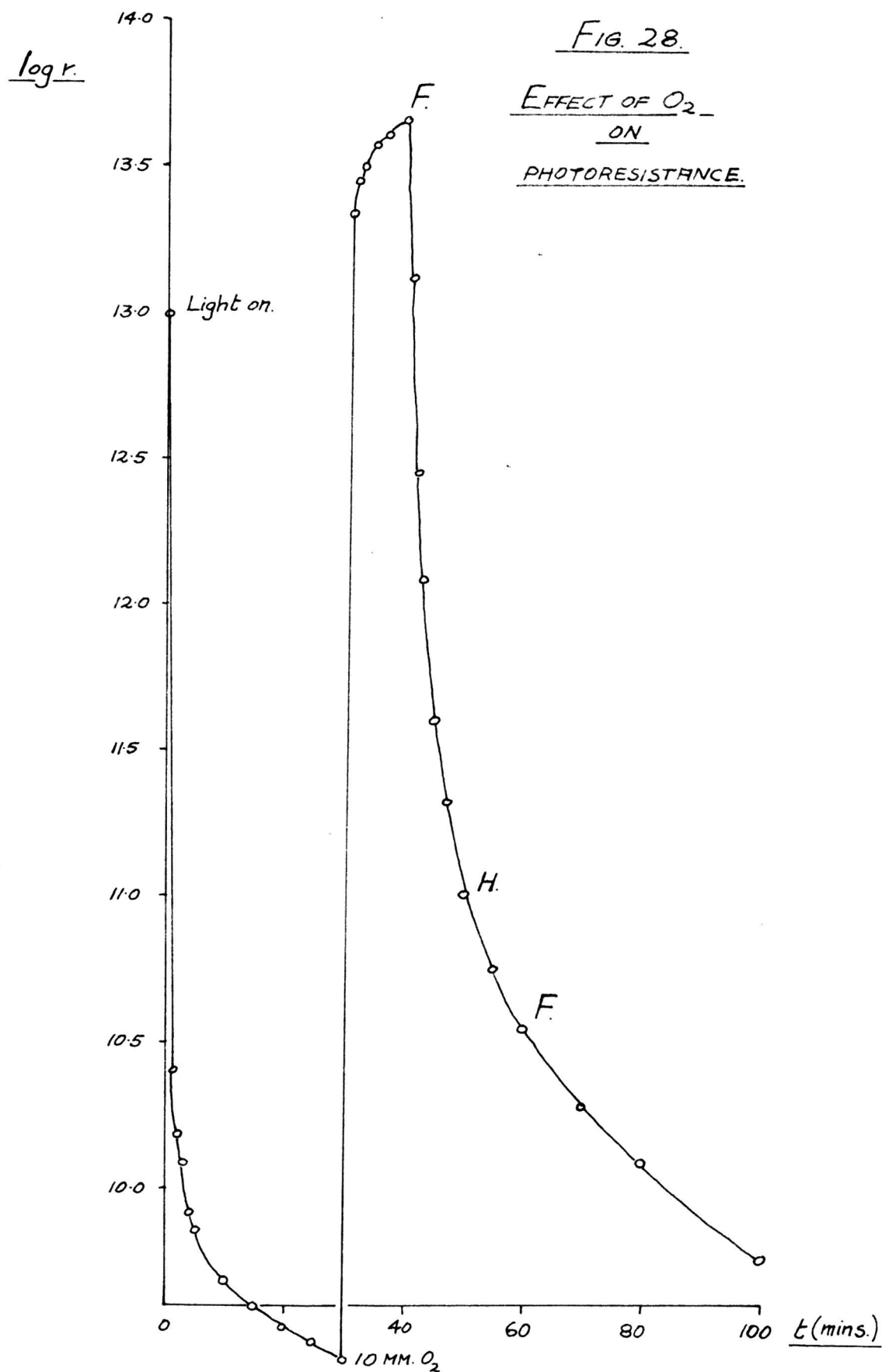


smaller changes illustrated in Fig.25 are possibly secondary ones associated with surface water on the solid.

Admission of  $O_2$  increased the photoresistance of  $TiO_2$  pellets, by an amount much larger than that described above for the dark resistance. The resistance increased from its value under illumination to a value of the order of the original dark resistance. Again the resistance increased very rapidly after the admission of  $O_2$ , but small differences in behaviour were noted if the admission of gas occurred during the decay of photoconductance rather than while the sample was under illumination. The results of some typical experiments are now given.

Table 16 and Fig.27 show the effect of admitting (point A) 10 mm. of  $O_2$  one minute after the start of photoconductance decay in vacuo. The resistance rose rapidly and attained a steady value within 3 mins. (B). Evacuation at  $20^\circ C$  after a further 12 mins. in the absence of illumination produced another small increase in resistance, complete within 5 mins. (C). When the system was isolated from the pumps the resistance fell again very slightly. Once again these small resistance changes are possibly secondary effects associated with surface water. Re-illumination in vacuo (D) then resulted in a large time-dependent decrease in resistance; the system was isolated from the pumps at this stage and no pressure increase was detected on the Pirani gauge. A period of evacuation (E) during this re-illumination had no observable effect on the rate of decrease in resistance. These results are in accordance with a thermal (dark) desorption of freshly photoadsorbed oxygen at  $20^\circ C$ .

When oxygen (10 mm.) was admitted while illumination was still in

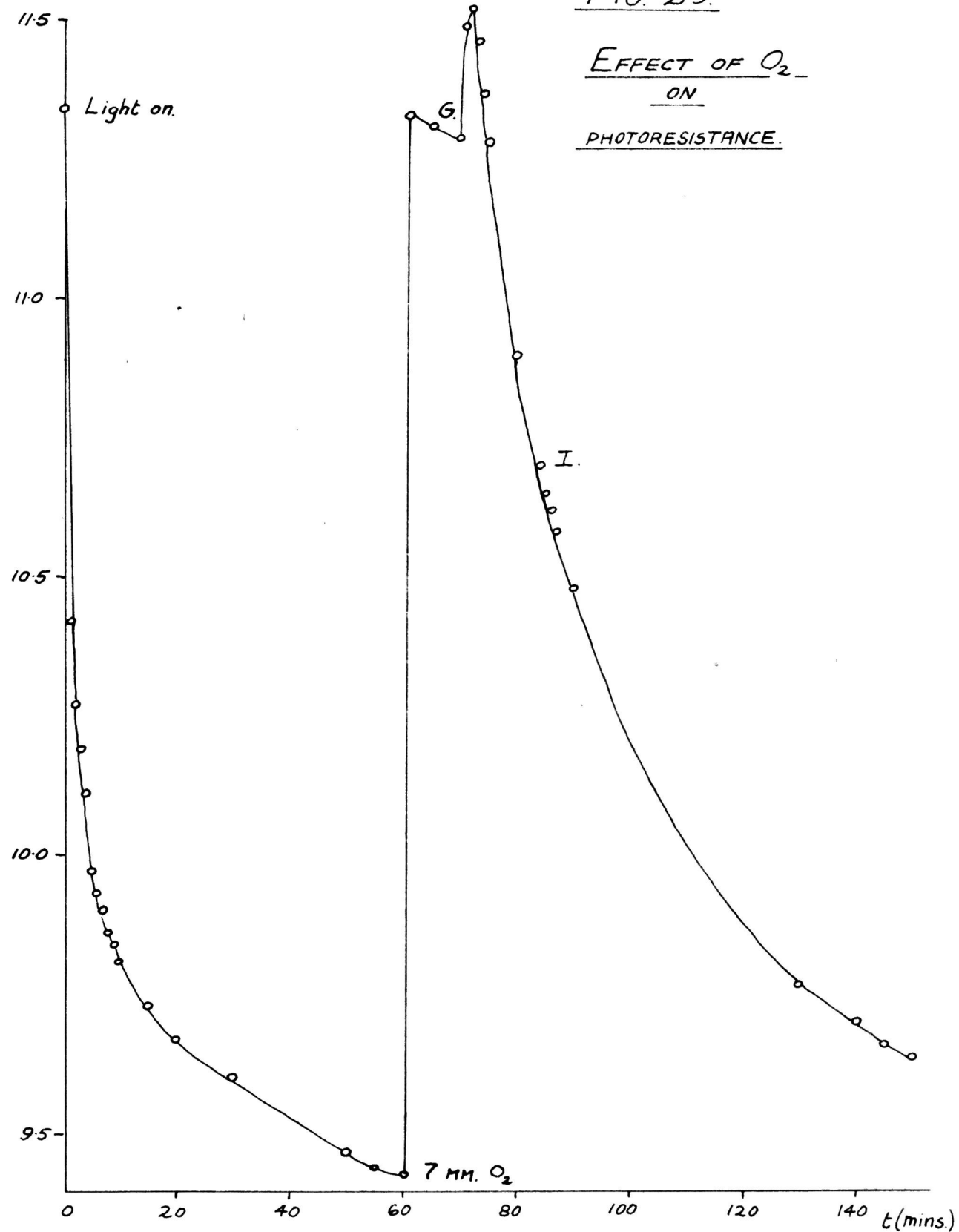




log r.

FIG. 29.

EFFECT OF  $O_2$   
ON  
PHOTORESISTANCE.



progress the resistance again increased rapidly. Some pellets gave a resistance against time plot corresponding to Fig.28 and Table 17, and some to Fig.29 and Table 18. That is, the increase in resistance either :

- (i) decreased in rate with time,
- or (ii) attained a maximum value almost instantaneously and then decreased slightly.

In either case, evacuation at 20°C under illumination reversed the increase in resistance almost completely (F and G), the rate of reversal decreasing with time in the manner of a photoconductance development. Isolation of the evacuated system from the pumps during this period caused no observable discontinuity (Hand I) in the resistance against time plot and no pressure increase was detectable by Pirani gauge. In case (ii) above, the decrease in resistance on evacuation was preceded by a small resistance increase (J). These results are consistent with a thermal desorption of oxygen at 20°C, with a simultaneous re-development of photoconductance.

In a further experiment, 25 mm. of oxygen were added to an illuminated pellet. The normal rapid resistance increase occurred and the resistance then remained approximately constant during 1000 mins. of illumination in oxygen, (although fairly large and random fluctuations were observed in the resistance value); after this treatment, however, the resistance did not decrease when the pellet was evacuated under illumination.

The amount by which the photoresistance of a  $\text{TiO}_2$  pellet was increased on admission of oxygen was shown to be independent of oxygen pressure in the range of 1-30 mm.

It is evident that the procedures so far described for pressure measurements of oxygen photoadsorption and conductivity changes during this photo-

adsorption differ in one important respect. In the first case, oxygen was admitted to the solid before illumination commenced; excitation of photoelectrons to conduction levels would therefore be in progress during the photoadsorption. In the second case, a steady photoconductance was established before admission of oxygen, and electrons may be expected to be already in conduction levels during the entire photoadsorption.

An experiment was therefore carried out (62) to determine whether the large and rapid increase in photoresistance of Figs. 28 and 29 was associated with an appreciable photo-uptake of oxygen. A  $\text{TiO}_2$  film was illuminated in vacuo in the Bourdon reaction system for 5 hours. A known pressure of oxygen was then admitted from a calibrated volume and the pressure decrease which occurred was all accounted for by the expansion of oxygen from this calibrated volume into the known volume of the reaction system. It was, therefore, concluded that the large and rapid increase in photoresistance was caused by a relatively small amount of photoadsorbed oxygen.

Conversely, an experiment was carried out in which 30 mm.  $\text{O}_2$  were admitted to a  $\text{TiO}_2$  pellet in the dark. The normal relatively small increase in dark resistance was observed (Fig. 26). On illuminating (K) this system a small and rapid decrease in resistance was observed and was followed by a gradual increase to a constant resistance whose value was less than that prior to illumination. Evacuation of the illuminated pellet at this stage (L) resulted in the gradual development of a normal photoconductance. The data covering this experiment are presented in Table 19 and Fig. 26.

### 3. Effect of water vapour

The effect of bringing various pressures of water vapour (0.01-2.0 mm.)

Fig 30.

EFFECT OF WATER VAPOR ON RESISTANCE.

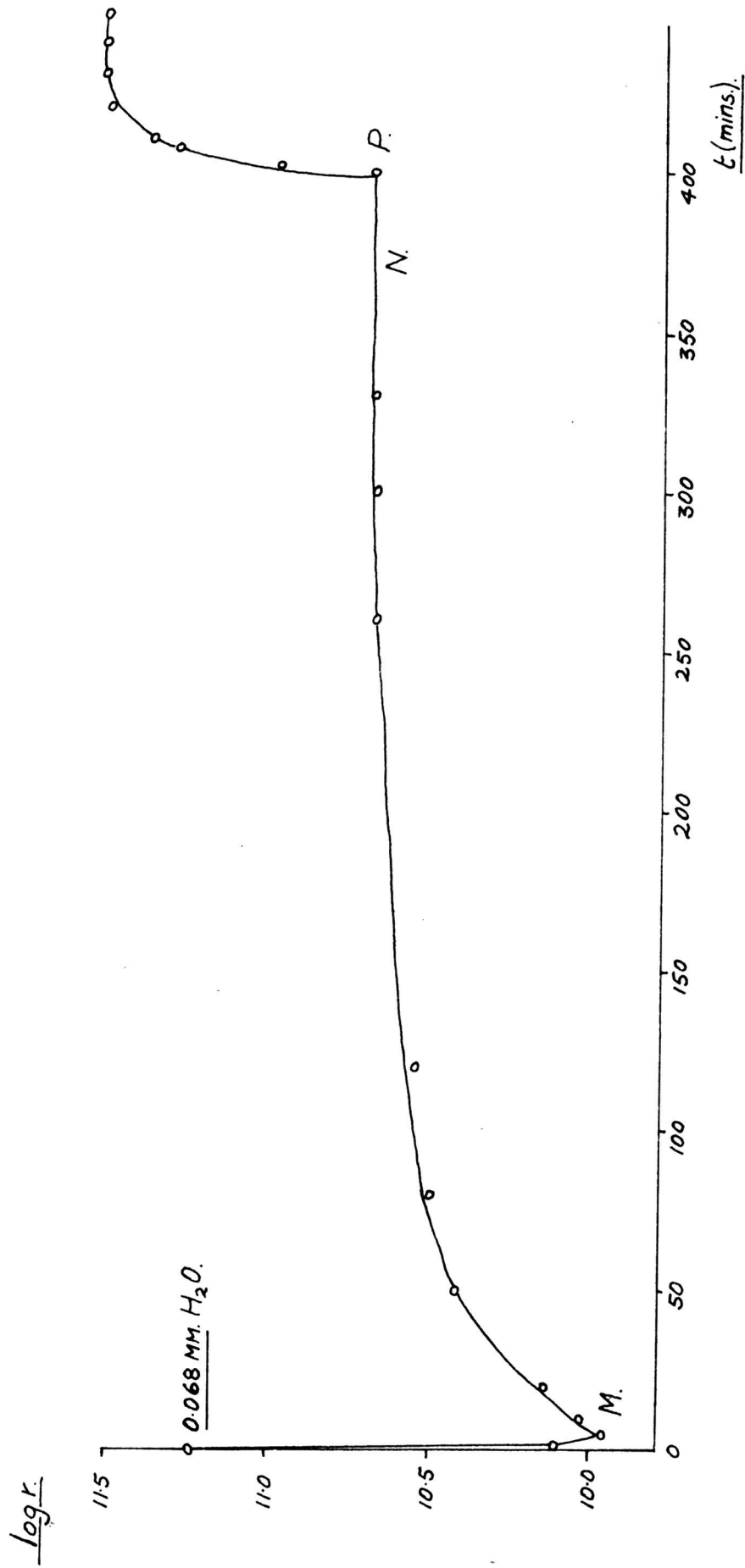
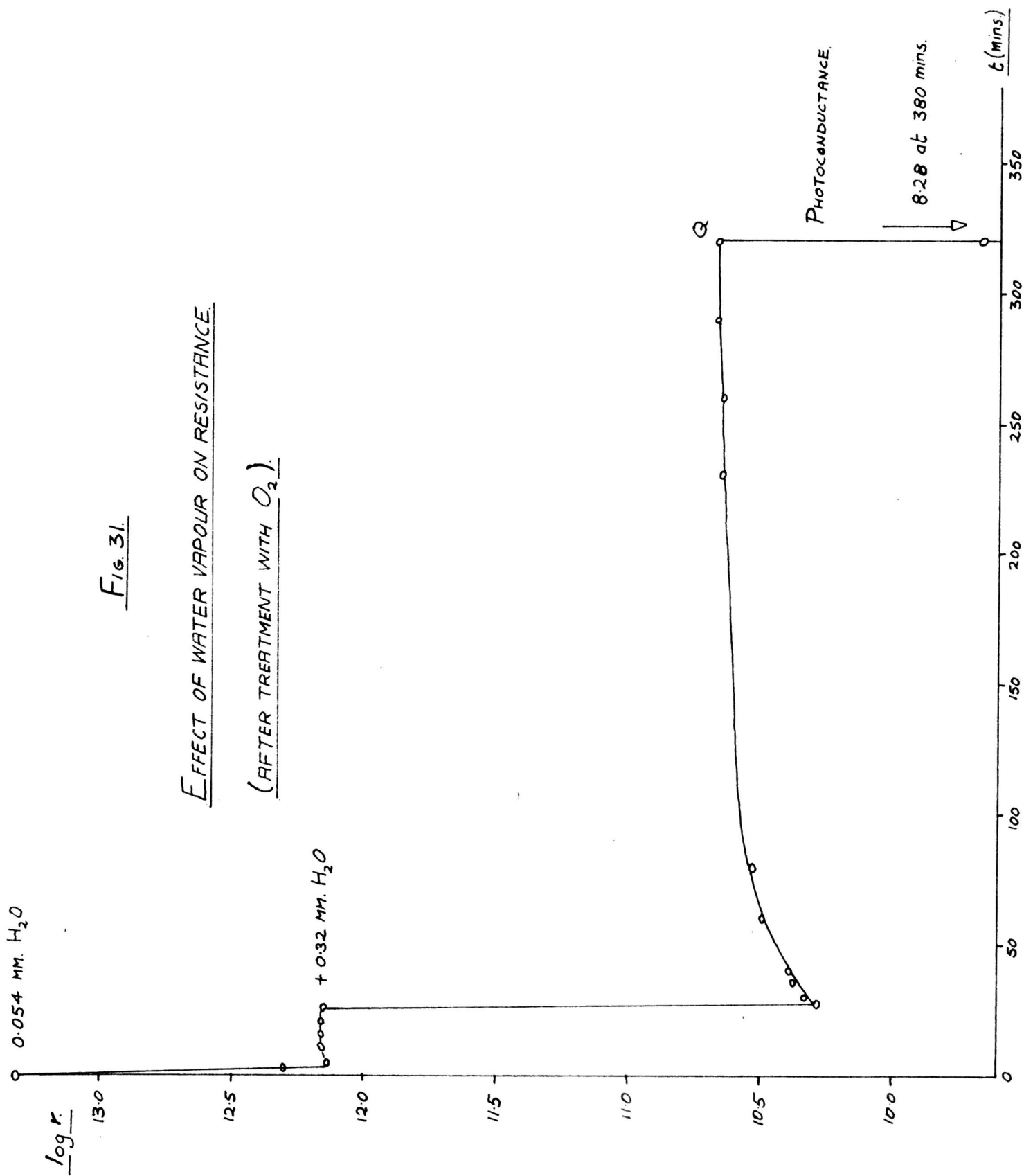


Fig. 31.

EFFECT OF WATER VAPOUR ON RESISTANCE.

(AFTER TREATMENT WITH  $O_2$ ).



in contact with evacuated  $\text{TiO}_2$  was studied both in the presence and absence of illumination. The pressure of the water vapour was controlled by cooling a cold trap at measured temperatures in the range  $-10^\circ$  to  $-60^\circ\text{C}$ . The pressure of vapour in contact with condensed water at a given temperature was obtained from International Critical Tables.

Water vapour, in the absence of illumination, decreased the resistance of  $\text{TiO}_2$  pellets rapidly within a few minutes; the decrease for pressures greater than about 0.5 mm. exceeded that which occurred on illumination. A typical experiment is recorded in Table 20 and Fig.30, where 0.068 mm. of water were admitted. This decrease in resistance was followed by a slower increase in resistance (Fig.30, M). The rate of this subsequent increase in resistance decreased with time. A steady resistance value (N) was attained c.300-500 mins. after admission of the water vapour. This final resistance was always less than the original resistance of the pellet. Evacuation in the dark (P) at  $20^\circ\text{C}$  produced a rapid but time-dependent increase in resistance to a value equal to, or sometimes greater than, the original resistance of the pellet. This was observed also if evacuation was commenced at a stage corresponding to the minimum resistance obtained.

Generally, the size of the initial decrease in resistance increased with increasing pressure of water vapour. Pressures of about 0.5 mm. were sufficient to produce an initial decrease equal to the steady value attained on continued illumination. If the sample was illuminated after admission of about 0.5 mm. water vapour and when the resistance had reached this minimum value there was only a negligible further increase in resistance. In other words, no appreciable photoconductance was developed.

Photoadsorption of oxygen prior to admission of water vapour in the

dark altered the characteristics of the subsequent resistance changes. In experiments which illustrated this effect the following procedure was adopted: Oxygen was admitted during the decay in photoconductance of a fresh pellet. The usual large and rapid increase in resistance was observed. The oxygen in the gas phase was then removed by pumping. Admission of water then gave the usual sharp fall in resistance, but the subsequent slow increase in resistance was largely suppressed. Fig.31 and Table 21 illustrate the suppression of this effect for two successive additions (0.054 and 0.32 mm.) of water vapour. Illumination (Q) of the pellet after this treatment decreased its resistance to the value developed during the original illumination.

#### 4. Effect of unsaturated hydrocarbons

Because of the resistance changes produced by small amounts of water vapour, the hydrocarbons were admitted to the measurement system, where possible, from a trap cooled to  $-110^{\circ}\text{C}$ . The effect of admitting ethylene, propylene and benzene vapour separately to  $\text{TiO}_2$  pellets at  $20^{\circ}\text{C}$  both in the presence and absence of illumination was investigated. No appreciable change in dark or photoresistance were observed for any of the hydrocarbons at pressures up to 30 mm.

In the dark, admission of an unsaturated hydrocarbon produced, on occasions, a very small decrease in resistance followed by an increase. The effect was not reproducible and can, perhaps, be attributed to a change in the character of surface water. The absence of any effect when the hydrocarbons were admitted (at pressures in the range 10-30 mm.) to an illuminated pellet at  $20^{\circ}\text{C}$

was particularly striking.

Ethylene and propylene are photoadsorbed on  $\text{TiO}_2$  to an extent comparable (page 32) to oxygen. Despite this no resistance changes were observed when they were brought into contact with illuminated  $\text{TiO}_2$ , whereas, under the same conditions, oxygen produces a large increase in resistance. This suggests that the small effects observed when the hydrocarbons were admitted in the dark are secondary effects. It is apparent that the primary photoadsorption of ethylene and propylene does not alter the resistance of the dioxide.



## DISCUSSION

## DISCUSSION

### Surface water and capacity for photoadsorption

The detailed structure of a  $\text{TiO}_2$  surface is not known. It is established (27) (29), however, that for samples evacuated at moderate temperatures (c.  $200^\circ\text{C}$ ) a considerable amount of adsorbed water remains on the surface. The existence of a qualitative correlation between residual surface water and other surface properties of the dioxide has already been mentioned on page 9.

In any investigation of adsorption on  $\text{TiO}_2$  it is, therefore, advisable to pre-treat each sample under standard conditions. Where a photo-oxidation with water as a product is being investigated, such a standardisation is essential. In the present investigation the standard pre-treatment of  $170^\circ\text{C}$  evacuation was adopted after extensive trials, with regard to the fact that extreme temperatures could result in surface sintering and a change in adsorption capacity.

The infra-red studies of Yates (30) have shown that after evacuation at  $150^\circ\text{C}$  molecular water is still present on a  $\text{TiO}_2$  surface; evacuation at  $350^\circ\text{C}$  removes all but surface OH groups. Differences in the OH spectra of anatase and rutile were tentatively ascribed to the different crystal faces involved. It was evident that the method of preparation of the  $\text{TiO}_2$  played a large part in determining the character of adsorbed water. This should, in turn, be reflected in a variation of adsorption properties with sample preparation.

The  $170^\circ\text{C}$  evacuation pre-treatment adopted in the present photo-adsorption studies is expected, therefore, to produce a  $\text{TiO}_2$  surface with a high OH content and a smaller amount of molecular water. The photoadsorption of oxygen on such a surface has been shown (page 35) to result in a displacement of water (and of  $\text{CO}_2$ ) from the surface; water and  $\text{CO}_2$  were recovered by  $170^\circ\text{C}$  evacuation,

following an oxygen photoadsorption. The amounts of water and  $\text{CO}_2$  recovered were small ( $\sim 1 \mu$  mole) and no correlation between their amounts and the amount of photoadsorbed oxygen was apparent. The results (20) of Maclean, which established an equimolar relation between displaced water and photoadsorbed oxygen, have therefore been confirmed only qualitatively. Maclean worked with films which had been evacuated at  $20^\circ\text{C}$ , however, and the smaller amounts of water recovered from films pre-treated at  $170^\circ\text{C}$  are consistent with the lower water content of these films. The lack of equimolar correlation in the present studies is in accord with the idea that only water adjacent to photoadsorption sites will be displaced. In other words, surface water or OH groups do not, themselves, constitute a site for oxygen photoadsorption.

The amount of oxygen photoadsorbed is not increased by evacuation at  $170^\circ\text{C}$  instead of  $20^\circ\text{C}$ . The  $170^\circ\text{C}$  evacuation merely provides more definite confirmation of a water displacement reaction, since it is no longer necessary to estimate (20) a correction for thermally desorbed water. The photoadsorption of ethylene does not appear to affect the bond between adsorbed water and the surface. Circumstantially this may indicate that the sites for oxygen photoadsorption either differ from, or are not all available for, ethylene photoadsorption.

Oxygen and ethylene were photoadsorbed on films whose only pre-treatment was the standard evacuation at  $170^\circ\text{C}$ . The uptakes involved were of the order  $40\text{--}50 \mu$  moles per g.  $\text{TiO}_2$  and  $20 \mu$  moles per g.  $\text{TiO}_2$  respectively. The  $\text{TiO}_2$  had a B.E.T. surface area of  $100 \text{ m}^2/\text{g}$ . On the assumption that there were approximately  $10^{19}$  surface titanium ions per  $\text{m}^2$ , this means that there were approximately  $10^{21}$  surface metal ions per g. On this basis the surface

coverage during photoadsorption of ethylene or of oxygen is very small and of the order of a few percent or less, even if the molecules dissociate on adsorption or are bound to more than one surface atom. The specific nature of the photoadsorption sites, and the probability that they are related to the defect nature of the surface, is emphasised by these low coverages. Maclean has reported (20) a similarly low concentration (170 per g.) of sites for oxygen photoadsorption on another sample of  $\text{TiO}_2$ .

The photoadsorptions of oxygen and of ethylene were irreversible in that neither oxygen nor ethylene were recovered on evacuation at  $170^\circ\text{C}$ . Nevertheless, this treatment (page 23) resulted in a partial renewal of the capacity of the solid for further photoadsorption (page 36). Since no detectable desorption occurred, the treatment at  $170^\circ\text{C}$  must either have generated new adsorption sites or regenerated original sites by, for example, causing a surface migration of photo-adsorbed species. A similar effect has been observed (33) in the case of hydrogen photoadsorbed on  $\text{TiO}_2$ . A process akin to the second suggestion is the more likely, since films pretreated at  $250^\circ\text{C}$  and  $170^\circ\text{C}$  did not differ in their capacity for ethylene photoadsorption, whereas a  $250^\circ\text{C}$  evacuation subsequent to an ethylene photoadsorption was generally the more effective in renewing photo-adsorptive capacity. No ethylene or oxidation products were obtained on  $250^\circ\text{C}$  evacuation.

#### Photoconductance in titanium dioxide

When semiconductors are illuminated with radiation of a suitable wavelength an increase in the conductivity of the solid is observed (e.g. Refs: (1) (2) (42) (63) and present results). In the case of an n-type semiconductor, this is a

reflection of an increased concentration of electrons in the conduction band. Adsorption of light quanta has excited electrons into the conduction band and, at the same time, produced positive holes in either the valence band or at a localised impurity level. The photoconductive<sup>ity</sup> rises rapidly at first and then more slowly; a constant value of photoconductance is attained only after prolonged illumination. The final photoconductance developed is the result of an equilibrium between at least two processes,

- (1) Generation of photoelectrons and positive holes.
- (2) Recombination of photoelectrons with positive holes.

The recombination process (2) proceeds by a slower mechanism than (1) and the final result of illumination is to increase the equilibrium concentration of electrons in the conduction band.

In addition, electrons may be removed from the conduction band by shallow surface "traps" (47). On an energy basis these may be situated just below the bottom of the conduction band. Electrons can be thermally excited from these traps into the conduction band. The slow decay of photoconductance on ceasing illumination can be explained on this basis. Alternatively, the slow photoconductance decay is explicable solely on the basis of a slow recombination between electrons and positive holes.

It is further proposed here that all the original electronic states may never be regained once the solid has been illuminated. It is possible that on ceasing illumination the electrons are removed from the conduction band fairly rapidly by surface traps and then more slowly by deeper traps from which they can be promoted later by illumination. A series of such traps could exist at levels below the conduction band of the same order as that of the original

FIG 32.

POSSIBLE ELECTRONIC TRANSITIONS IN  $TiO_2$ .

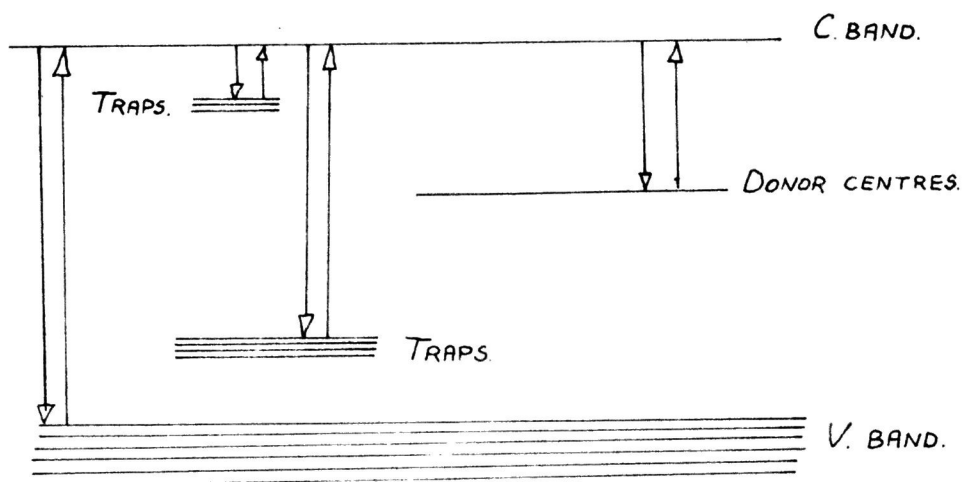
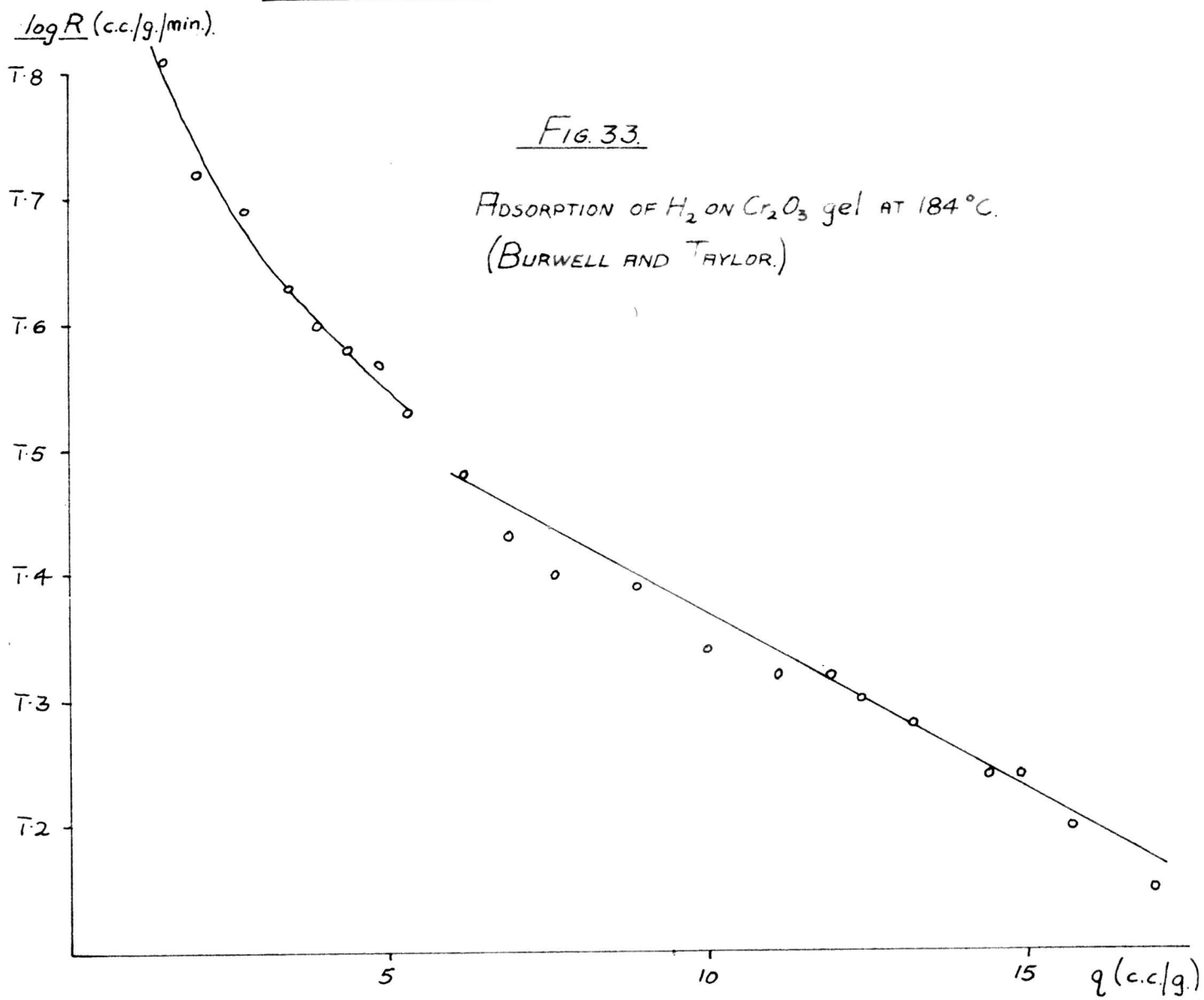


FIG. 33.

ADSORPTION OF  $H_2$  ON  $Cr_2O_3$  gel AT  $184^\circ C$ .  
(BURWELL AND TAYLOR.)



donor levels.

Shallow surface traps are known to exist (11) (40) on  $\text{TiO}_2$  and to be responsible for some observed infra-red adsorption bands. The faster rate of photoconductance development on re-illumination of  $\text{TiO}_2$  during the decay period (Fig.24) suggests that under these conditions photoelectrons are being excited from traps whose response to illumination is faster than that of the original donor centres. It is, therefore, suggested that deeper traps for conduction electrons exist on the  $\text{TiO}_2$  surface involved in the present investigations.

It has been mentioned on page 6 that there is a difference of opinion as to the source of photoconductance electrons in  $\text{TiO}_2$ . There is no definitive evidence as to whether positive holes are produced in the valence band or at localised impurity levels. Possible electronic transitions in illuminated  $\text{TiO}_2$  are postulated in Fig.32 on the basis of the considerations outlined above.

Positive holes in the valence band will be mobile and available to contribute towards a photoconductance. Those at impurity levels will normally be located at specific points on the solid and will not normally constitute conducting species. The fact that oxygen completely destroys the photoconductance of  $\text{TiO}_2$  (page 59) suggests that the positive holes produced on illumination do not contribute to the photoconductance. It is, therefore, proposed that on illumination, electrons are raised from impurity levels rather than the valence band.

It is apparent from the present results that the measured conductivity is a surface conductivity, since it is completely suppressed by oxygen photo-adsorption at  $20^\circ\text{C}$ . At this temperature adsorbed oxygen will not affect the bulk properties of the solid.

### Kinetics of photoadsorption

All the photo-uptakes measured were initially described (pp. 30 to 34) by a parabolic uptake against time relationship:

$$(q + q_0)^2 = kt + q_0^2$$

where  $q$  = uptake at time  $t$ .

$k$  = constant

and  $q_0$  is a small constant or zero.

This was followed by a stage which fitted the Elovich equation:

$$\frac{dq}{dt} = ae^{-\alpha q} \quad (\underline{a} \text{ and } \alpha \text{ are constants})$$

in so far as a plot of  $\log \left(\frac{dq}{dt}\right)$  against  $q$  was linear during this stage. The integrated form of the Elovich equation can be written:

$$q = \frac{2.3}{\alpha} \log (t+t_0) - \frac{2.3}{\alpha} \log t_0$$

where  $t_0 = \frac{1}{\alpha a}$ , and in the second stage of the uptake a plot of  $q$  against  $\log (t+t_0)$  should be linear, provided that a suitable value of the disposable parameter  $t_0$  is chosen. The gradient of this plot will give a value of  $\alpha$ , and a value of  $\underline{a}$  can then be obtained from the relationship  $\underline{a} = \frac{1}{\alpha t_0}$ . This value of  $\underline{a}$  should be the observed initial rate of exponential uptake. The application of the equation in this integrated form should be quantitatively more precise than in the differentiated form; at advances stages in the uptake the graphical calculation of the small rate values involved becomes highly imprecise. Nevertheless, plots of  $\log \left(\frac{dq}{dt}\right)$  against  $q$  may be used to demonstrate the qualitative applicability of the Elovich equation to the data (cf. Figs. 11 and 15).



Generally the integrated form of the Elovich equation is applied to chemisorption data with a  $t_0$  value chosen to give a linear plot over the entire course of the adsorption. The calculated  $a$  values so obtained are normally much less than the initial experimental rates. Thus, in analysing the figures of Burwell and Taylor for  $H_2$  chemisorption on  $Cr_2O_3$  at  $184^\circ C$ , Taylor and Thon have chosen (49) a  $t_0$  value, 22, which gives a linear  $q$  against  $\log(t + t_0)$  plot over the entire chemisorption. The resultant  $a$  value (0.54 cc/g/min.) is much less than the initial experimental rate (1.5 cc/g/min.). Taylor and Thon did not produce a plot of  $\log(\frac{dq}{dt})$  against  $q$  but when this is done (Fig.33) it can be seen that there is a discontinuity at  $q \sim 6$  cc/g, with an approximately linear plot only for  $q$  values  $> 6$  cc/g. This, in the light of the present studies, is taken to mean that the Elovich equation is not obeyed in the initial stages of the chemisorption. In fact, in analogy with the present photoadsorption on  $TiO_2$ , the uptake from  $q = 0$  to  $q = 5.5$  cc/g./min. can be adequately described by the parabolic expression:

$$(q + 1.3)^2 = 4.1 t + 1.7$$

The integrated form of the Elovich equation was applied to this chemisorption and to the present photoadsorptions as follows. The Elovich kinetics were considered to commence at a time  $t_1 = 0 = (t - I)$ , where  $I$  is the time for which parabolic kinetics hold. (The time  $I$  was found by fitting the parabolic expression into the original data). It was then found that a value of  $t_0$  exists such that a plot  $q$  against  $\log(t_1 + t_0)$  is linear from  $t_1$  onwards and has a gradient  $\frac{2.3}{\alpha}$ . The values of  $t_0$  and  $\alpha$  are such that  $\frac{1}{t_0 \alpha} = \frac{a}{\alpha}$  is in

TABLE 22

Elovich parameters for a selection of typical photoadsorptions

	I	$\alpha$	a	R	$\alpha^1$	$a^1$	$R^1$	$\alpha^{11}$	$a^{11}$	$R^{11}$
1. O <sub>2</sub> on untreated film (Table 1)	900	0.17	0.006	0.006	0.13	0.002	0.002			
2. O <sub>2</sub> on C <sub>2</sub> H <sub>4</sub> - treated film (Table 8)	7	✓ 0.14	0.20	0.20	✓ 0.01	✓ 0.044	0.043	✓ 0.075	✓ 0.015	✓ 0.013
3. O <sub>2</sub> on C <sub>3</sub> H <sub>6</sub> - treated film (Table 7)	6	0.12	0.33	0.33	0.15	0.16	0.16			
4. C <sub>2</sub> H <sub>4</sub> on untreated film (Table 3)	250	0.94	0.013	0.013	0.59	0.003	0.003			
5. C <sub>2</sub> H <sub>4</sub> on O <sub>2</sub> - treated film (Table 6)	10	0.29	0.17	0.17	0.36	0.05	0.05	0.43	0.003	0.003
6. C <sub>3</sub> H <sub>6</sub> on O <sub>2</sub> - treated film (Table 5)	14	✓ 0.36	0.09	0.09	0.40	0.01	0.01			

very close agreement with the experimental rate at time  $t_1$ . This general pattern held for all the photoadsorptions studied on  $\text{TiO}_2$ . In most cases, a further characteristic of the Elovich plots is evident. The plots of  $q$  against  $\log(t_1 + t_0)$  consisted of two, or sometimes three, distinct linear portions with correspondingly different values of  $\alpha$ . The second and third portions could be represented by a value  $\alpha^1$  and a value  $t_0^1$ , where  $t_0^1$  is the sum of  $t_0$  and the time for which the previous Elovich section(s) had been in force. Here again the value of  $\frac{1}{t_0^1 \alpha^1} = \underline{a}^1$  was in good agreement with the experimental rate at the time of the break in the plot.

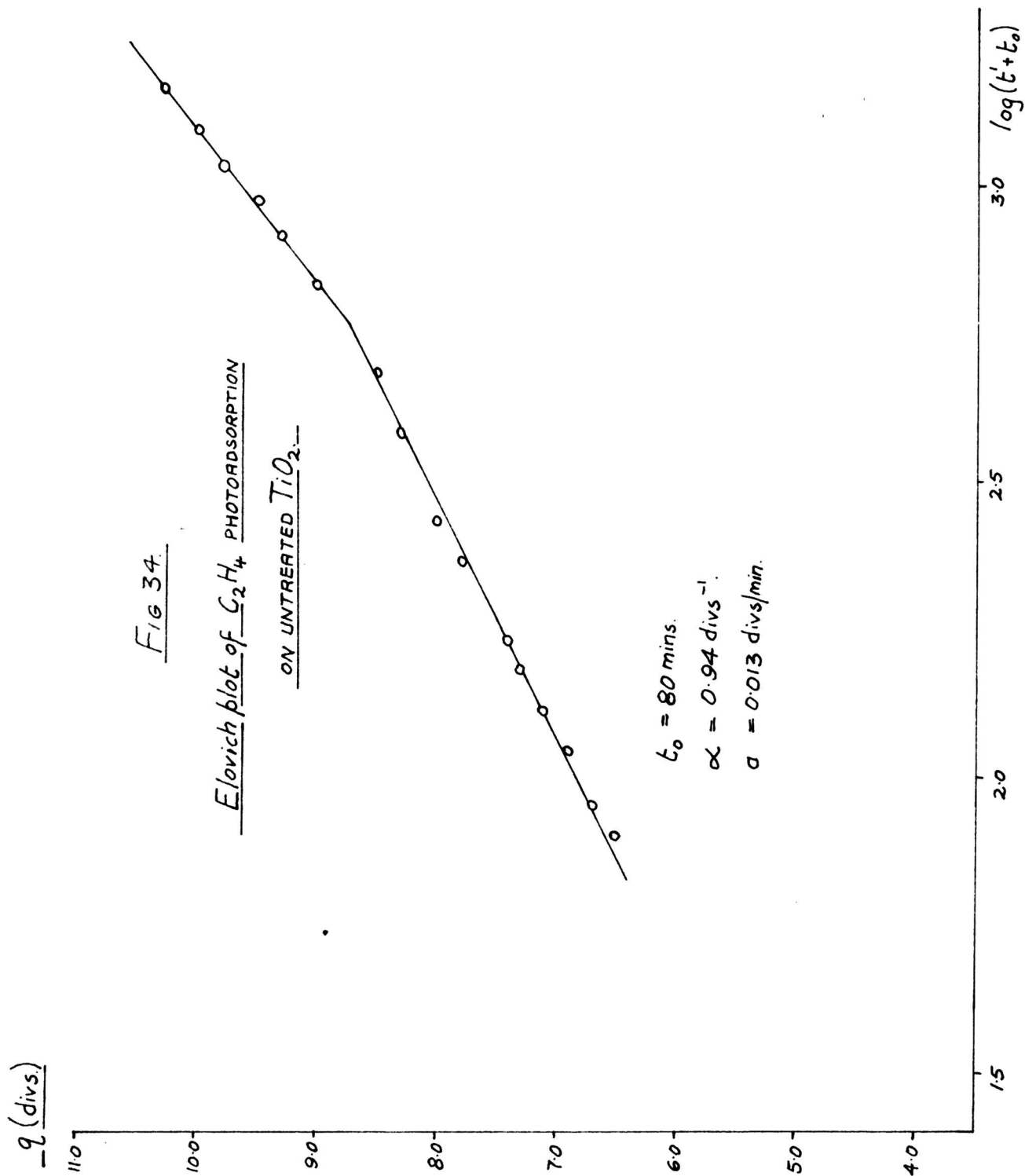
Fig.34 serves as an example of the type of Elovich plots which are obtained; the data are those of the ethylene photoadsorption of Table 3.

The total photoadsorption can, in each case, therefore, be represented by an initial stage which obeys parabolic kinetics and thereafter by two or more stages described by the Elovich equation with appropriate values of  $\alpha$  and  $\underline{a}$ .

Examples of the results obtained are given in Table 22, for a selection of the various types of photoadsorption. Here  $I$  is in minutes,  $\alpha$  values are in  $\text{divs}^{-1}$  and  $\underline{a}$  values are in  $\text{divs}/\text{min}$ .  $R(\text{divs}/\text{min.})$  is the experimental rate which should correspond to  $\underline{a}$ . The quantities  $\alpha^1$ ,  $\underline{a}^1$  and  $R^1$  refer to a second Elovich section and  $\alpha^{11}$ ,  $\underline{a}^{11}$  and  $R^{11}$  to a third Elovich section (where this occurs).

The initial parabolic kinetics for each of the photoadsorptions in Table 22 are given by :

1.  $(q - 0.2)^2 = 0.11t$
2.  $q^2 = 1.15t - 0.2$
3.  $q^2 = 1.75t - 0.4$
4.  $(q + 1.15)^2 = 0.23t + 1.3$



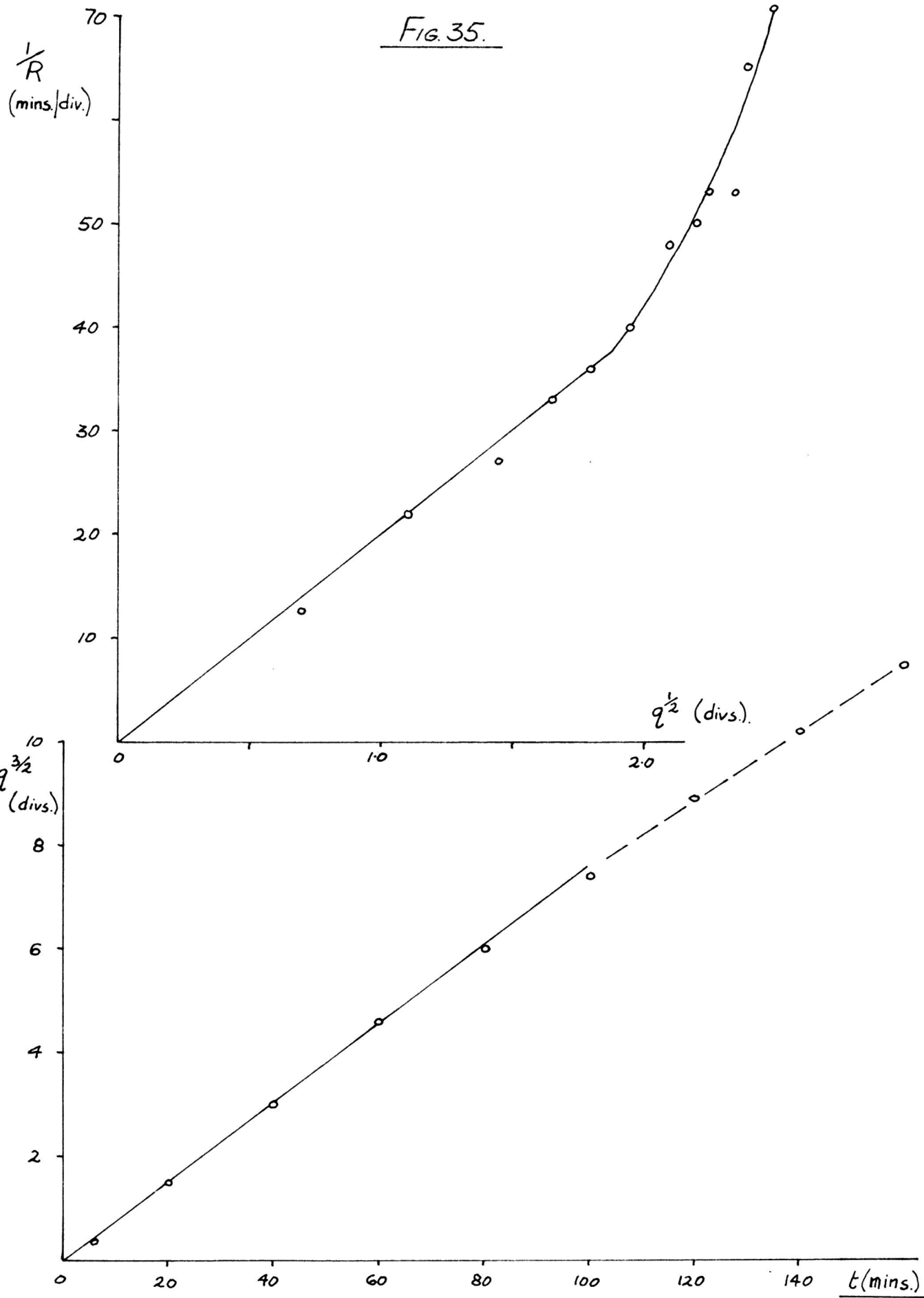
$$5. (q + 0.7)^2 = 1.8t + 0.5$$

$$6. (q + 0.43)^2 = 0.45t + 0.2$$

The data for the chemisorption of  $H_2$  on  $Cr_2O_3$  can be analysed in the same way. The parabolic kinetics end at a time  $I = 11$  mins. A  $t_0$  value of 47 gives an unbroken Elovich plot for the remainder of the chemisorption. The resultant  $a$  value of 0.32 cc./g./min. is in exact agreement with the experimental rate at  $t = 11$  mins.

The data of Kennedy (32) for oxygen photoadsorption on  $TiO_2$  are amenable to a similar analysis; again excellent agreement between  $a$  values and experimental rates is obtained. On the other hand some of the oxygen photoadsorptions of Maclean (20) on a third sample of  $TiO_2$  did not fit parabolic kinetics closely over their initial stages. In more recent preliminary investigations (62) on yet another sample of  $TiO_2$  it has been found necessary to employ excessively large values of  $q_0$  before parabolic kinetics will describe the initial stages of ethylene photoadsorption; an expression of the type  $q^{\frac{3}{2}} = kt$  was found to describe the initial stages more accurately and the remainder of the uptake obeyed normal parabolic and eventually Elovich kinetics. Parabolic kinetics are consistent with a rate which is related linearly to  $1/q$ , whereas the  $q^{\frac{3}{2}}$  type of kinetics is consistent with a rate related linearly to  $1/q^{\frac{1}{2}}$ . Examination of the photoadsorptions quoted in Table 22 demonstrates that in at least one instance expressions involving  $q^{\frac{3}{2}}$  describe the initial section of the pre Elovich stages as adequately as do the parabolic kinetics. (Fig.35). The photoadsorption data illustrated on Fig.35 are those of ethylene on untreated  $TiO_2$ .

FIG. 35.



Possible significance of the kinetics

In the context of the photoadsorptions on  $\text{TiO}_2$  the form of the kinetics appears to vary from sample to sample, especially with regard to the initial stages. Charman and Dell have reported (64) parabolic kinetics for oxygen adsorption on irradiated  $\text{NiO}$ , but have attached no fundamental significance to them. In the case of the photoadsorptions on  $\text{TiO}_2$  it is, therefore, suggested that the eventual Elovich kinetics are the characteristic property of the processes.

It may be noted here, however, that the kinetics of oxygen photoadsorption on  $\text{TiO}_2$  have previously been interpreted in terms of an activated surface migration of adsorbed oxygen, this migration being initially rate-determining and responsible for the parabolic kinetics (page 11). The rate of migration of adsorbed species over a limited area of surface covered with a quantity  $q$  of adsorbed gas will be proportional to  $\frac{1}{q}$  and parabolic kinetics will result. On the other hand, where adsorbed species are migrating outwards from the centre of a circular area of surface with steadily increasing radius ( $r$ ) their rate of migration will be proportional to  $\frac{1}{r}$  and hence to  $\frac{1}{q^{1/2}}$ , where  $q$  is the amount of adsorbed oxygen in the area of radius  $r$ . The data of photoadsorption do not allow a choice to be made between these two alternatives.

In fact, the wider application of these kinetics to hydrocarbon photoadsorption suggests that the parabolic kinetics may have no physical significance, and that a less specific mechanism might be necessary. Since all the photoadsorptions involve an electronic rearrangement in the surface layers of the solid, it is possible that the observed kinetics are a reflection of a slow attainment of electronic equilibrium under illumination and in the presence of

adsorbed species. The Elovich kinetics are of more mechanistic significance from this viewpoint than are the kinetics of the initial stages.

It has been mentioned on page 18, that several proposed mechanisms of chemisorption lead to Elovich kinetics and it would be highly speculative to interpret these kinetics in terms of a unique mechanism. Melnick has shown (42) (56) that Elovich kinetics can result from electrons having to surmount a potential energy barrier whose height increases with coverage. In view of the undoubted electronic nature of the photoadsorptions such an explanation is favoured in the present instance.

The existence of "breaks" in Elovich plots has been taken (49) as evidence for the presence of distinct types of adsorption site. The constant  $\alpha$  has been taken as a measure of the deceleration of the chemisorption. If Elovich kinetics are due to an increasing energy of activation as photoadsorption proceeds, then the  $\alpha$  value will be related to the rate at which the energy of activation increases with coverage. The distinct linear portions in the Elovich plots will then represent distinct types of site with consecutively increasing initial energies of activation for chemisorption and corresponding values of  $\alpha$ . It may be noted that  $\alpha$  need not increase with consecutive linear portions, although the value of the initial activation energy for a set of sites must do so.

The form of the Elovich kinetics for the photoadsorptions on  $\text{TiO}_2$  suggests that the various types of site are not filled concurrently, but rather that one set of sites becomes practically exhausted before photoadsorption commences on a second set. Such an extreme situation will not hold in practice but the indication is that the sets of sites differ markedly in initial energy of activation for photoadsorption. It is possible that photoactive electrons (or



positive holes) are located preferentially at one type of site until this type is practically exhausted.

It is difficult, in the absence of information on the structure of the  $\text{TiO}_2$  surface, to suggest how the sites might differ physically. However, Yates has reported (30) that two types of OH group are present on anatase surfaces and he has suggested that this might be related to a difference between crystal faces. The work of Haber and Stone (37) has shown the difference in activity with crystal face for oxygen adsorption on  $\text{NiO}$ . Each linear portion in the Elovich plots of the present photoadsorption might relate, therefore, to photoadsorption on a particular crystal face; the presence of both anatase and rutile in the sample could lead to further types of adsorption site. "Pre-treatment" of the  $\text{TiO}_2$  films could also be expected to provide yet another type of site and it is noteworthy that only such films provided three linear portions (Table 22).

#### Mechanism of photoadsorption

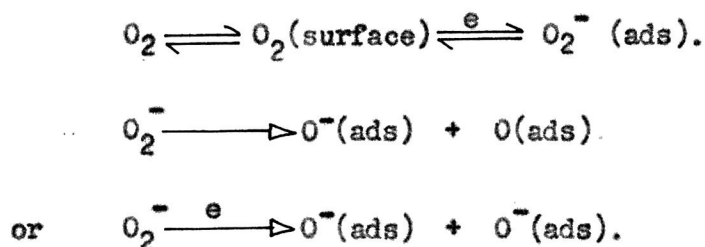
##### 1. Oxygen

The very rapid increase in photoresistance which occurs (page 60) when oxygen is admitted to illuminated  $\text{TiO}_2$  confirms that the photoadsorption of oxygen involves electron transfer from solid to gas. Possible structures for the photoadsorbed oxygen are  $\text{O}_2^-$ ,  $\text{O}^-$  or  $\text{O}^{2-}$ .

When the illuminated solid is evacuated immediately after the completion of a photoresistance increase caused by admission of oxygen, a gradual decrease in resistance occurs (Figs. 28 and 29). At this stage the photoadsorption of oxygen is obviously reversible. Other evidence (pages 35 and 60) indicates that

on prolonged illumination oxygen is photoadsorbed as an irreversible species. The chemisorption of oxygen on oxides as  $O_2^-$  and  $O^-$ , with formation of  $O_2^-$  at higher temperatures has been proposed by several authors (35) (65). The  $O_2^-$  species is to be regarded as an adsorbed surface species distinct from lattice oxygen; incorporation of adsorbed oxygen into the lattice is considered to take place at still higher temperatures. The general consensus of opinion is that  $O_2^-$  will be a reversibly chemisorbed and catalytically active species, whereas  $O^-$  will be more strongly chemisorbed and consequently less active catalytically (65), but a similar relationship has been proposed (35) for the  $O^-$  and  $O_2^-$  species respectively.

It is suggested that, in the present investigations, the most probable form for the reversibly photoadsorbed oxygen is  $O_2^-$  and that this becomes irreversibly converted to  $O^-$  or a related species on prolonged illumination:



The last of these reactions involves the localisation of a second electron from the solid. It might be expected that a slow increase in photoresistance would occur on prolonged illumination if this reaction took place. The measurements of photoresistance during prolonged illumination in oxygen show marked non-reproducibility, but the suggestion is that no further extensive increases in photoresistance occur. (Non-reproducibility at this stage is possible connected with changes in the surface water content; the pellets

used here were evacuated at 20°C only and will have a high water content). It is shown a little later that this result is still consistent with the formation of two adsorbed  $O^-$  species, since electrons can be imagined to come from levels in which they are not directly available to contribute towards a photoconductance.

Irreversibly photoadsorbed oxygen was responsible for an increased ethylene photo-uptake but no oxidation products were detected unless the conditions were such as to bring photoadsorbed ethylene into contact with freshly photoadsorbed oxygen. In contrast, irreversibly photoadsorbed oxygen appears capable of photoadsorbing and photo-oxidising propylene on the surface. The experiment (page 48) which compares the rates of separate photo-uptake of oxygen and propylene with the rate of pressure decrease in a gas phase where both are present, however, provides inconclusive evidence that freshly photoadsorbed oxygen is more reactive than oxygen photoadsorbed over a longer period of illumination. These results are again indicative of two types of photoadsorbed oxygen. In line with current ideas it is suggested, as above, that  $O_2^-$  is the reversibly photoadsorbed and more reactive form.

It is appropriate, at this point, to point out that conductivity experiments (page 58) provide evidence for a small adsorption of oxygen in the dark at 26°C. This adsorption is rapid and is not reversed by evacuation at 20°C. A third type of oxygen adsorption is evident. The dark pressure decreases which occur in propylene-oxygen mixtures in contact with  $TiO_2$  suggest that this third form is reactive. There is the possibility that the same type of adsorbed oxygen is involved but that the source of electrons differs from that which provides the photoelectrons.

It was established (page 61) that a small amount of photoadsorbed oxygen is effective in completely suppressing the photoconductance. This shows that

relatively few electrons are available for photoconduction. The situation can be described in terms of surface traps for photoelectrons and a comparison can be drawn with the photoconduction scheme proposed earlier. It is suggested that photoelectrons in the conduction band are in equilibrium with electrons trapped at lower levels (cf. page 69). Admission of oxygen to a pre-illuminated sample removes conduction electrons rapidly and upsets the electronic equilibrium between trapping levels and conduction band.

The subsequent rate of photo-uptake of oxygen is determined by the rate of excitation of electrons from these lower levels to the conduction band. The rate of excitation will decrease with an accumulation of negatively charged surface oxygen and Elovich kinetics will be encountered. (42), (56).

The previous paragraph has considered the case where electronic equilibrium is established under illumination before oxygen is admitted to the sample. It has been pointed out on page 61 that in a typical photo-uptake experiment oxygen is admitted before this equilibrium is attained; during the course of the photo-uptakes, therefore, the generation of photoelectrons from donor levels will still be proceeding. Again it is suggested that the rate of generation of photoelectrons on a surface with increasing content of negatively charged adsorbed oxygen controls the overall photo-uptake. A small photocurrent is in fact developed (Fig.26) under these conditions and it appears that some electrons do not become available to photoadsorb oxygen immediately on their excitation to conduction levels.

The general shape of the oxygen photo-uptake curve does not alter if the  $\text{TiO}_2$  film is illuminated overnight before the admission of oxygen. (Work by Macfarlane (62) shows, however, that in some instances such pre-illumination has the effect of replacing an initial  $(q + q_0)^2$  relationship by a  $q^{\frac{3}{2}}$  against

time relationship). On the basis of the preceding discussion this would indicate that the rate of photo excitation of electrons from donor levels does not differ markedly from the rate at which trapped electrons are raised to the conduction band.

## 2. Ethylene

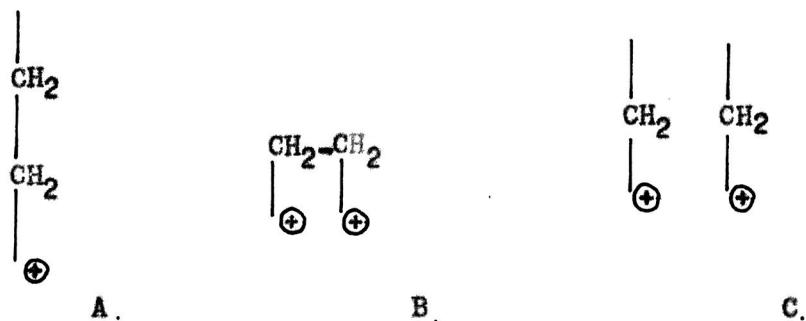
Any discussion as to the mechanism of ethylene photoadsorption is limited by lack of information as to the form in which the gas is attached to the surface. No ethylene adsorption was observed on  $\text{TiO}_2$  at  $25^\circ\text{C}$  unless the system was illuminated. Since the gas itself does not absorb the wavelengths employed, the photo effect is, therefore, a result of radiation absorbed by the solid. The conduction levels of the solid are not involved in the photoadsorption since ethylene does not affect the photoconductance of  $\text{TiO}_2$ . The photoadsorption must, therefore, involve interaction between ethylene and the positive holes produced at donor levels. A similar type of adsorption has been suggested (47) for hydrogen and isobutene adsorption on  $\gamma$ -irradiated  $\text{ZnO}$ . Work on other systems (48) suggests that the dark chemisorption of unsaturated hydrocarbons on oxides involves electron donation from the adsorbed molecule to the surface.

If the final photoconductance of  $\text{TiO}_2$  illuminated in vacuo is a result of an electronic equilibrium between electron generation by light absorption and electron recombination with positive holes, then ethylene photoadsorption would be expected to upset this equilibrium. A change in photoresistance would be observed (47). Since no change in photoresistance is observed experimentally, it is unlikely that the generation and recombination processes are in simple equilibrium.

At least one explanation is possible. Electron-hole recombination is slow and after several hours illumination in vacuo practically all the donor levels have been emptied; electrons in the conduction band are in equilibrium with electrons in trapping levels. No photodesorption or thermal desorption of ethylene was observed and trapping of photoelectrons by positive holes which have reacted with ethylene does not appear to occur to any extent. This explanation again calls for the existence of surface traps which can localise photoelectrons, and such traps have already featured in the discussion on photoconductance and oxygen photoadsorption.

The colour change observed (page 55) in  $\text{TiO}_2$  when ethylene is photoadsorbed on it suggests that the surface of the dioxide is reduced during the photo-uptake. This is consistent with a higher surface concentration of electrons when ethylene combines with positive holes, the extra electrons being localised at specific adsorption sites and not available to contribute towards the photoconduction. The reversal of the colour change on evacuation at  $170^\circ\text{C}$  indicates a change in the character of the ethylene-surface bond, although this does not result in the desorption of ethylene.

In analogy with the schematic representation of Wolkenstein (66) possible forms of photoadsorbed ethylene are:



where  $\oplus$  represents a positive hole. Forms B and C can only be produced at

sites where positive holes are located in close proximity to one another. Wolkenstein's ideas would predict that forms A and C would be reactive and available for photo-oxidation by adsorbed oxygen. It is found experimentally that photo-oxidation of the photoadsorbed ethylene does occur (page 35).

In analogy with the general discussion on the mechanism of oxygen photoadsorption it is proposed that the slow photo-uptake of ethylene is a result of the slow generation of available positive holes in the surface of the illuminated solid. A gradually increasing concentration of electrons and adsorbed ethylene at the surface will result in a progressive decrease in the rate of generation of photoelectrons and positive holes. Elovich kinetics will be a reflection of the increasing difficulty with which positive holes are produced.

### 3. Ethylene and propylene on oxygen-pretreated $\text{TiO}_2$

Whereas ethylene was photoadsorbed on fresh  $\text{TiO}_2$  surfaces, no photoadsorption of propylene was normally observed unless the solid had been pretreated by a photoadsorption of oxygen. The rate and extent of ethylene photoadsorption were increased by such a pretreatment with oxygen. The irreversibly photoadsorbed oxygen was active in this respect (cf. page 33).

On the supposition that photoadsorption of oxygen will produce species of the type  $\text{O}^- \oplus$ , it appears that ethylene will react with positive holes alone, whereas propylene requires the presence of a surface  $\text{O}^-$  species. This is discussed further in the section on photo-oxidation. It is obvious that positive holes produced by prior oxygen photoadsorption are not available as such until the solid is again illuminated, since no dark adsorption of either hydrocarbon was observed.

Some photo-oxidation of propylene was observed under these conditions

(page 36 ). A colour change analogous to that occurring during an ethylene photoadsorption on fresh  $\text{TiO}_2$  was observed during photoadsorption of either hydrocarbon on oxygen pre-treated films. In the propylene case the reversal (evacuation at  $\leq 170^\circ\text{C}$ ) of this colour change before desorption of products had taken place indicates that this reversal was a result of a change in the character of adsorption.

The kinetics of both photoadsorptions were identical in form with those of the photoadsorption on untreated films. It is reasonable to suppose that the electronic nature of the photoadsorptions again leads to this type of kinetics.

#### 4. Oxygen on hydrocarbon-treated $\text{TiO}_2$

The situation here is complicated by the fact that a photo-oxidation reaction is involved in addition to a simple photoadsorption. If it is assumed that ethylene and propylene combine with photo-produced positive holes in a largely irreversible reaction (page 36) then the electrons originally excited from donor levels will not recombine with those positive holes which have reacted with hydrocarbon molecules. On discontinuing illumination they will be trapped at levels from which it is conceivable that they may be regenerated in positions more available to photoadsorb further oxygen.

Added to this is the possibility that limited surface migration of photoadsorbed oxygen towards photoadsorbed hydrocarbon may take place. Photo-oxidation of the hydrocarbon and regeneration of oxygen photoadsorption sites would result.

Direct reaction between gas phase oxygen and photoadsorbed hydrocarbon does not seem likely. This reaction might be expected to occur in the dark, but the observed oxygen uptake is a photo effect. Added to this, the identical form of the kinetics suggests that an electronic property of the solid surface is again involved.



Photo-oxidations on TiO<sub>2</sub>

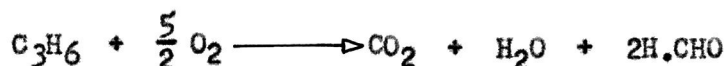
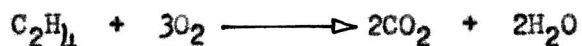
It has been shown in the present investigations that photo-oxidation of ethylene and of propylene occurs in the presence of oxygen and of illuminated TiO<sub>2</sub> at 25°C. Oxygen photoadsorbed on TiO<sub>2</sub> which has previously photoadsorbed hydrocarbon has been shown qualitatively (page 35) to be capable of photo-oxidising the pre-adsorbed hydrocarbon. In addition, some photo-oxidation appears to occur when propylene is photoadsorbed on a TiO<sub>2</sub> surface which contains previously photoadsorbed oxygen, although this is not observed with ethylene.

The products of photo-oxidation under the above conditions were CO<sub>2</sub>, water and formaldehyde, and these were not desorbed in detectable amount until the solid was evacuated at 170°C. A surface reaction between photoadsorbed species is indicated.

In the case of propylene a series of 170°C evacuations appears (page 44) to deactivate the photoadsorbed species until the solid becomes saturated with respect to separate photoadsorptions of propylene and oxygen. No comparable results are, as yet, available for ethylene. In general, however, for each hydrocarbon a series of alternate hydrocarbon-oxygen photoadsorptions could be carried out (in the absence of 170°C evacuations). The total pressure decreases measured in such a series corresponded to an uptake many times greater than the capacity of the fresh solid for hydrocarbon or oxygen photoadsorption. A process of site generation and/or regeneration is indicated here.

The amounts of reactants and products in these systems is relatively small (1-5  $\mu$  moles). It was only when more extensive reaction had taken place that quantitative results of any significance were obtained. Thus, large pressure

decreases occurred when ethylene-oxygen or propylene-oxygen mixtures were in contact with illuminated  $\text{TiO}_2$  at  $25^\circ\text{C}$ . When such illuminations were carried out for prolonged periods, analysis of the amounts of reactants and products indicated that ethylene and propylene were being photo-oxidised according to the equations:



It must be pointed out, however, that in one series of experiments (page 40) an incomplete oxidation of ethylene to  $\text{CO}_2$ , water and formaldehyde was encountered, even although oxygen was in large excess in the gas phase. The amounts of reactants and time of illumination were smaller in these experiments, but the anomalous nature of the results here is not at all clear.

In experiments where hydrocarbon-oxygen mixtures are illuminated over  $\text{TiO}_2$  it is again evident that reactants and products were held on the surface in amounts much greater than those corresponding to the capacity of the film for hydrocarbon or oxygen photoadsorption. Products of the reaction were held on the surface until extensive pressure decreases had occurred; the gradual decrease in the rate of the observed pressure decrease could be due to blocking of surface sites in the initial period of reaction, coupled with a desorption of products in later stages.

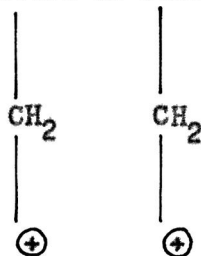
A surface reaction between photoadsorbed hydrocarbon and a photoadsorbed oxygen species ( $\text{O}_2^-$  or  $\text{O}^-$ ) is again indicated. The probability that oxygen

is initially photoadsorbed in a specially reactive form has already been discussed. The dark pressure decreases which occur in propylene-oxygen mixtures over  $\text{TiO}_2$  provide further evidence of some type of reactive, intermediate adsorbed species or complex, since this dark reaction occurs over dioxide which is saturated with respect to separate propylene and oxygen photoadsorptions. The extensive photoreaction which follows the dark reaction under these circumstances could be a result of a reaction involving especially reactive photo-adsorbed species (perhaps  $\text{O}_2^-$ ), or else a result of surface modification brought about by the dark reaction.

In the light of these complexities it is not at present possible to elucidate the mechanism of the photoreactions. That the mechanism will indeed be complex is obvious from the fact that several adsorbed oxygen species must be involved in the photo-oxidation of one hydrocarbon molecule. It is probable that reaction proceeds after surface migration of adsorbed oxygen towards adsorbed hydrocarbon, and in this event it is probable that  $\text{O}_2^-$  (ads.) would be utilised wherever possible.

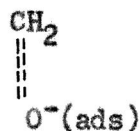
A tentative and schematic outline of a possible path for each photoadsorption is now presented.

Ethylene is photoadsorbed on surfaces which have not been pre-treated with oxygen, a process represented as follows :



It is now proposed that each of these species reacts with photoadsorbed

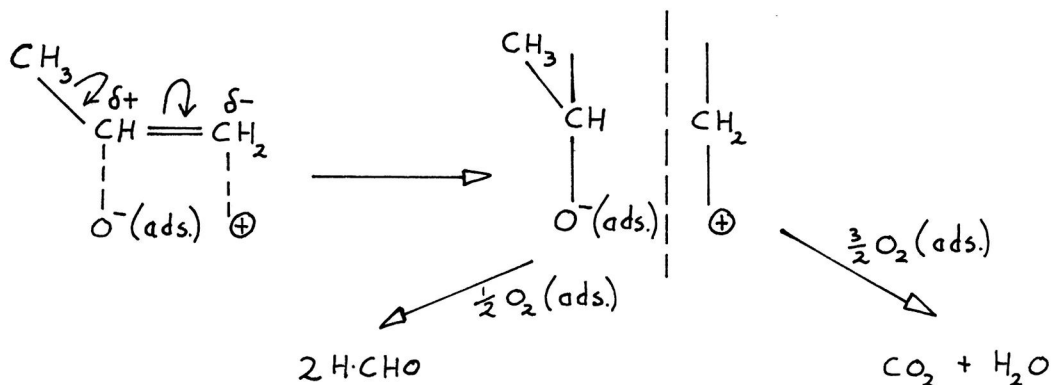
oxygen to give  $\text{CO}_2$  and  $\text{H}_2\text{O}$ . On a surface which has been pretreated with oxygen, photoadsorbed species of the form :



may be present, giving rise to  $\text{H}\cdot\text{CHO}$ .

It should be noted here that extensive oxidation of photoadsorbed  $\text{H}\cdot\text{CHO}$  was not observed at  $25^\circ\text{C}$ ; photoadsorption of  $\text{H}\cdot\text{CHO}$  was largely reversible at  $25^\circ\text{C}$ . This result is in agreement with the suggested scheme for ethylene photo-oxidation if it is assumed that photoadsorbed  $\text{H}\cdot\text{CHO}$  is attached to the surface via its oxygen atom and that such a surface species is not photo-oxidisable at  $25^\circ\text{C}$ . Partial oxidation of a  $(-\text{CH}_2 - \oplus)$  species is taken to produce a  $(\text{O}-\text{CH}_2 -)$  intermediate attached to the surface by a carbon atom; within the context of the preceding picture of ethylene oxidation, such a species will be photo-oxidisable at  $25^\circ\text{C}$ .

Propylene, on the other hand, is photoadsorbed only on surfaces which contain photoadsorbed oxygen. It is suggested that propylene photoadsorption and subsequent photo-oxidation involve reactions of the type:



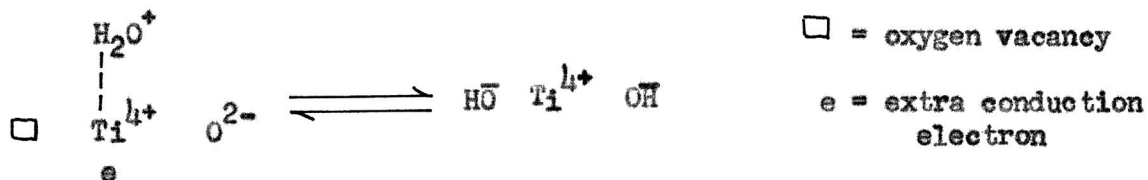
Again the (  $-\text{CH}_2 - \oplus$  ) species reacts to give  $\text{CO}_2$  and  $\text{H}_2\text{O}$ . It is suggested that the other section of the molecule is photo-oxidised via formation of two species of the type (  $\text{CH}_2 \equiv \text{O}^-(\text{ads})$  ), and in line with the ethylene analogue this will result in the formation of 2  $\text{H}\cdot\text{CHO}$  (non-photo-oxidisable). The resemblance of the  $\text{CH}_3\text{CH}$  fragment to acetaldehyde is noteworthy. There is no evidence for the production of acetaldehyde as an oxidation product of propylene under these conditions, but a study of the properties of acetaldehyde in relation to illuminated  $\text{TiO}_2$  would be of interest.

The present studies have also demonstrated a photo-oxidation of ethylene and propylene oxides on illuminated  $\text{TiO}_2$ . The detected products were again  $\text{CO}_2$ , water and formaldehyde. Species of the ethylene or propylene oxide type might well act as intermediates in the hydrocarbon photo-oxidations. The present preliminary results on the two oxides serve only to demonstrate that the presence of such intermediates cannot be ruled out.

Adsorption of water vapour on titanium dioxide

Titanium dioxide surfaces have a high capacity for the adsorption of water vapour. Coverages of over a monolayer have been reported (29). The measurements of resistance change in  $\text{TiO}_2$  pellets in contact with water vapour (page 61) were not carried out in conjunction with adsorption measurements; it is possible, therefore, that only a small proportion of the total adsorbed water is responsible for the resistance changes.

The resistance measurements indicate the presence of at least two types of adsorbed water. These may be adsorbed simultaneously, or alternatively one type may be converted by a slow surface process to the second type. A comparison may be drawn with the resistance changes which occur (68) during the chemisorption of CO on the p-type semiconductor  $\text{Cu}_2\text{O}$ . Here an initial rapid increase in resistance followed by a slower decrease is taken to indicate an initial adsorption as  $\text{CO}^+$  followed by reaction with lattice oxygen to give a surface  $\text{CO}_3^-$  species; the existence of the latter has been conclusively demonstrated. One possible interpretation of the present results is that water is first adsorbed rapidly as  $\text{H}_2\text{O}^+$ ; this gives rise to the initial resistance decrease. A slower process then occurs in which the initially adsorbed water is converted to surface  $\text{OH}^-$ . This slow process is responsible for the subsequent slow increase in resistance and may be represented diagrammatically :



The slow process involves localisation of the extra conduction electron

(donated by the water molecule) at a surface OH species. The incomplete reversal of the initial resistance decrease indicates that only a portion of the  $\text{H}_2\text{O}^+$  can be incorporated with surface  $\text{O}^{2-}$ . It is obvious that both types of water are loosely held, since the original pellet resistance can be attained on evacuation at  $20^\circ\text{C}$ .

The measurements also demonstrate a relation between adsorbed water and oxygen photoadsorption, in that the slow increase in resistance is suppressed by a prior oxygen photoadsorption. In terms of the model proposed above, photoadsorbed oxygen may fill surface vacancies and prevent the formation of OH<sup>-</sup> species. The previous evidence for a relation between surface water and oxygen photoadsorption has been mentioned on page 9.

Finally it should be noted that water vapour adsorbed in the form ( $\text{H}_2\text{O}^+$ ) which decreases the pellet resistance is effective in suppressing the photo-conductance. This could arise in two ways, either :

- (1) The electrons donated by the initially adsorbed water are sufficient to fill the available conduction levels,
- or (2) Water is adsorbed at sites which normally act as donors of photo-conductance electrons, and the photoactivity of these sites is somehow destroyed.

It is not possible to comment further on these possibilities without information as to the density of conduction levels and donor sites. It may be pointed out again, however, that this result is again in agreement with a relation between surface water and the photo-properties of the dioxide.

It is to be noted that the conductivity changes measured here when small pressures of water vapour were brought in contact with  $\text{TiO}_2$  are of the same

nature as those reported by Maclean (20) for the case of  $\text{TiO}_2$ , in contact with ammonia (10-30 mm). It is possible that the conductivity changes measured by Maclean were the result of small amounts of water present in the ammonia.



### CONCLUSION

Photoadsorptions of ethylene and of propylene have been studied on a laboratory prepared sample of  $\text{TiO}_2$  at  $25^\circ\text{C}$ . The electronic nature of the adsorptions has been established. The ability of the dioxide to act as a photo-oxidative catalyst at  $25^\circ\text{C}$  has been demonstrated.

The Elovich nature of the kinetics of photoadsorption of oxygen, ethylene and propylene suggests an adsorption process whose energy of activation increases with coverage. A study of the processes at higher temperatures would therefore be of interest and would provide some information as to the variation of energy of activation with coverage. These high-temperature studies could be extended to investigate photoelectron-hole recombination processes or the possibility of a purely thermal photocatalysis.

The work is hindered at the moment by ignorance as to the nature of a  $\text{TiO}_2$  surface and the adsorbed species. Infra red studies of the photoadsorbed gases should provide useful information on the latter.

T A B L E S

TABIE 1.

O<sub>2</sub> on untreated TiO<sub>2</sub>

Volume of reaction system = 31.4 ml.

Gauge sensitivity = 0.0776 mm/div.

Weight of film = 0.074 g.

t mins.	$\Delta p$ Divs.	t	$\Delta p$	t	$\Delta p$
0	0.0	150	4.2	2600	15.8
0.5	0.4	180	4.3	2840	16.8
1	0.7	210	4.7	3020	16.8
2	0.8	240	5.8	3260	16.8
5	0.8	400	6.8	3800	18.7
10	1.4	700	9.0	4280	19.9
15	1.7	1000	10.5	4640	19.9
60	2.8	1400	12.8	5690	22.1
90	3.4	1520	12.8	6110	21.9
120	3.8	2000	14.6	7220	23.7

Total uptake = 3.1  $\mu$  moles = 42  $\mu$  moles per g. TiO<sub>2</sub>

TABLE 2.

O<sub>2</sub> on untreated TiO<sub>2</sub>

Volume of reaction system = 32.2 ml.

Gauge sensitivity = 0.0776 mm/div.

Weight of film = 0.073 g.

t mins.	$\Delta p$ Divs.	t	$\Delta p$	t	$\Delta p$
0	0.0	630	11.2	3390	20.4
1	0.2	1230	14.3	3540	21.1
3	0.6	1290	14.3	4260	23.1
5	1.1	1380	15.1	4440	23.2
7	1.2	1440	15.2	4620	23.3
10	1.6	1500	15.4	5880	25.5
15	2.1	1620	16.1	5920	25.2
20	2.3	1890	17.0	6000	25.3
25	2.9	2100	17.2	6100	25.9
80	5.1	2760	19.2	6210	26.2
100	5.3	2940	19.4	6790	26.2
120	6.0	3000	19.8	7480	27.7
360	9.2	3060	20.0	7540	27.7
420	9.3	3120	20.4		

Total uptake =  $3.7 \mu$  moles =  $51 \mu$  moles per g. TiO<sub>2</sub>

TABIE 3

C<sub>2</sub>H<sub>4</sub> on untreated TiO<sub>2</sub>

Volume of reaction system = 31.6 ml.

Gauge sensitivity = 0.0776 mm/div.

Weight of film = 0.075 g.

t mins.	$\Delta p$ Divs.	t	$\Delta p$	t	$\Delta p$
0	0.0	80	3.2	440	8.0
1	0.1	100	3.9	470	8.1
2	0.2	140	4.7	500	8.2
3	0.2	180	5.4	530	8.3
5	0.4	230	6.1	560	8.3
10	1.0	240	6.2	640	8.4
15	1.1	280	7.2	670	8.6
20	1.3	300	7.3	900	9.0
25	1.5	330	7.3	1300	9.9
30	2.0	360	7.3	1670	10.4
50	2.3	390	7.5	1860	10.4
60	2.7	400	7.9	1980	10.5
70	3.0	410	8.1	2700	10.5

Total uptake =  $1.4 \mu$  moles =  $18 \mu$  moles per g. of TiO<sub>2</sub>.

TABLE 3a.

Derived rate values from Table 3

$\Delta p$	R	$\frac{1}{R}$	log R.	$\Delta p$	R	log R.
0.5	0.079	12.7	2.90	7.1	0.0095	3.98
1.3	0.045	22.0	2.66	7.3	0.0080	3.90
2.1	0.037	27.0	2.57	7.4	0.0080	3.90
2.75	0.030	33.3	2.48	7.5	0.0060	3.78
3.3	0.028	36.4	2.44	7.8	0.0055	3.74
3.8	0.025	40.0	2.40	8.0	0.0045	3.65
4.3	0.021	47.6	2.32	8.3	0.0018	3.26
4.7	0.020	50.0	2.30	8.5	0.0022	3.34
5.1	0.019	52.6	2.28	9.0	0.0018	3.26
5.5	0.019	52.6	2.28	9.3	0.0018	3.26
5.8	0.015	64.5	2.19	9.5	0.0015	3.18
6.1	0.014	71.4	2.15	9.8	0.0012	3.08
6.4	0.013	77.0	2.11	10.0	0.0010	3.00
6.7	0.013	77.0	2.11	10.3	0.0005	4.7
6.9	0.0105	95.4	2.02			

TABLE 4.

C<sub>2</sub>H<sub>4</sub> on untreated TiO<sub>2</sub>

Volume of reaction system = 32.2 ml.

Gauge sensitivity = 0.0776 mm/div.

Weight of film = 0.069 g.

t mins.	Δ p divs.	t	Δ p	t	Δ p
0	0.0	60	1.9	1660	6.8
1	0.5	70	2.1	1690	6.8
2	0.7	120	2.8	1750	6.9
3	0.8	160	3.0	1990	7.3
4	0.8	220	3.6	2400	7.8
5	0.8	280	3.8	2920	8.4
10	0.9	340	3.9	3580	8.9
15	1.0	500	4.6	4400	8.9
25	1.5	640	4.9	4500	8.9
30	1.8	820	4.9	4600	8.9
40	1.8	1200	6.2	5200	8.9
50	1.8	1630	6.8		

Total uptake = 1.20  $\mu$  moles = 17.5  $\mu$  moles per g. of TiO<sub>2</sub>.

TABIE 5.

C<sub>3</sub>H<sub>6</sub> on O<sub>2</sub><sup>-</sup> treated TiO<sub>2</sub>

Volume of reaction system = 32.2 ml.

Gauge sensitivity = 0.0776 mm/div.

Weight of film = 0.073 g.

t mins.	Δ p divs.	t	Δ p	t	Δ p
0	0.0	50	4.2	690	10.1
1	0.1	60	4.7	1000	11.0
2	0.5	70	5.0	1410	12.0
3	0.9	80	5.1	1530	12.0
4	1.0	90	5.2	1560	12.0
5	1.1	100	5.5	2100	12.6
10	1.9	120	6.0	2670	13.0
12	2.0	140	6.2	2820	13.0
15	2.0	180	7.0	2940	13.0
20	2.7	300	8.2	3240	13.0
25	3.0	500	9.4	4200	14.0
30	3.2	600	10.0	4400	14.0
40	4.0	630	10.0	4530	14.0

Prior oxygen photoadsorption = 3.7 μ moles

Total propylene uptake = 1.9 μ moles



TABLE 6.

C<sub>2</sub>H<sub>4</sub> on O<sub>2</sub>- treated TiO<sub>2</sub>

Volume of reaction system = 32.2 ml.

Gauge sensitivity = 0.0776 mm/div.

Weight of film = 0.076 g.

t mins.	$\Delta p$ divs.	t	$\Delta p$	t	$\Delta p$
0	0.0	40	6.6	1520	15.5
0.5	0.5	60	7.8	1760	15.6
1	0.7	80	8.5	2020	16.4
2	1.4	100	9.1	2780	17.4
3	1.6	130	9.5	2900	17.4
4	2.1	180	10.6	3080	17.4
5	2.5	280	11.6	3380	17.6
7	2.6	340	12.2	3740	18.6
10	3.5	500	13.3	4400	19.4
20	4.9	640	14.0	6200	21.3
25	5.5	1000	15.2	7220	21.3
30	5.9	1340	15.5		

Prior oxygen photoadsorption = 1.3  $\mu$  moles.

Total ethylene uptake = 2.9  $\mu$  moles.

TABLE 7.

O<sub>2</sub> on C<sub>3</sub>H<sub>6</sub>- treated TiO<sub>2</sub>

Volume of reaction vessel = 32.2 ml.

Gauge sensitivity = 0.0776 mm/div.

Weight of film = 0.087 g.

t mins.	Δp divs.	t	Δp	t	Δp
0	0.0	10	4.3	200	18.8
0.5	0.7	15	5.7	250	20.0
1	1.2	20	6.7	300	21.0
1.5	1.6	25	7.7	400	23.0
2	1.8	30	8.5	500	24.3
3	2.1	40	9.7	600	25.3
4	2.7	50	11.0	800	27.6
5	2.8	60	11.8	1000	29.1
6	3.2	75	12.7	1400	31.3
7	3.6	100	14.4	1600	32.2
8	3.7	120	15.5	2000	33.7
9	4.0	150	17.5	2200	34.1

Prior propylene photoadsorption = 1.2 μ moles.

Oxygen photoadsorption in 2200 mins. = 4.6 μ moles .

TABLE 7a.

Derived rate values from Table 7

$\Delta p$	R	$\frac{1}{R}$	$\log R$	$\Delta p$	R	$\frac{1}{R}$	$\log R$
0.75	1.44	0.69	0.16	7.7	0.18	5.6	$\bar{1}.26$
1.2	0.70	1.43	$\bar{1}.85$	8.45	0.14	7.1	$\bar{1}.15$
1.75	0.48	2.08	$\bar{1}.68$	9.1	0.12	8.3	$\bar{1}.08$
2.2	0.42	2.38	$\bar{1}.62$	10.5	0.10		$\bar{1}.00$
2.55	0.34	2.9	$\bar{1}.53$	11.5	0.09		$\bar{2}.95$
2.9	0.34	2.9	$\bar{1}.53$	12.2	0.07		$\bar{2}.85$
3.2	0.32	3.1	$\bar{1}.51$	14.3	0.065		$\bar{2}.81$
3.55	0.32	3.1	$\bar{1}.51$	16.5	0.045		$\bar{2}.65$
3.85	0.30	3.3	$\bar{1}.48$	18.8	0.032		$\bar{2}.51$
4.15	0.28	3.6	$\bar{1}.45$	21.2	0.022		$\bar{2}.34$
4.4	0.28	3.6	$\bar{1}.45$	23.0	0.015		$\bar{2}.18$
5.7	0.25	4.0	$\bar{1}.40$	25.6	0.012		$\bar{2}.08$
6.8	0.20	5.0	$\bar{1}.30$	27.9	0.010		$\bar{2}.00$

TABLE 8.

O<sub>2</sub> on C<sub>2</sub>H<sub>4</sub> - treated TiO<sub>2</sub>

Volume of reaction system = 31.4 ml.

Gauge sensitivity = 0.0776 mm/div.

Weight of film = 0.074 g.

t mins.	Δ p divs.	t	Δ p	t	Δ p
0	0.0	15	4.1	1320	34.8
0.5	0.7	20	5.0	1360	34.9
1	1.0	25	5.8	1460	35.9
2	1.2	30	6.1	1560	36.9
3	1.8	90	11.0	1860	38.9
4	2.0	100	11.9	3000	46.0
5	2.1	190	16.0	4320	51.0
6	2.6	250	18.0		
7	2.9	460	23.1		
8	3.0	490	23.9		
9	3.0	590	25.9		
10	3.1	620	26.2		
12	3.9	1280	34.1		

Prior ethylene photoadsorption = 3.5 μ moles.

Oxygen uptake in 4320 mins. = 6.7 μ moles.

TABLE 9.

40 mm. C<sub>2</sub>H<sub>4</sub> + 40 mm. O<sub>2</sub>

Volume of reaction system = 31.4 ml.

Gauge sensitivity = 0.0776 mm./div.

Weight of film = 0.072 g.

t mins.	$\Delta p$ divs.	t	$\Delta p$	t	$\Delta p$
0	0.0	280	103.8	960	152.0
1	0.4	380	128.2	1010	260.2
2	1.8	400	133.4	1030	262.4
3	2.4	420	138.2	Overnight dark period	
4	3.4	440	142.4	1050	266.6
5	4.0	460	148.0	1080	271.2
11	8.0	480	152.8	1120	278.8
15	10.0	520	160.8	1150	284.6
25	15.4	540	165.0	1180	290.0
30	17.6	560	169.8	1210	294.0
60	32.0	580	174.0	1300	308.2
80	39.6	590	176.2	1330	313.2
100	47.0	Overnight dark period		1360	318.0
120	53.8	600	179.8	1390	323.2
140	60.0	610	182.2	1650	366.2
160	66.4	630	186.8	1670	369.6
Overnight dark period		670	196.2	1720	372.2
170	70.6	710	204.0	Overnight dark period	
190	78.2	790	220.4	1745	377.2
210	84.2	840	230.4	1765	381.8
250	95.8	890	239.6	1790	386.0

Total pressure decrease in 1790 mins. = 30.0 mm.

= 50.5  $\mu$  moles.

TABLE 10 on page 39

TABLE 11 facing page 40

TABLE 12.

35 mm. C<sub>3</sub>H<sub>6</sub> + 35 mm. O<sub>2</sub>

Volume of reaction system = 31.4 ml.

Gauge sensitivity = 0.0776 mm/div.

Weight of film = 0.075 g.

t mins.	$\Delta p$ divs.	t	$\Delta p$	t	$\Delta p$
Dark		1	1.6	17	15.8
0	0.0	2	2.8	21	18.9
1	3.0	3	3.8	25	22.0
2	5.0	4	4.8	30	25.7
4	8.0	5	5.8	42	33.0
5	9.0	6	6.8	45	35.4
10	11.0	7	7.8	50	38.8
15	12.0	8	8.8	55	41.8
20	13.0	9	9.5	60	44.8
30	13.0	10	9.9	105	70.0
60	14.0	11	10.8	125	80.3
120	15.0	12	11.7	130	83.2
Light on		13	12.6	140	87.5
0	0.0	14	13.3	Light off	
0.5	0.8	15	13.9		

Total pressure decrease during 140 minutes of illumination = 6.8 mm.

= 11.5  $\mu$  moles.

TABLE 13

Photoconductance rise and decay

	t mins.	log r (ohms)	t	log r	t	log r
Light on	0	10.96	150	8.35	390	8.53
	0.5	9.70	195	8.32	425	8.82
	1	9.42	370	8.27	500	9.17
	2	9.16	Light off		610	9.47
	3	9.05	371	8.30	1000	10.00
	4	8.98	372	8.32	1750	10.40
	5	8.93	373	8.34	1800	10.42
	10	8.78	374	8.36	3130	10.70
	40	8.54	375	8.38	4500	10.78
	100	8.42	380	8.44		

TABLE 14

Photoconductance rise and decay

	t mins.	log r (ohms)	t	log r	t	log r
Light on	0	14.38	20	10.41	260	10.44
	0.5	11.55	120	9.90	270	10.62
	1	11.31	240	9.73	Light on	
	2	11.12	Light off		271	10.21
	3	10.95	242	9.95	272	10.08
	4	10.86	243	10.00	273	10.03
	5	10.79	244	10.03	274	9.97
	10	10.60	245	10.07	275	9.94
	15	10.48	250	10.22	310	9.73



TABLE 15.

Effect of O<sub>2</sub> on dark resistance

	t mins.	log r (ohms)	t	log r	t	log r
20 mm. O <sub>2</sub>	0	11.66	7	12.76	20	12.61
	0.5	12.77	8	12.75	25	12.58
	1	12.77	9	12.75	30	12.56
	1.5	12.77	10	12.74	Evacuated	
	2	12.78	64 mm O <sub>2</sub>		32	12.58
	3	12.78	11	12.71	35	12.59
	4	12.78	12	12.69	55	12.63
	5	12.78	13	12.68	65	12.66
	40 mm O <sub>2</sub>		14	12.66	70	12.67
	6	12.76	15	12.65		

TABLE 16

Admission of O<sub>2</sub> during photoconductance decay

	t mins.	log r (ohms)	t	log r	t	log r
Light on	0	11.48	162	12.16	187	12.95
	0.5	9.55	163 (B)	12.17	190	12.82
	1	9.30	164	12.17	Light on (D)	
	2	9.09	165	12.17	190.5	10.50
	3	8.98	166	12.17	191	10.14
	4	8.90	167	12.17	192	9.70
	5	8.84	168	12.17	193	9.51
	10	8.68	169	12.17	194	9.38
	15	8.59	170	12.17	195	9.27
	20	8.52	175	12.17	200	8.99
	30	8.43	Evacuated		Evacuated (E)	
	40	8.32	175.5	12.48	201	8.91
	120	8.16	176	12.57	202	8.89
	150	8.14	177	12.80	205	8.84
	159	8.13	178	12.92	210	8.71
Light off			179	12.99	240	8.39
	159.5	8.18	180 (C)	13.03	270	8.27
	160	8.19	185	13.01	285	8.24
+ 10 mm.O <sub>2</sub> (A)			Isolated		290	8.23
	160.5	11.65	185.5	13.00		
	161	12.10	186	12.99		

TABLE 17

Effect of O<sub>2</sub> on photoresistance

	t mins.	log r (ohms)	t	log r	t	log r
Light on	0	12.99	32	13.45	46	11.44
	0.5	10.62	33	13.50	47	11.32
	1	10.40	34	13.53	48	11.20
	2	10.18	35	13.57	49	11.10
	3	10.09	36	13.59	50	11.00
	4	9.92	37	13.61	Isolated (H)	
	5	9.86	38	13.62	51	10.95
	10	9.69	39	13.63	52	10.90
	15	9.60	40	13.65	53	10.85
	20	9.53	Evacuated (F)		54	10.80
	25	9.48	40.5	13.36	55	10.75
	30	9.42	41	13.12	60	10.55
+ 10 mm. O <sub>2</sub>			42	12.45	Evacuated (F)	
	30.5	13.20	43	12.08	70	10.28
	31	13.34	44	11.76	80	10.09
	31.5	13.43	45	11.60	100	9.76

TABLE 18

Effect of O<sub>2</sub> on photoresistance

	t mins.	log r (ohms)	t	log r	t	log r
Light on	0	11.34	55	9.44	74	11.37
	1	10.42	60	9.43	75	11.28
	2	10.27	+ 7 mm.O <sub>2</sub>		80	10.90
	3	10.18	60.5	11.31	84	10.70
	4	10.11	61	11.33	Isolated (I)	
	5	9.97	62	11.33	85	10.65
	6	9.93	63	11.32	86	10.62
	7	9.90	64	11.31	87	10.58
	8	9.86	65	11.31	88	10.55
	9	9.84	70	11.29	89	10.51
	10	9.81	Evacuated (G)		90	10.48
	15	9.73	70.5	11.41	130	9.77
	20	9.67	71	11.49	140	9.70
	30	9.60	72	11.52	145	9.66
	50	9.47	73	11.46	150	9.64

TABIE 19

Illumination of a  $TiO_2 - O_2$  system

	t mins.	log r (ohms)	t	log r	t	log r
+30 mm $O_2$	0	12.20	8	12.46	29	11.76
	0.5	12.74	9	12.48	30	11.67
	1	12.78	10	12.50	31	11.62
	2	12.82	15	12.52	32	11.58
	3	12.82	20	12.54	35	11.45
	4	12.82	25	12.55	40	11.29
	5	12.82	Evacuation (L)		50	11.08
Light on (K)			25.5	12.42	80	10.76
	5.5	12.41	26	12.23	110	10.58
	6	12.41	27	12.00	140	10.50
	7	12.43	28	11.88	150	10.47

TABIE 20

Effect of water vapour on resistance

t mins.	log r (ohms)	t	log r	t	log r
0	11.23	10	10.03	401	10.90
0.25	10.43	15	10.09	402	10.99
0.5	10.32	20	10.14	403	11.08
0.75	10.25	50	10.42	404	11.16
1	10.21	80	10.50	405	11.23
1.5	10.15	120	10.55	406	11.25
2	10.11	260	10.68	407	11.30
3	9.97	300	10.68	410	11.38
4	9.95	330	10.69	415	11.49
5 (M)	9.96	400 (N)	10.70	420	11.51
6	9.98	Evacuated (P)		425	11.52
7	9.99	400.25	10.78	430	11.53
8	10.00	400.5	10.82	440	11.53
9	10.02	400.75	10.86	450	11.53

TABLE 21.

Effect of water vapour on resistance  
(after treatment with O<sub>2</sub>)

	t mins.	log r (ohms)	t	log r	t	log r
+ 0.054 mm H <sub>2</sub> O	0	13.30	15	12.16	80	10.53
	0.25	12.30	20	12.16	230	10.65
	0.5	12.19	25	12.15	260	10.65
	1	12.15	+ 0.32 mm.H <sub>2</sub> O		290	10.67
	1.5	12.13			320	10.67
	2	12.13	26	10.26	Light on (Q)	
	3	12.13	26.5	10.27	320.5	9.83
	4	12.14	27	10.28	321	9.67
	5	12.15	28	10.30	321.5	9.40
	6	12.15	29	10.31	323	9.22
	7	12.16	30	10.33	325	8.97
	8	12.16	35	10.37	330	8.74
	9	12.16	40	10.39	340	8.54
	10	12.16	60	10.48	380	8.28

TABLE 22 facing page 72

BIBLIOGRAPHY



REFERENCES

1. CRONEMEYER and GILIEO, Phys. Rev., 82, 975 (1951).
2. CRONEMEYER and GILIEO, ibid 87, 876 (1952).
3. GOODEVE, Trans. Farad. Soc., 33, 340 (1937).
4. WEYL and FORIAND, Ind. Eng. Chem., 42, 257 (1950).
5. GOODEVE and KITCHENER, Trans. Farad. Soc., 34, 902 (1938).
6. MARKHAM, J. Chem. Ed., 32, 540 (1955).
7. JACOBSEN, Ind.Eng. Chem., 41, 523 (1949).
8. McTAGGART and BEAR, J.Appl. Chem., 8, 72 (1958).
9. GRANT, Revs. Mod. Phys., 31, 646 (1959).
10. CRONEMEYER, Phys. Rev., 113, 1222 (1959).
11. C.A. 53, 9818e (1959), Filiminov, Optika i Spektroskopiya, 5, 709 (1958).
12. GRAY et al, J.Phys. Chem., 63, 472 (1959).
13. EARIE, Phys. Rev., 61, 56 (1942).
14. HURIEN, Acta.Chem. Scand., 13, 365 (1959).
15. BRECKENRIDGE and HOSLER, Phys. Rev., 91, 793 (1953).
16. FREDERIKSE, J.Appl. Phys., 32, 2211 (1961).
17. CHESTER, ibid., 32, 2233 (1961).
18. for example, JOHNSON, J.Am.Ceram.Soc., 36, 97 (1953),  
HAUFFE et al, Z. Elektrochem, 56, 937 (1952).
19. RITCHIE et al., Trans. Farad. Soc., 54, 119 (1958).
20. MacLEAN, Ph.D. Thesis, University of Edinburgh.
21. HAUFFE, Reaktionen in und Festen Stoffen, Springer Verlag, Berlin, (1955).
22. GEBHART and HERRINGTON, J.Phys. Chem., 62, 120 (1958)
23. KATAOKA and SUZUKI, Bull.Electrotech. Lab. Tokyo, 18, No.1, 732 (1954)

24. BOLTAKS, et al., Zhur.Tekh. Fiz, 21, 532 (1951). cf. C.A. 45, 9950 f.
25. HENISCH, Elec. Commun. 25 No.2, 163 (1948).
26. EHRLICH, Z.Electrochem. 45, 362 (1939).
27. IATTY, J. Appl. Chem. 8, 96 (1958).
28. GREGG, "Chemisorption", Proc.Symposium, Keele (1956) page 68 (Butterworths).
29. ASHER and GREGG, J.Chem.Soc., 1960, 5057.
30. YATES, J.Phys.Chem., 65, 747 (1961).
31. McTAGGART and BEAR, J.Appl.Chem., 5, 643 (1955).
32. KENNEDY, Ph.D. Thesis, University of Edinburgh.
33. C.A. 53, 6788a, Rapaport and Solonitsyn, Dokl. Akad, SSSR, 143, 1149 (1962).
34. KENNEDY, Unpublished results, University of Edinburgh.
35. STONE, Advances in Catalysis, 13, 1 (1962).
36. HABER and STONE, J.Chem.Soc., 1961, 424.
37. HABER and STONE, Trans. Farad. Soc., 59, 192 (1963).
38. BARRY and STONE, Proc. Roy. Soc. (London), A.255, 124 (1960).
39. FUJITA and KWAN, J.Research Inst., Hokkaido University, I, 24 (1960).
40. TEREININ and SOLONITSYN, Disc.Farad.Soc., 28, 28 (1959).
41. MEDVED, J.Chem. Phys., 28, 870 (1958).
42. MELNICK, ibid., 26, 1136 (1957).
43. KOBAYASHI and KAWAJI, ibid., 24, 907 (1956).
44. KESAVULU and TAYLOR, J.Phys. Chem., 66, 54 (1962)
45. SCHWAB, Advances in Catalysis, 9, 229 (1957).
46. GRAY and SAVAGE, Disc.Farad.Soc., 28, 159 (1959).
47. BARRY and KILIER, ibid., 31, 219 (1961).
48. CLARK and BERETS, Advances in Catalysis, 9, 204 (1957).

49. TAYLOR and THON, J.A.C.S., 74, 4169 (1952).
50. TAYLOR and THON, ibid., 75, 2747 (1953).
51. IOW, Chem.Reviews, 60, 267 (1960).
52. PARRAVANO and BOUDART, Advances in Catalysis, 8, 50 (1953).
53. GRAY, "Chemistry of the Solid State", Ed.Garner (Butterworths, 1955).
54. LAIDIER, Catalysis (Reinhold Publ. Co., N.Y.), Ed.Emmett (1952).
55. CIMINO et al., Actes du deuxieme congres International de catalyse,  
1, 263 (1961).
56. MORRISON, Advances in Catalysis, 7, 259 (1955).
57. GERMAIN, Compt.rend., 238, 236 and 345 (1954).
58. WEISER and MULLIGAN, J.Phys.Chem., 38, 513 (1934).
59. GILES et al., J.Chem.Soc., 1960, 3973.
60. GILES and NAKHWA, J.Appl.Chem., 12, 266 (1962).
61. GREGORY, Unpublished results, University of Edinburgh.
62. MacFARLANE, Unpublished results, University of Edinburgh.
63. G.A. 56, 9567 e, Izvozhikov, Fiz. Tverdogo Tela 3, 3229 (1961).
64. CHARMAN and DEIL, Trans. Farad. Soc., 59, 470 (1963).
65. CHAPMAN et al., ibid., 59, 453 (1963).
66. WOIKENSTEIN, Advances in Catalysis, 12, 189 (1960)
67. G.A. 52, 16898 d. Solonitsyn, Zhur. Fiz. Khim. 32, 1241 (1958)
68. GARNER et al, Proc.Roy.Soc., A197, 294 (1949).

ACKNOWLEDGMENTS

The author expresses his gratitude to Dr. M. Ritchie for invaluable help and encouragement. He is indebted, also, to the Department of Scientific and Industrial Research for their award of a Research Grant.

---